DEVELOPMENT OF A 3–D KINEMATIC MODEL OF HUMAN ARM AND MOMENT AND ENERGETIC ANALYSES OF FUNCTIONAL HUMAN ARM MOTION

by

Yu Li

A Thesis

Submitted to the Faculty of Graduate Studies

in Partial Fulfillment of the Requirements for the Degree of

Master of Science

The University of Manitoba

Department of Electrical Engineering

Winnipeg, Manitoba

August, 1991

ISBN 0-315-77957-8

DEVELOPMENT OF A 3-D KINEMATIC MODEL OF HUMAN ARM AND MOMENT AND ENERGENTIC ANALYSES OF FUNCTIONAL HUMAN ARM MOTION

BY

YU LI

A Thesis submitted to the Faculty of Graduate Studies of the University of Manitoba in partial fulfillment of the requirements for the degree of

MASTER OF SCIENCE

ABSTRACT

To gain an understanding of the causes of the functional movement of human upper limb, an approach to analyze the muscle moments and the resultant energetics of human upper limb motion is developed. This approach is based on a 3–D kinematic model of the upper limb which was developed in this study. The 3–D kinematic model allows 3 DOF (Degrees Of Freedom) at the shoulder, 2 DOF at the elbow and 3 DOF at the wrist. A simple but effective algorithm is developed to smooth out the noise in the raw motion data without losing useful sharp information in the data. Lagrangian dynamics is utilized to formulate the equations of motion of the upper limb, from which net muscle moments at each joint are obtained.

The net muscle moments at the different joint answer the question of which group of muscles contribute to the particular motion. It is concluded that the active groups of muscles for the three functional upper limb movements at the shoulder are the extensors, inward rotators and the abductors; at the elbow pronators and mainly extensors are active; both flexors and extensors are active at the wrist. To analyze energy exchange within each segment the energy variation of each segment is analyzed. It is concluded that the energy levels of each segment show similar variation patterns; three energy exchanges are noticeable and all are in phase. Finally a power/work approach is developed focusing on the human muscles themselves as generators and absorbers of energy. This method answers the question of where the energy is generated and where it is absorbed.

ACKNOWLEDGEMENTS

The author wishes to express her sincere appreciation and gratitude to Dr. S. Onyshko for his wise supervision, valuable guidance and inspiration during the progress of this work and for his suggestions in preparing this thesis.

The appreciation and gratitude are extended to Dr. E. Shwedyk for his generous counsel, valuable guidance and encouragement.

Special thanks are due to Dr. J.E. Cooper and Ms. J. Miller who contributed to this work by devoting their time and helping in obtaining and interpreting data.

The author also wishes to thank all those who generously helped her in solving problems associated with several computer systems and software packages.

In addition, the author is grateful to the financial support of the University of Manitoba Graduate Fellowship.

Finally, the author wishes to dedicate this thesis to her motherland—China which she loves dearly.

TABLE OF CONTENTS

LIST OF FIGURES

CHAPTER 1

INTRODUCTION

1.1 Preface

Understanding the dynamics and kinematics of human movement has both a basic and an applied value in medicine, biology and robotics. In comparison with the great deal of research into the dynamics and kinematics of the human lower extremity, less information is available on the dynamics and kinematics of the human upper extremity. Analysis of human upper limb movement is of importance to ergonomics in improving the environment of workplace where manual and repetitive task is needed and injuries or disorders may occur [1, 2, 3]. Analysis of the functional performance of the upper limb under normal and abnormal conditions [4, 5, 6, 7, 8] is the foundation of arm prosthesis design to restore the functions [9, 10, 11] and as a design and aid for the paralyzed [12, 13, 14]. Studies of human upper limb movement are also the bases for the design and simulation in robotics [15, 16, 17]. The importance of human upper limb motion has evoked considerable interest in the measuring, modeling and synthesis among many investigators.

The basic kinematic and dynamic analyses of human upper limb motion can be categorized as followings:

(1) Measurement of the joint motion data [18, 19, 20, 21] and the anthropometric parameters [22, 23, 24, 25];

(2) Joint model [26, 27, 28, 29] and skeletal–muscular model [30, 31, 32, 33];

(3) Analysis of movement causes such as muscle forces [34, 35, 36], joint moments [37] and energetics [38, 39];

(4) Muscle mechanics and EMG [40];

(5) Neuromotor control of the upper limb motion.

The complexity of these problems results mainly from the complicated anatomical structure of the human musculo–skeletal system, which causes difficulties in both the measurement and description of human motion.

1.2 The Objective of This Study

The purpose of this study is threefold: (1) establishment of 3–D kinematic multisegmental model of the upper limb; (2) smoothing of the raw motion data of human upper limb; (3) joint moment and energetics analyses of the upper limb motion. The approach is based on the motion data of human upper limb available in the Biomedical Engineering Laboratory and a 3–D anatomical model of the upper limb. Therefore the first phase of this study is to establish a 3–D multisegmental model of the upper limb. The second phase is to formulate the mathematical model of the upper limb by applying Lagrange's dynamics. The third phase is to develop a smoothing algorithm to filter out the noises in the raw upper limb motion data. The fourth phase is to solve for the joint moments from the Lagrangian equations of motion. The last phase is to analyze the joint moments and the resultant energetics.

1.3 Literature Review

1.3.1 Joint Model, Degrees of Freedom and Motion Description

When the motion associated with an anatomical joint is to be measured, a kinematic model for the joint must be established [27]. Joint function is determined primarily by the shape and contour of the contact surfaces and constraints of the surrounding soft tissue. From the medical point of view, joint classification is usually based on the shape of the joint surface [41]. On the other hand, from the biomechanics point of view, the classification of the joint models depends on the degrees of freedom (DOF) of the joint motion.

The motion which occurs in most anatomical joints involves 3–D movement which is described by six independent coordinates or degrees of freedom. Three are used to describe translational movement of the joint and another three are used to describe rotational movement of the joint [42, 43]. Because of the difficulties and complexity of both measurement and description of six degrees of freedom motion, only a few investigators have considered both the translation and rotation which occurs between body segments such as vertebral bodies of the spine [44, 45], the wrist [46], the knee [47], and the shoulder [48]. To date, most experimental studies of the joint motion have considered only the relative rotational motion between the articulating bones [49].

Various joint models have been reported in the literature. Of all these joint models, five seem to be used most often [27]. These are (classified according to DOF):

(1) The one–DOF hinge joint. The simplest and common model used to simulate an anatomical joint in planar motion about a single axis embedded in the fixed segment;

(2) The three–DOF (two translations and one rotation) planar joint, used to simulate more general planar joint movement in which relative motion between all points takes place in parallel planes without a single fixed axis or center of rotation;

(3) The three–DOF spherical or ball and socket joint. A joint which consists of a ball–shaped head that fits into a concave socket where movement of the moving segment takes place through rotation about three axes that intersect at the joint center;

(4) The two–DOF spherical joint, which allows rotation about two axes through the joint;

(5) The six–DOF (three translations and three rotations) spatial joint. A general spatial joint which does not assume any limitation on the number of degrees of freedom between the moving and fixed segment.

It should be noted that linkage chains involving more than two rigid bodies have also been used to model anatomical joints such as the wrist [50].

Revolve Joints

In general revolve motion (or hinge motion) includes both ginglymoid movement, such as in the elbow joint and the interphalangeal joints of the finger, as well as pivotal movement, such as the articulation between the radius and ulna where an arch–shaped surface rotates about a rounded, or peg–like pivot. It has been used frequently for the human elbow [51], wrist [52], and occasionally for the human shoulder [53], and fingers [54].

Planar Joint

The motion in this joint consists of gliding movement such as that between the carpal bones of the wrist [41]. This three–DOF planar joint is often used as a model for the shoulder [55], elbow [56], and the radio–ulnar joint [57].

It should be pointed out that a three–DOF planar analysis of a joint can be performed accurately only on a joint that is indeed planar [58]. If a joint is not truly planar, points on the moving body will appear to move along instantaneous elliptical pathways about the fixed body as the viewer looks normal to the supposed plane of motion. This can

result in great deviation of the instant center locations because an ellipse has no fixed center of curvature [27].

Three–DOF Spherical Joint

The relative motion is characterized by all points of the moving segment on concentric spheres about a single center point on a fixed body. For this model the moving segment usually has a fairly well–defined longitudinal axis. This model is frequently assumed for the human shoulder [56], elbow [59], and wrist [46].

The position of the moving member with respect to the fixed is defined in a variety of ways. In Figure 1.1, it is assumed that the location of the center of the joint is known. The relative position is defined by the coordinates of two points A and B which are not colinear with the sphere center [27]. The relative position can also be defined by the rotations about three general axes intersecting at the center of the joint. For anatomical purposes, the position is often defined by rotations in three orthognal planes (sagittal, frontal, and transverse), as well as the rotation about the long axis of the body segment [56, 57], although other systems are also used [46]. Four systems to define relative position are outlined in [27]. When translations are zero, Euler angles are the most convenient to define the relative motion [49, 60].

Many investigators have made it clear that for finite spatial rotation, the sequence of rotation is extremely important and must be specified for a unique description of joint motion [27, 41, 61]. In contrast, it has been noted [60, 62] that finite rotations performed about axes of a joint coordinate system are not dependent upon sequence. The sequence independence or commutative nature can be achieved with proper selection and description of the axes of rotation [49, 60, 62]. In this study, one axis is fixed to the stationary segment and the other is fixed to the moving segment, which results in the sequence being dependent [61].

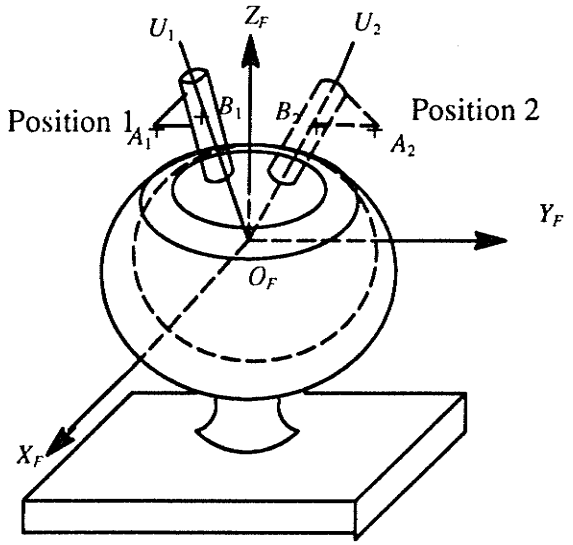

Fig. 1.1 Three–DOF spherical joint

This three–DOF spherical joint model is used in this study to describe the motion at the shoulder and wrist. Euler angles are used to describe the rotation.

Two–DOF Spherical Joint

The two–DOF spherical joint models are special cases of the three–DOF models. Two versions have appeared in the medical literature and they are illustrated in Figure 1.2 (a) and (b) [27]. The model in Figure 1.2 (a) has been used for the human shoulder [63], elbow [64] and wrist. It differs from the general three–DOF spherical joint in that axial rotation is neglected.

The second type of two–DOF spherical joint can be modeled as a slotted ball and socket joint and is illustrated in Figure 1.2 (b). This joint permits rotation about two axes through the joint center. One axis is perpendicular to the plane of the slot, and the other lies in the plane of the slot and corresponds to the longitudinal axis of the moving segment. This model has been used for the human elbow [56] and differs from the general three–DOF spherical joint in that one axis of rotation is constrained to a fixed plane, usually the sagittal

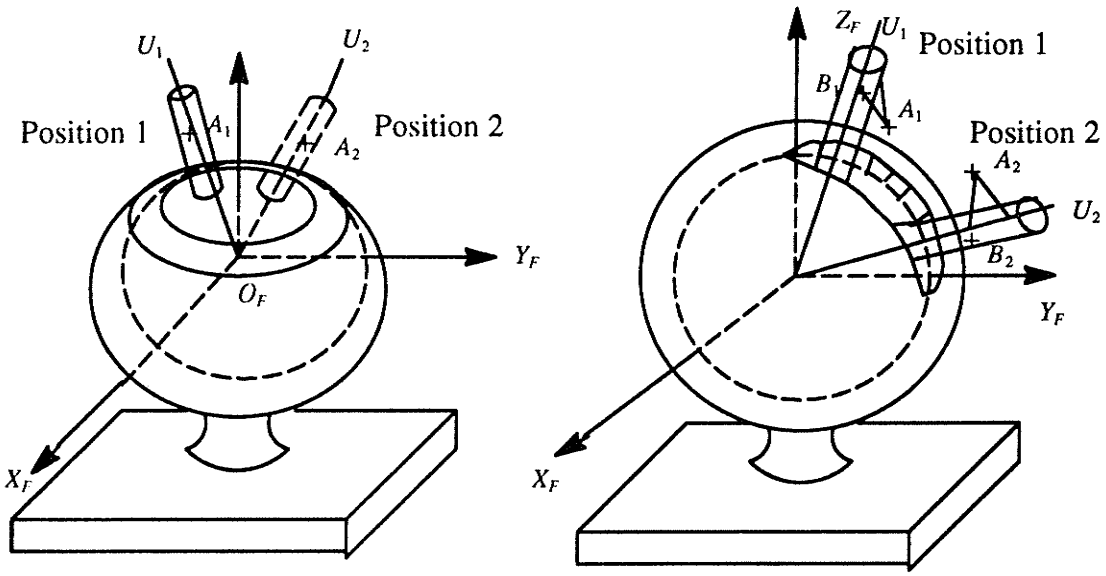

(a). Two–DOF Spherical Joint

(Axial rotation is neglected)

(b). Two–DOF Spherical Joint

(Axial rotation and flexion/extension are allowed)

Fig. 1.2 Two–DOF spherical joint

plane. The angles usually used to describe the relative motion are the flexion–extension angle and the axial rotation angle.

Because of the fact that the second two–DOF spherical joint model is the best and simplest to describe the human elbow, as well as that the same Euler angle coordinate system can be applied as that for the three–DOF spherical shoulder and wrist model, it was used in this study to describe the elbow motion.

General Six–DOF Joint

The six–DOF joint has been used for the human wrist [46], and canine shoulder joint [65].

The most commonly used analytic method for the description of six–DOF spatial motion is the use of a screw displacement axis (SDA) [46]. Unfortunately, the screw axis

parameters are highly sensitive to measurement errors [48], and these errors increase as the motion is approximated by increasingly finer displacements.

Although the six–DOF joint model permits both overall consideration of the gross relative motion between two segments, the relative motion is difficult both to measure and to describe. Therefore, the general six–DOF joint model was not used in this study.

1.3.2 Equation of Motion, Muscle Model, and an Indeterminate Problem

An understanding of the statics, kinematics and dynamics of human motion is fundamental. Kinematics is the position, velocity, and acceleration relationships between manipulator segments. Statics is the relationship between the forces and torques at the segment. Dynamics is the relationship between the kinematics and the statics [66].

Conceptually, there are two types of rigid body dynamics [26, 67]. One is classified as the Direct Dynamics Problem (DDP) in which the external forcing functions applied to the mechanical system are known and the objective is to determine the resulting motion of the system due to the applied forces and moments. The other type of problem is defined by the authors as the Inverse Dynamics Problem (IDP). In these problems the motion of the mechanical system is known in various forms but the externally applied forces and moments are to be determined. No matter which of the two problems is dealt with, to analyze the dynamic behavior of a mechanical system a mathematical model must be established. As a matter of fact, in the analysis, design or identification of manipulators, or robotics, the first step is the derivation of the system's equations of motion [68].

The dynamic behavior is described in terms of the time rate of change of the system configuration in relation to the joint torques exerted by the muscles. This relationship

can be expressed by a set of differential equations, called the equations of motion, that govern the dynamic response of the links to input joint torques [69].

Two methods can be used in order to obtain the equations of motion: the Newton–Euler formulation, and the Lagrangian formulation [69, 70]. The Newton–Euler formulation is described by the direct interpretation of Newton's Second Law of Motion, which describes dynamic systems in terms of force and momentum. The equations incorporate all the forces and moments acting on the individual links. The equations obtained from the Newton–Euler method include the constraint forces acting between adjacent links. Thus, additional operations are required to eliminate these terms and obtain explicit relations between the joint torques and resultant motion in terms of joint displacement. In the Lagrangian formulation, on the other hand, the system's dynamic behavior is described in terms of work and energy using generalized coordinates. All the workless forces and constraint forces are automatically eliminated in this method [69]. Considering the advantages (to be discussed in detail in Chapter 2) of the Lagrangian formulation over the Newton–Euler method, Lagrangian formulation was used in this study.

The joint moments obtained by Lagrangian formulation is only a 'net' or resultant moment exerted by all the muscles that do work during the motion. But information on the forces produced by individual skeletal muscles or muscle groups during normal motion is important to the understanding of muscle mechanics, muscle physiology, musculo–skeletal mechanics, neurophysiology and motor control [71]. In IDP cases, the problem is generally indeterminate, that is, there are more unknowns than available equations. Therefore, no unique solution can be obtained. The indeterminacy of individual muscle is explained as follows: (1) when an external moment must be equalibrated across a joint, a biomechanical model of the joint and its muscles can be established, and a set of muscle forces that equilibrate that external moment found; (2) however, most joints of the human body are

crossed by a large number of muscles. There are at most six equations of equilibrium (three force equations and three moment equations) to be satisfied, but there are often more than six muscle forces to be calculated [72]. For example, An et al [34] included nine muscles in their model of the elbow. In such models, the calculation of the muscle contraction forces constitutes a statically indeterminate problem. Meanwhile, the following three reasons cause discrepancies in the results of muscle forces obtained by different investigators [31]: (1) differences in the way the joint is modeled (as we discussed above); (2) differences in how the muscle force line–of–action is represented (i.e., differences in the muscle model); (3) differences in the way the three joint axes are defined (i.e., differences in decomposing the force vector into three unique components to classify each component based on its algebraic sign). Additional complication arises in the case of multiple–joint muscle or muscles that cross two or more joints [31].

An approach often taken to solve this indeterminate problem is to use an optimization technique [72, 73, 74]. In this method, an optimization scheme is required and an objective function needs to be identified to generate extra equations needed to solve the problem [75, 76, 77]. Muscle EMG method may be used to predict individual muscle force for the elbow flexor muscles. But the primary problem in using the EMG is its sensitivity to varying conditions such as muscle action types, velocity of contraction, fatigue, training and detraining [71]. Although other investigators have proposed an in vivo or direct measurement of the forces of individual muscles by implanting a special transducer on the selected tendons [71], this in vivo recording is still doubted in the application of human motion by many investigators.

1.3.3 Joint Moment of Force (or Torque) Analysis

In order to investigate the patterns of human motion and muscular activity responsible for the motion, not only the moments of individual muscle or muscle group are important, but also the resultant joint moment and the moment components at the local principle axes (i.e., moments produced by the force that is normal to the local motion plane) [78, 79]. Schneider et al [37], in a dynamic analysis of human multisegmental movement during a task involving the upper extremity, partitioned the moments into four categories that can be defined generally as follows [80, 81]:

(1) Net joint moment. The sum of all the positive and negative moment components (gravitational, interactive and muscle) that act at a joint;

(2) Gravitational moment. A passive moment resulting from gravity acting at the center of mass of each segment;

(3) Interactive moments. Passive moments arising from mechanical interactions between segments, such as inertial forces proportional to segmental accelerations or centripetal forces proportional to the square of segmental velocities.

(4) Generalized muscle moment. A 'generalized' moment that includes forces arising from active muscle contractions and from passive deformations of muscles tendons, ligaments, and other periarticular tissues. Because the effects of muscular forces are embedded within this component, the generalized muscle moment comprises the actively–controlled elements of limb–trajectory motor programs.

Schneider pointed out that the net, gravitational and interactive moments can be calculated directly from the limb kinematics. Therefore the generalized muscle moment can be calculated as a 'residual' term, because the sum of the generalized muscle moment, gravitational moment and interactive moments equals the net moment. This generalized

muscle moment or 'residual' moment has also been called 'joint torque' [82], 'muscle moment' [83], and 'moment of force' [84, 85, 70].

When investigating the patterns of motion of the serving arm during the performance of the tennis serve, Bahamond [79] calculated the resultant joint torque and forces at the shoulder and elbow joints by utilizing the inverse dynamic approach. The resultant torques were then projected onto rotation and horizontal adduction torques at the shoulder and flexion–extension and pronation–supination torques at the elbow. Then conclusions were drawn as the contribution of each torque at different phases during the tennis serving.

Andersson et al [86] reported their study on elbow flexion–extension moments when subjects were doing heavy exertion, and divided the moments into active joint moment (caused by active muscle contraction) and passive muscle moment. The passive joint moment was reported negligible in situations of heavy exertion. Two terms, 'muscle contraction moment' and 'moment of force', were used by Jensen et al. [85] when they studied the relationship between upper extremity moments and swimming training. The moments for shoulder and elbow extension were demonstrated in two ways. Firstly, swimmers in a training program tended to increase their contraction moments. Secondly, faster swimmers tended to have greater contraction moments. These results were of use in providing insight into the relative contribution of upper extremity contraction moments to frontal swimming.

1.3.4 Mechanical Work, Energy and Power

No movement takes place without energy flow. Determination of the variables related to the energetics during human motion is a matter of considerable interest to researchers and clinicians. Without that information, nothing is known about the energy flow that causes the observed movement. Diagnostically, it is found that joint mechanical powers

are the most discriminating of all in the assessment of pathological gait. Without joint mechanical power, erroneous or incomplete assessments would be made that would not be detected by EMG or moment–of–force analyses [70]. Also, valid mechanical work calculations are essential to any efficiency assessments that are made in sports and work–related tasks and rehabilitation [89].

Following is a review of the approaches utilized by researchers in the analysis of mechanical energetics of human motion.

In general, two main methods are available to compute the mechanical energetics of human movement: (1) to infer the work performed by examining the energy changes of the body and its constituent segment; (2) to compute the work from the knowledge of the resultant moments of force at the joint and their angular displacements (or directly using muscle force and muscle length changes) [87]. Most researchers have used the energy based approach, no doubt because of its methodologically simpler process of recording segment energetics rather than joint kinetics.

Early attempts based on the energy approach utilized the moments of the center of gravity of the body, eg. [88]. When more than one segmental energy was determined some means of combining them became necessary [89, 90]. These investigators measured the energy components of each limb segment and added them to obtain a measure of total body energy. The changes in this curve were then taken as being representative of the internal work to move the body. A number of other formulations of limb segment energies, eg. [91], defined transfers within the segments. Winter [92] then proposed that the absolute changes in the total body energy be taken into account for both the positive and negative work of the musculature.

This straight algebraic summation of energies demanded by the work/energy relationship implies that decreases in the segmental energy could be 'traded off' against in-

creases in another segment. This process is termed transfer between segments. But it has been noted by a number of investigators that under many circumstances transfer between segments as defined by the above authors is not taking place because these transfers are dependent on the interconnections between segments [87]. Williams and Cavanagh [93] reviewed these problems and highlighted some of the difficulties associated with the computation of mechanical power from segmental energies only. Zatsiorski et al. [94] calculated mechanical power from segmental energies using a number of the methods noted above and commented on the huge discrepancies between different methods.

A parallel approach, which requires knowledge of the joint kinetics, also allows calculation of mechanical work and transfers. Using the joint moments and joint kinematics, Hubley and Wells [95] computed the work while Winter and Robertson [96] computed the power.

Winter and Robertson [96] and Robertson and Winter [83] have described in detail how the energy flow or transfer in a link segment model of the human body can be computed and interpreted. Standard procedures [97] are used to obtain the net joint moments and forces. These are then used to define four energy flows per segment, two at each end: (1) The joint power P_j is the rate at which energy is entering or leaving a segment through the joint (either through bone on bone contact or ligamentous forces) and is passive in nature and requires no metabolic expenditure. It is defined as the vector dot product of the joint velocity and the net joint reaction force. (2) The muscle power P_m is the power generated through the muscle and under certain circumstances, through the ligament. It is defined as the product of the net joint moment and the segment's angular velocity [97]. It should be noted that this technique automatically calculates any external work that is done. The external power will be reflected in increased joint moments, which when multi-

plied by the joint angular velocity will show an increased power equal to that done externally [71]. Therefore, this approach allows one to separate transfers segment by segment.

Unfortunately, the energy approach and the work approach do not, in general, lead to the same conclusions regarding transfer and saving of energy. The causes of the discrepancy were clearly demonstrated by Wells [87] with three experiments on three type of transfers. Firstly, a standing person rising slowly onto tiptoes was considered. Because the potential and thus the total energy of all segments increases in phase , the energy base method will predict no transfer between segments. But the joint–work approach will show that positive work is done at the ankle joint and that transfers through the joint centers of all segments have occurred by virtue of their non–zero velocity. Therefore the joint–work approach allows us to determine where the energy came from (ankle joint in this example) and how energy is redistributed through the skeletal system. The second experiment considered the person swinging one arm as a pendulum. In the ideal case, when the potential and kinetic energies are in anti–phase and of equal amplitude, the total segment energy will be constant. If the energies are not so related the segment's total energy varies and net work must have been done on the segment. The transfer within the segment can be calculated [91] using the energy based method. The joint–work approach is insensitive to these types of transfer within a segment. The third experiment considered a standing person who slowly raises one arm and lowers the other in the frontal plane. In this example, the energy is mainly in potential form, and the energy based method will predict a transfer between the segments (one arm is increasing energy and the other is decreasing). The joint–work approach will show no transfer across the shoulder, but it will show generation of energy at one shoulder joint and an absorption at the other. In this example, one set of shoulder abductors must perform positive work and the other must perform negative

work. One can not be 'traded off' against the other as is implied in the energy method. The energy based method therefore gives erroneous information in this situation.

In addition, the energy based approach has been criticized in recent years not only because it gives erroneous information by denying the energy exchanges taking place within each segment, or between adjacent segments [84], but also that even a correctly calculated total body energy curve yields no information as to the source of generation and absorption of that energy. On the other hand, the joint–work approach has attracted a great deal of attention in the study of human movement energetics.

CHAPTER 2

ESTABLISHMENT OF THE KINEMATIC

MODEL OF HUMAN UPPER LIMB

2.1 Introduction to Lagrangian Formulation of Equations of Motion

Simple motions (single joint, or one, or two–dimensional motions) have been modeled with reasonable success. For the dynamic analysis of connected segment systems, mathematical models consisting of interconnected mass elements, springs, dampers, and actuators (muscles, motion generators) are often used. The complexity increases when the motion of such models is to be determined by defining the time history of the position of individual segments, or by application of motor forces. In fact, as more segments are involved in the problem, the computation required increases rapidly due to the interactions of forces and moments between joints.

Formulating the equations of motion can be done in several ways. The first and most direct, but possibly the least efficient way, is to apply Newton's law of dynamics to each segment in the model. Although the reaction forces and moments caused by the constraints due to the connections between adjacent segments are obtained as by-products of the solution, the method is cumbersome and does not lend itself easily to a general dynamic simulation program. However, if some concepts of graph theory are incorporated with Newton's laws of motion, a methodical procedure can be used to write dynamic simulation programs which are self–formulating.

The second method to formulate the equations of motion is to utilize Lagrangian dynamics, which accommodates constraints much better. This procedure for writing equations of motion was developed by J. L. Lagrange around 1780. It is based on the energy method, and can be used in the general, many–degrees–of–freedom case. Lagrange's equations require the concept of virtual displacement and employ system energy and work, as a function of the generalized coordinates to obtain a set of second–order differential equations of motion. Equations can be obtained by describing either forces, for linear coordinates, or moments, for angular coordinates. To a large extent the method reduces the entire field of dynamics to a single procedure involving the same basic steps, regardless of the number of segments considered, the type of coordinates employed, the number of constraints on the model, whether the system is conservative or not. This method has been employed by many investigators in the formulation of equations of motion [1, 2].

Which method is more suitable? Each method has its advantages and disadvantages. However, the Lagrangian method is systematic in any suitable coordinates. A procedure based on Lagrange's dynamics was developed in this study and it is suitable for computer implementation using symbolic manipulation language. Before we go any further, a review of Lagrange's method is necessary. The derivation of Lagrange's equations can be found in any advanced dynamics or robotics textbook such as [3].

2.1.1 Degrees of Freedom, Generalized Coordinates

An important concept in the description of a dynamic system is that of degrees of freedom (DOF). The number of degrees of freedom is equal to the number of coordinates used to specify the configuration of the system minus the number of independent equations of constraint. A particle that can move freely in space has six DOF, three rotations and

three translations. Usually, it is possible to find a set of independent coordinates which describe the configuration and which can vary freely without violating the constraints, In this case, there are as many degrees of freedom as there are coordinates.

The configuration of a given system may be expressed in terms of various sets of coordinates. Hence no specific set of coordinates is uniquely suited to the analysis of a given mechanical system. Many coordinate systems are possible; in fact, there is an infinite number. But, in any case, the number of coordinates is equal to the number of degrees of freedom plus the number of independent equations of constraint. Any set of numbers which serve to specify the configuration of a system is an example of *generalized coordinates*, even though they do not have a discernible geometrical significance. The term generalized coordinates can refer to any of the commonly used coordinate systems.

As we proceed to a discussion of Lagrange's equations, it will become apparent that the mathematical analysis of a dynamical system is simplified by choosing a set of *independent generalized coordinates*. In this case, the number of independent generalized coordinates is equal to the number of degrees of freedom; hence there are no equations of constraint. Any additional coordinates in the model are known as superfluous or dependent coordinates. The relations between the independent and superfluous coordinates are in fact constraint equations. If the dependent coordinates can be eliminated, the system is called holonomic. Nonholonomic systems always require more coordinates for their description than there are degrees of freedom. By definition, the first and second derivatives of a generalized coordinate q_i with respect to time are called the generalized velocity $\dot{q}_i$ and the generalized acceleration $\ddot{q}_i$ respectively. The relation between the position vector $\vec{\mathbf{r}}_i$ of a point i in the system and the generalized coordinates $[\mathbf{q}]^t$ are called transformation equations. It is assumed that these equations are in the form:

$$\left.\begin{aligned} x_i &= f_{xi}\ (\ q_1,\ q_2,\ q_3,\ \ldots\ q_n,\ t\ ) \\ y_i &= f_{yi}\ (\ q_1,\ q_2,\ q_3,\ \ldots\ q_n,\ t\ ) \\ z_i &= f_{zi}\ (\ q_1,\ q_2,\ q_3,\ \ldots\ q_n,\ t\ ) \end{aligned}\right\} \qquad 2.1$$

2.1.2 The Lagrangian Function

The Lagrangian function L is defined as the difference between the total kinetic energy (KE) and the total potential energy (PE) in the system, i.e.,

$$L = KE - PE$$

The kinetic energy for a system is defined as the work done on the system to increase its velocity from rest to some value that is measured relative to a global (inertial) reference system. The existence of an inertial reference system is a fundamental postulate of classical dynamics. Potential energy exists if the system is under the influence of conservative forces. Hence the segment potential energy here is defined as the energy possessed by virtue of a segment's position in a gravity field relative to a selected datum level (usually ground level) in the system. In the case of a spring, potential energy is the energy stored in the spring due to its elastic deformation.

2.1.3 Generalized Forces Q

A nonconservative force $\mathbf{F}_j$ action on a system can be resolved into components corresponding to each generalized coordinate q_i (i=1, ..., n) in the system. This is also true for constraint forces. A generalized force Q_i is the component of the forces that do

work when q_i is varied and all other generalized coordinates are kept constant. In more useful terms, if f forces are acting on the system, then

$$Q_i = \sum_{j=1}^{j=f} \lambda_j \left(\frac{F_{x_j} \partial R_{x_j}}{\partial q_i} + \frac{F_{y_j} \partial R_{y_j}}{\partial q_i} + \frac{F_{z_j} \partial R_{z_j}}{\partial q_i} \right) \qquad 2.2$$

where $\mathbf{R}_j$ is the position vector of the force $\mathbf{F}_j$, and λ_j is the constraint force.

In an angular coordinate system this generalized force becomes a moment.

2.1.4 Lagrange's Equations

One of the principle forms of Lagrange's equations is

$$\frac{d}{dt}\left(\frac{\partial L}{\partial \dot{q}_i}\right) - \frac{\partial L}{\partial q_i} = Q_i \quad , \qquad i=1, ..., n \qquad 2.3$$

in which the Q_i 's are generalized forces (forces in linear coordinates, moments in angular coordinates), q_i 's are independent generalized coordinates, and L is the Lagrangian function, n is the number of independent generalized coordinates (or in holonomic systems, the number of DOF).

In the next section, the procedure to model human upper limbs and the application of Lagrangian dynamics to establish the equations of motion for the system is developed in detail. Before the development, the principle advantages of Lagrange's method are outlined below.

(1). The amount of geometric reasoning required may be substantially less because only velocity, and not acceleration, is required. Further, the sign problem is easier because the square of velocity is used.

(2). The method deals essentially with scalar, rather than vector relations.

(3). For conservative systems, forces are not considered.

(4). The method avoids consideration of inertial forces within the system.

(5). The number of equations is determined automatically once the independent generalized coordinates are correctly chosen.

(6). For holonomic systems, no constraint equations are needed.

(7). It is a systematic method and can be implemented by computer programers.

The principle disadvantages of Lagrange's method are:

(1). It proceeds in a routine way without indicating physical cause and effect until the final step. Thus physical intuition is severely limited.

(2). The amount of algebra may be substantially greater than in a force equilibrium procedure, particularly if the system is nonconservative.

2.2 Review of the Kinematics of the Shoulder Complex, Elbow Complex and Hand

Lack of the published studies about movement of human upper limbs as a whole is one of the reasons for doing this study. The modeling of joints of the upper limb has been one of the targets of many investigators. Unfortunately, these models have not satisfied many investigators either because only one joint was considered or because the motion was limited to only one or two dimensions. Modeling the shoulder complex has been a challenge to the investigators, because of the lack of an appropriate biomechanical database, as well as the anatomical complexity of the shoulder and its multi–joint nature. The term 'shoulder complex' refers to the combination of the shoulder joint (the glenohumeral joint) and the shoulder girdle which includes the clavicle, scapula and their articulations. An anatomical description and a brief account of studies on the shoulder complex is given

in [4] and more details can be found in textbooks [5]. Recently, Engin et al. [6] described work on the proper biomechanical description and simulation of the human shoulder complex. Engin and his associates [7], proposed a kinematic data collection methodology by means of sonic emitters and associated data analysis technique. Based on this data collection methodology, they established a statistical database for the shoulder complex sinus for the male population, aged 18–32. The statistical database established by Engin and Chen [8] was cast in a form compatible with the model by obtaining a set of unit vectors describing circumductory motion of the upper arm as a torso–fixed coordinate system. This set of unit vectors was then employed to determine the parameters of a composite shoulder complex sinus of a simplified version of the proposed model. Later on, a mathematical description of the humerus orientation with respect to the torso was given in terms of eight joint variables [9]. Since the system was a kinematically redundant one, an optimization method using a 'minimum joint motion' criterion was introduced to obtain the solution for the joint variables.

Compared to the shoulder complex, the human elbow joint (or complex) is a bit easier to model and describe. In the past two decades, elbow prostheses have been developed and widely used for joints destroyed by disease or trauma. The elbow complex is composed of three articulations: the humeroradial, the humeroulnar, and the superior radioulnar; it has been modeled as a trochoginglymus joint possessing two rotation degrees of freedom (flexion–extension and pronation–supination) by most investigators [10].

Investigations of normal wrist kinematics date back to the late nineteenth century. These early studies were largely limited to planar motion analyses. The need for accurate, quantitative description of wrist kinematics became more apparent with the introduction of total wrist arthroplastry as a method of treatment for advanced rheumatoid arthritis and post–traumatic osteoarthritis. Total wrist prostheses reflected widely differing design

criteria. The prostheses developed by Menli [11] and Hamas [12] are both of a ball–and socket design and differ kinematically in the location of the center of rotation. A quantitative three–dimensional description of wrist kinematics obtained from a statistically significant number of normal subjects was reported by Brumbaugh et al. [13]. The screw displacement axis (SDA) concept was introduced to describe the motion of the hand relative to a reference frame embedded in the radius. From the degrees of freedom point of view, the wrist modeled by the above authors has only two DOF: flexion–extension and ulnar–radial deviation. The third DOF was introduced in this study, i.e., the inward–outward rotation of hand relative to the forearm.

2.3 Kinematic Model of Human Upper Limb and Choice of Coordinate System

The complexity of the function and anatomy of the human upper extremity has been long recognized from a biomechanical standpoint. The upper extremity is a remarkable manipulator possessing both strength and control. A three–dimensional kinematic model and a description of human upper limb have not been well developed. Although the kinematic model of upper limb developed by Langrana [14] included three–dimensional motion of shoulder complex and elbow complex, the wrist joint, a significant joint in the human upper limb, was not considered. Model of upper limb reported by Jackson [15] was made to swing only in the sagittal plane. In this study, a three–dimensional model of upper limb is developed. But due to the difficulties and lack of data for the hand (finger) and shoulder complex, the upper limb was modeled as three connected rigid bodies: upper arm–forearm–hand.

2.3.1 Anatomy and Motion of Upper Limb, and DOF

Figure 2.1 shows the anatomical structure of the human upper extremity from the posterior view.

(1) Movements of the Shoulder Joint

As is well known, the shoulder joint and shoulder girdle comprise the shoulder complex. Because of the lack of motion data on the shoulder girdle, only the shoulder joint is considered in this study.

The shoulder joint, formed by the articulation of the humerus with the scapula, is modeled as a ball–and–socket joint (three–dimensional spherical joint). This structural nature of the shoulder joint makes possible a wide variety of movements and combinations of movements.

Typical movements in the shoulder joint are shown in Figure 2.2:[16]

(a) Ab– and ad– duction (shown in Figure 2.2 (a))

Abduction is sideward elevation of the arm; adduction is the return movement. Humerus movement from the sideposition is common in throwing, tackling, and striking activities.

(b) In– and out– ward rotation (shown in Figure2.2 (b))

Inward rotation is the turning of the humerus around its long axis to the medial side. Outward rotation is the opposite, with the humerus turning around its long axis to the lateral side.

(c) Flexion and extension (shown in Figure 2.2 (c))

A forward elevation of the arm is called flexion; the return movement is extension. Flexion and extension of the shoulder joint are performed frequently supporting the body weight in a hanging position or in a movement from a prone position on the ground.

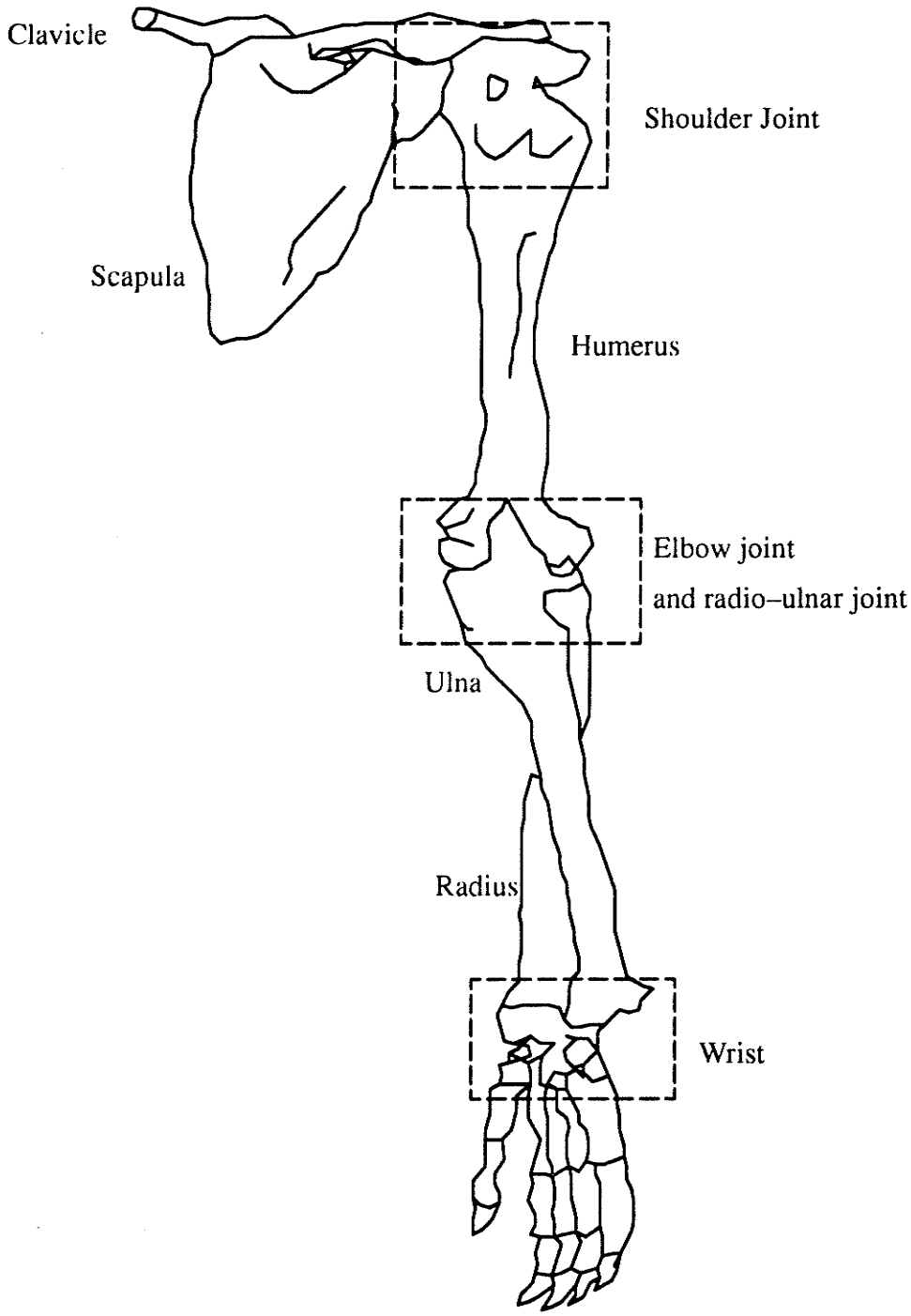

Fig. 2.1 Anatomical structure of the human upper extremity from the posterior view

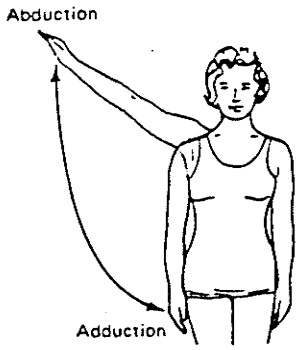

(a). Abduction and Adduction

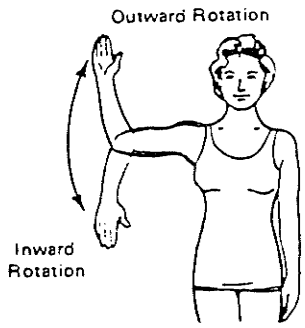

(b). In– and outward Rotation

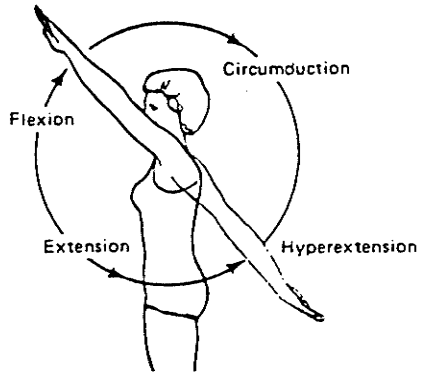

(c). Flexion and Extension

Fig. 2.2 Motion of human arm at the shoulder

(2) Movements of the Elbow and Radio–Ulnar Joints

Functionally, there is distinct separation between the elbow joint and the radio–ulnar joints, the former allowing flexion and extension of the radius and ulna with respect to the humerus, and the latter allowing pronation and supination of the forearm [16]. The motion of the arm at the elbow is shown in Figure 2.3.

Flexion — movement of the hand to the shoulder by bending the elbow

Extension — return to the straight arm

Pronation — movement of the radius on the ulna by moving the hand from palm up to palm down position

Supination — movement of the radius on the ulna by moving the hand from palm down to palm up

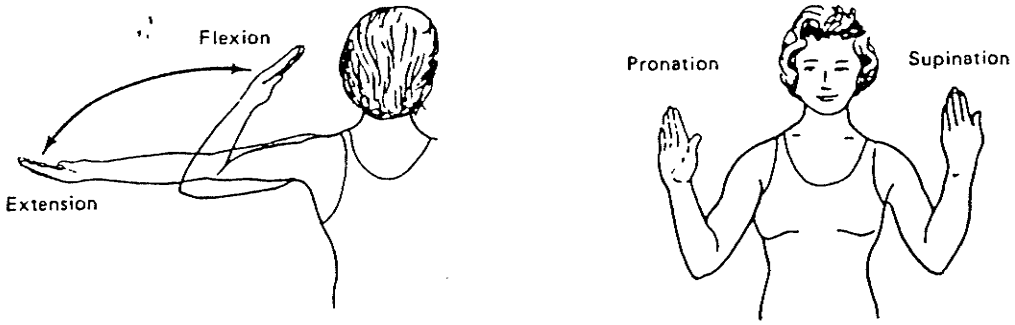

(a) Flexion and Extension (b) Pronation and Supination

Fig. 2.3 Motion of human arm at the elbow

As a matter of fact, the elbow joint serves the shortening and lengthening of the upper extremity, and the radio–ulnar joint moves the hand in pro– and supi– natory direction. The whole complex has two degrees of freedom, hinge motion as well as axial motion (i.e., a two–dimensional spherical joint).

(3) Movements of the Wrist

Anatomically and structurally the wrist and hand of man is a highly developed, complex mechanism capable of a variety of movements. This is due to the arrangement of the 29 bones, 25 moveable joints, and over 30 muscles.

A complete discussion of all the complexities of the wrist and hand is far beyond the scope of this study. Our concern is with the wrist movement, not its anatomical structure. Thus the hand will be modeled as one rigid body connected to the forearm (radius and ulna) by the wrist joint. Typically, the wrist joint permits ulnar flexion, radial flexion,

flexion, extension, and circumduction [16]. The third motion, i.e., inward–outward rotation was also studied in [17].

Flexion/extension and abduction/adduction are shown in Figure 2.4. Circumduction is a combination movement, consisting of flexion, abduction, hyperextension, and adduction occurring in sequence in either this or the reverse order. Thus, the wrist joint has three degrees of freedom, one describing flexion and extension, one describing abduction and adduction, one describing inward and outward rotation.

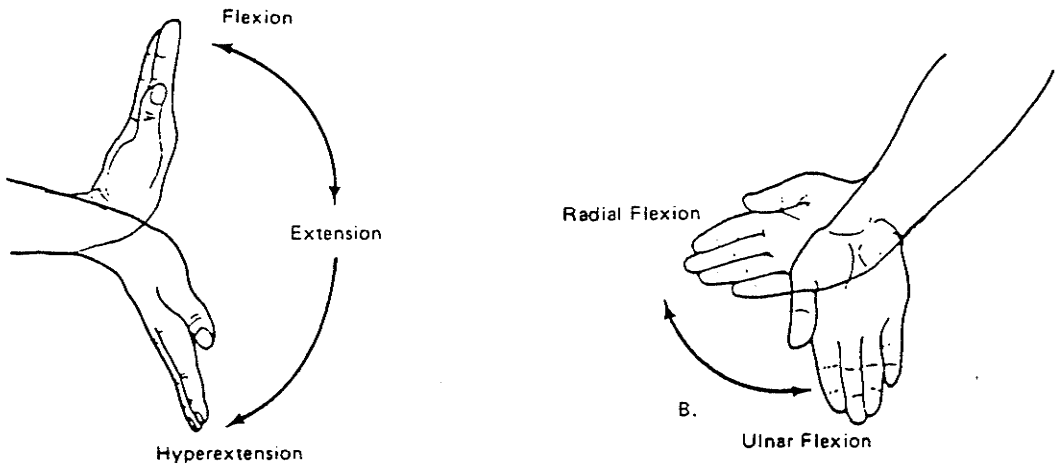

(a). Flexion and Extension (b). Radial Flexion and Ulnar flexion

Fig. 2.4 Motion of human arm at the wrist

(4) Summary of the DOF and Movements of the Human Upper Limb

At the Shoulder:

1 DOF ⇔ Flexion/extension

1 DOF ⇔ Abduction/adduction

1 DOF ⇔ Inward/outward rotation

At the elbow:

1 DOF ⇔ Flexion/extension

1 DOF ⇔ Pronation/supination

At the wrist:

1 DOF ⇔ Flexion/extension

1 DOF ⇔ Radial flexion/ulnar flexion

1 DOF ⇔ Inward/outward rotation

2.3.2 Analytical Description of the Movements of the Shoulder, Elbow and Wrist Joint

Based on the discussion of movements at the shoulder, elbow and wrist joints (section 2.3.1), two types of spherical joint models were used in describing their movements: a three–dimensional spherical joint model for shoulder and wrist joints, a two–dimensional spherical joint model for the elbow (and radio–ulnar joint). As mentioned in Chapter 1, the two–dimensional spherical joint model is a special case of the three–dimensional spherical joint model; therefore, a description of the system that is used to describe the three–dimensional spherical joint model is applicable to the two–dimensional spherical joint model. In this section, it is shown that the Eulerian angle description matches the rotational motion of the spherical joint model.

(1) Eulerian Angle System

The spherical joint model is commonly used for analyzing anatomical joints. This type of joint allows three DOF of rotation; in other words, three angles are required to specify the relative position between the moving and the fixed segments. It has been pointed out that for finite spatial rotation, the sequence of rotation is extremely important and must specified for a unique description of joint motion. Although it is possible to make the finite rotation sequence independent or commutative by proper selection and definition

of the axes of rotation between two bony segments, an ordinary Eulerian angle system with rotation sequence dependence is introduced. This description system is easy to define and understand.

Several different Eulerian angle systems have been used. The one used here is the type that is widely used in aeronautical engineering and also in the analysis of missiles and other space vehicles [18]. This type has also been used recently in the functional study of arm movement [17].

In Figure 2.5 (a), (b) and (c), let X, Y, Z be unit vectors along three orthognal axes (sagittal , frontal and transverse). The order of the rotations and the Euler angles are defined as follows:

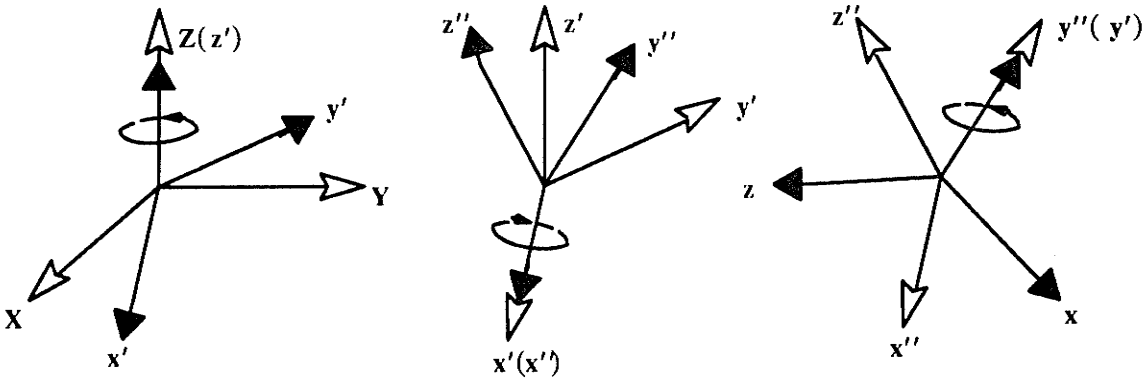

Fig. 2.5 Z–X–Y Euler Angles

(a). rotation about the **Z** axis through an angle ϕ :

$$\begin{aligned} & \phi \\ \mathbf{Z} &\rightarrow \mathbf{z'} \quad (=\mathbf{Z}) \\ \mathbf{X} &\rightarrow \mathbf{x'} \\ \mathbf{Y} &\rightarrow \mathbf{y'} \end{aligned}$$

(b). rotation about x' axis through an angle θ :

$$\theta$$

$$x' \rightarrow x'' \ (= x')$$

$$y' \rightarrow y''$$

$$z' \rightarrow z''$$

(c). rotation about y'' axis through an angle ψ :

$$\psi$$

$$x'' \rightarrow x$$

$$y'' \rightarrow y \ (= y'')$$

$$z'' \rightarrow z$$

These three rotations can be expressed by the following three rotation matrix equations:

$$\begin{bmatrix} x' \\ y' \\ z' \end{bmatrix} = \lambda_\phi \begin{bmatrix} X \\ Y \\ Z \end{bmatrix} \quad , \qquad \lambda_\phi = \begin{bmatrix} Cos\phi & Sin\phi & 0 \\ -Sin\phi & Cos\phi & 0 \\ 0 & 0 & 1 \end{bmatrix} \qquad 2.4$$

$$\begin{bmatrix} x'' \\ y'' \\ z'' \end{bmatrix} = \lambda_\theta \begin{bmatrix} x' \\ y' \\ z' \end{bmatrix} \quad , \qquad \lambda_\theta = \begin{bmatrix} 1 & 0 & 0 \\ 0 & Cos\theta & Sin\theta \\ 0 & -Sin\theta & Cos\theta \end{bmatrix} \qquad 2.5$$

$$\begin{bmatrix} x \\ y \\ z \end{bmatrix} = \lambda_\psi \begin{bmatrix} x'' \\ y'' \\ z'' \end{bmatrix} \quad , \qquad \lambda_\psi = \begin{bmatrix} Cos\psi & 0 & -Sin\psi \\ 0 & 1 & 0 \\ Sin\psi & 0 & Cos\psi \end{bmatrix} \qquad 2.6$$

It is important to recognize that two of the rotational axes (Z, x', y'') are nonorthogonal; consequently, the system is difficult to use readily in kinetic analysis. We will see that angular velocity and acceleration have to be transformed into a set of principle axes or body axes (axes fixed in the segment) in terms of the defined Euler angles ($\phi \quad \theta \quad \psi$).

(2) Coordinate Systems

Normally, to describe the spatial position of a rigid body, two sets of coordinate systems are needed. The first coordinate system, which is common to all body segments is the inertial coordinate system or fixed frame of reference. The second coordinate system is the body (or principle in mechanics) coordinate system. These orthognal axes are defined as follows (shown in Figure 2.6):

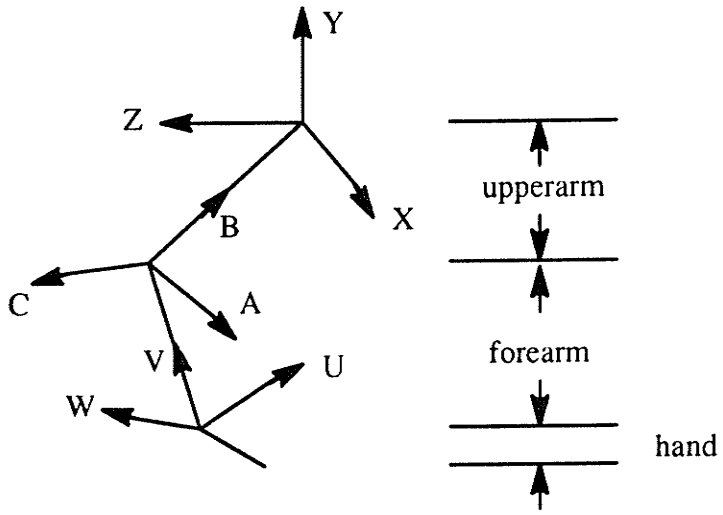

Fig. 2.6 Coordinate system for the description of the arm motion

XYZ: inertial axes or fixed frame of reference with origin fixed in the center of the shoulder.

xyz: principle or body axes, fixed in the upper arm, with origin at the shoulder.

ABC: same as xyz except that their origin is fixed at the elbow.

abc: principle or body axes, fixed in the forearm with origin at the elbow.

UVW: same as abc except that their origin is fixed at the wrist.

uvw: principle or body axes, fixed in the hand, with origin at the wrist.

The relations between XYZ and xyz, ABC and abc, UVW and uvw are shown in the following transformation matrix between the orthognal axes:

$$\begin{bmatrix} x \\ y \\ z \end{bmatrix} = \lambda_{\psi_1}\lambda_{\theta_1}\lambda_{\phi_1} \begin{bmatrix} X \\ Y \\ Z \end{bmatrix} \qquad 2.7$$

$$\begin{bmatrix} a \\ b \\ c \end{bmatrix} = \lambda_{\psi_2}\lambda_{\phi_2} \begin{bmatrix} A \\ B \\ C \end{bmatrix} \qquad 2.8$$

$$\begin{bmatrix} u \\ v \\ w \end{bmatrix} = \lambda_{\psi_3}\lambda_{\theta_3}\lambda_{\phi_3} \begin{bmatrix} U \\ V \\ W \end{bmatrix} \qquad 2.9$$

where matrices λ_{ψ_1} , λ_{θ_1} , λ_{ϕ_1} , λ_{ψ_2} , λ_{ϕ_2} , λ_{ψ_3} , λ_{θ_3} , λ_{ϕ_3} are given by the Equations 2.4, 2.5 and 2.6.

The Euler angles of each body axis with respect to a fixed frame of reference can be calculated, to give the rotation of each body segment (upper arm, forearm and hand) with respect to the fixed frame of reference. For joint rotation, the relative motion of the body axes with respect to each other is needed to simplify the formulation of equations of motion. Therefore, relative rotation angles are used in this study for convenience and classification.

To specify the different motions at different joints, ϕ, θ and ψ with number subscript (1: upperarm; 2: forearm; 3: hand) are assigned as follows:

At the Shoulder:

ϕ_1 : Flexion/extension

θ_1 : Abduction/adduction

ψ_1 : Inward/outward rotation

At the elbow:

ϕ_2 : flexion/extension

ψ_2 : pronation/supination

At the wrist:

ϕ_3 : flexion/extension

θ_3 : ulnar flexion/radial flexion

ψ_3 : inward/outward rotation

(3) Derivation of angular velocity in terms of the Euler angles

As it will be seen later, angular velocity is needed in the Lagrangian formulation of equations of motion. Therefore, derivation of the angular velocity in terms of the Euler angles is discussed here.

As the angles ϕ, θ and ψ vary, the body moves, and has therefore an angular velocity vector. An obvious form for this vector is

$$\omega = \dot{\phi}\mathbf{Z} + \dot{\theta}\mathbf{x}' + \dot{\psi}\mathbf{y}'' \qquad 2.10$$

but this suffers from the defect of being expressed in terms of several different reference frames. That axes **Z**, $\mathbf{x}'$ and $\mathbf{y}''$ are not perpendicular to each other makes this angular velocity vector difficult to use in mechanical analysis. To do an energy analysis, one needs moments of inertia. For this purpose it is more convenient to express ω in terms of its components relative to **xyz** (axes fixed in the body or principle axes). Then,

$$\omega = \omega_x\mathbf{x} + \omega_y\mathbf{y} + \omega_z\mathbf{z} \qquad 2.11$$

and the following obvious identities can be use (derived from matrix Equations 2.4, 2.5 and 2.6)

$$\left.\begin{aligned} \mathbf{Z} &= -cos\theta \sin\psi \mathbf{x} + \sin\theta \mathbf{y} + \cos\theta \cos\psi \mathbf{Z} \\ \mathbf{x}' &= \cos\psi \mathbf{x} + \sin\psi \mathbf{z} \\ \mathbf{y}'' &= \mathbf{y} \end{aligned}\right\} \qquad 2.12$$

and the angular velocities are derived as the following:

$$\left.\begin{aligned} \omega_x &= \dot{\phi} \cos\theta \sin\psi + \dot{\theta} \cos\psi \\ \omega_y &= \dot{\phi} \sin\theta + \dot{\psi} \\ \omega_z &= \dot{\phi} \cos\theta \cos\psi + \dot{\theta} \sin\psi \end{aligned}\right\} \qquad 2.13$$

ω_x, ω_y and ω_z are three components of angular velocity vector ω relative to body axes **xyz**. The above relations are sometimes called Euler's geometrical equations. The relationship between the first derivatives ($\dot{\phi}$, $\dot{\theta}$, $\dot{\psi}$) of Euler angles and the angular velocity components expressed in the **xyz** directions are given by the following transformation

$$\begin{bmatrix} \omega_x \\ \omega_y \\ \omega_z \end{bmatrix} = \begin{bmatrix} \cos\theta \sin\psi & \cos\psi & 0 \\ \sin\theta & 0 & 1 \\ \cos\theta \cos\psi & \sin\psi & 0 \end{bmatrix} \begin{bmatrix} \dot{\phi} \\ \dot{\theta} \\ \dot{\psi} \end{bmatrix} \qquad 2.14$$

If, now, we let I_x, I_y, I_z be the principle moments of inertia about body axes at the fixed point, the kinetic energy of the body is then given by

$$T = \frac{1}{2} (I_x\omega_x^2 + I_y\omega_y^2 + I_z\omega_z^2) \qquad 2.15$$

2.4 Energy forms Stored in Human Body

The purpose to introduce energy forms stored in human body is twofold: (1) to analyze energy variation of the upper limb movement;

(2) to form Lagrangian formulation of equations of motion.

2.4.1 Potential Energy and Kinetic Energy

Energy can be stored in two forms: kinetic and potential energy [19].

(1) Potential Energy (PE) is the energy due to gravity and, therefore, increases with the height of the body above ground or above some other suitable datum,

$$PE = mgh \qquad \text{Joules} \qquad 2.16$$

where m=mass, kg

g=gravitational acceleration, 9.8m/s^2

h= height of center of mass, m

The reference datum should be carefully chosen to fit the problem in question. Normally it is taken as the lowest point the body takes during the given movement. We chose the lowest point each subject's arm took during the given motion in this study.

(2). Kinetic Energy. There are two forms of kinetic energy (KE), that due to translational velocity and that due to rotational velocity,

$$translational\ KE = \frac{1}{2}mv^2 \qquad \text{Joules} \qquad 2.17$$

where v=velocity of center of mass, m/s

$$rotational\ KE = \frac{1}{2}\left(I_x\omega_x^2 + I_y\omega_y^2 + I_z\omega_z^2\right) \qquad \text{Joules} \qquad 2.18$$

where xyz: body axes (fixed in the body)

I_x, I_y, I_z: principle rotational moments of inertia with respect to **xyz**, $kg.m^2$.

ω_x, ω_y, ω_z: rotational velocity components at **xyz**, rad/s.

Note that these two energies increase as the velocity squared. The polarity of direction of the velocity is unimportant because velocity squared is always positive. The lowest level of kinetic energy is therefore zero.

(3) Total Energy. As mentioned previously energy of a body exists in three forms so that the total energy of a body is

$$E_t = PE + translational\ KE + rotational\ KE$$

$$= mgh + \frac{1}{2}mv^2 + \frac{1}{2}\left(I_x\omega_x^2 + I_y\omega_y^2 + I_z\omega_z^2\right) \qquad \text{Joules} \qquad 2.19$$

2.4.2 Formulation of the Lagrangian Function L and Generalized Forces (Moments)

At any given time the system energy may consist of

(1) the energy of segments due to their motion——kinetic energy, KE;

(2) the energy of segments due to the position of the system——potential energy, PE;

(3) the energy stored in springs due to their elastic deformation;

(4) the dissipation energy due to friction of the system.

The first, second and third types of energy are included in the Lagrangian function L (L=KE–PE) of the system. The fourth type can be treated as an external force applied to the system at the proper points rather than energy, and hence it could be covered under external forces. In the case of dampers it is possible to write an energy expression that may be included in Lagrangian equations. In order to do this, the spring constant and damping coefficient must be known. Unfortunately, although a few studies on spring constant and damping coefficient have been reported [20, 21], the elastic element and damping element of the muscle and soft tissue are not well understood and the results of most studies only apply to the specific conditions under which the studies were performed.

Practical numerical data are not available. Therefore, friction and elastic deformation at each joint were excluded in this study. It is assumed that each joint is frictionless and elastic deformation is negligible.

As part of the model description, the externally applied moments (i.e., generalized forces) are in a one–to–one correspondence with angular coordinates; moments are used to replace the generalized forces from now on) are always expressed as components in the directions of principle axes. In order to form the generalized forces required by Lagrange's equations, we developed the following transformations.

If the Euler angles ϕ, θ and ψ are given, then the infinitesimal virtual work of the generalized forces is

$$\partial W = Q_\phi \partial\phi + Q_\theta \partial\theta + Q_\psi \partial\psi \qquad 2.20$$

where $\partial\phi$, $\partial\theta$, $\partial\psi$ are infinitesimal virtual increments of ϕ, θ and ψ

Q_ϕ, Q_θ, Q_ψ are generalized forces required by Lagrange's equations.

But from $\partial\vec{\beta} = \vec{\omega} dt$,

where $\partial\vec{\beta}$: an infinitesimal angular displacement vector

$\vec{\omega}$: angular velocity vector

we have $\partial\beta_x = \omega_x dt$, $\partial\beta_y = \omega_y dt$, $\partial\beta_z = \omega_z dt$, and consequently, using the transformation in Equation 2.14 ,

$$\left.\begin{aligned} \partial\beta_x &= \omega_x dt = -Cos\theta Sin\psi\partial\phi + Cos\psi\partial\theta \\ \partial\beta_y &= \omega_y dt = Sin\theta\partial\phi + \partial\psi \\ \partial\beta_z &= \omega_z dt = Cos\theta Cos\psi\partial\phi + Sin\psi\partial\theta \end{aligned}\right\} \qquad 2.21$$

The infinitesimal virtual work ∂w can be also expressed as

$$\partial w = \vec{M}.\partial\vec{\beta} = M_x\partial\beta_x + M_y\partial\beta_y + M_z\partial\beta_z$$
$$= (-M_xCos\theta Sin\psi + M_ySin\theta + M_zCos\theta Cos\psi) \partial\phi + (M_xCos\psi + M_zSin\psi) \partial\theta + M_y\partial\psi \quad 2.22$$

Comparing Equation 2.20 and Equation 2.22 gives

$$\left.\begin{aligned} Q_\phi &= -M_xCos\theta Sin\psi + M_ySin\theta + M_zCos\theta Cos\psi \\ Q_\theta &= M_xCos\psi + M_zSin\psi \\ Q_\psi &= M_y \end{aligned}\right\} \quad 2.23$$

i.e., the transformation between the moments and the generalized forces

$$\begin{bmatrix} Q_\phi \\ Q_\theta \\ Q_\psi \end{bmatrix} = \begin{bmatrix} -Cos\theta Sin\psi & Sin\theta & Cos\theta Cos\psi \\ Cos\psi & 0 & Sin\psi \\ 0 & 1 & 0 \end{bmatrix} \begin{bmatrix} M_x \\ M_y \\ M_z \end{bmatrix} \quad 2.24$$

where M_x, M_y, M_z are externally applied moments in the directions of **xyz;**

Q_ϕ, Q_θ, Q_ψ are generalized moments required by Lagrange's equations.

Now since there are three sets of body axes **xyz**, **abc** and **uvw,** there are three sets of externally applied moments M_x, M_y, M_z, M_a, M_b, M_c, and M_u, M_v, M_w in the directions of **xyz**, **abc** and **uvw,** respectively. Therefore, according to the transformation in Equation 2.24, we obtain:

at the shoulder

$$\left.\begin{aligned} Q_{\phi 1} &= -M_xCos\theta_1Sin\psi_1 + M_ySin\theta_1 + M_zCos\theta_1Cos\psi_1 \\ Q_{\theta_1} &= M_xCos\psi_1 + M_zSin\psi_1 \\ Q_{\psi_1} &= M_y \end{aligned}\right\} \quad 2.25$$

at the elbow

$$\left.\begin{aligned} Q_{\phi_2} &= -M_a Sin\psi_2 + M_c Cos\psi_2 \\ Q_{\psi_2} &= M_c \\ M_a Cos\psi_2 &+ M_c Sin\psi_2 = 0 \end{aligned}\right\} \quad 2.26$$

at the wrist

$$\left.\begin{aligned} Q_{\phi_3} &= -M_u Cos\theta_3 Sin\psi_3 + M_v Sin\theta_3 + M_w Cos\theta_3 Cos\psi_3 \\ Q_{\theta_3} &= M_u Cos\psi_3 + M_w Sin\psi_3 \\ Q_{\psi_3} &= M_v \end{aligned}\right\} \quad 2.27$$

From Section 2.1, we know that Lagrange's equations are of the form

$$\frac{d}{dt}\left(\frac{\partial L}{\partial \dot{q}_i}\right) - \frac{\partial L}{\partial q_i} = Q_i \quad , \qquad i=1, ..., 8$$

where $q_1 = \phi_1$, $q_2 = \theta_1$, $q_3 = \psi_3$,

$q_4 = \phi_2$, $q_5 = \psi_2$,

$q_6 = \phi_3$, $q_7 = \theta_3$, $q_8 = \psi_3$.

Now, the question is how the generalized forces $Q_i's$, (i=1, ..., 8), are related to the nine moments. Their relationships are as followings:

$$Q_8 = Q_{\psi_3} = M_v$$

$$Q_7 = Q_{\theta_3} = M_u Cos\psi_3 + M_w Sin\psi_3$$

$$Q_6 = Q_{\phi_3} = -M_u Cos\theta_3 Sin\psi_3 + M_v Sin\theta_3 + M_w Cos\theta_3 Cos\psi_3$$

$$Q_5 = Q_{\psi_2} + Q_{\psi_3} = M_b + M_v$$

$$Q_4 = Q_{\phi_2} + Q_{\phi_3} = -M_a Sin\psi_2 + M_c Cos\psi_2 - M_u Cos\theta_3 Sin\psi_3 + M_v Sin\theta_3 + M_w Cos\theta_3 Cos\psi_3$$

$$Q_3 = Q_{\psi_1} + Q_{\psi_2} + Q_{\psi_3} = M_y + M_b + M_v$$

$$Q_2 = Q_{\theta_1} + Q_{\theta_3} = M_x Cos\psi_1 + M_z Sin\psi_1 + M_u Cos\psi_3 + M_w Sin\psi_3$$

$$Q_1 = Q_{\phi_1} + Q_{\phi_2} + Q_{\phi_3} = -M_x Cos\theta_1 Sin\psi_1 + M_y Sin\theta_1 + M_z Cos\theta_1 Cos\psi_1 - M_a Sin\psi_2 +$$

$$M_c Cos\psi_2 - M_u Cos\theta_3 Sin\psi_3 + M_v Sin\theta_3 + M_w Cos\theta_3 Cos\psi_3$$

and

$$M_a Cos\psi_2 + M_c Sin\psi_2 = 0$$

2.5 Formulation of Lagrangian Dynamic Equations of Motion

The derivation of Lagrangian dynamic equations of motion is a simpler process than the derivation of Newton's dynamic equations of motion. Still when the number of segments exceeds two and the motion is in three dimensions to derive the Lagrangian dynamic equations of motion by hand is time consuming. It is prone to human error due to the multiplicity of terms in the equations associated with computation of potential and kinetic energies. This problem becomes even more serious when an attempt is made to obtain the partial derivatives needed in Lagrangian equations. The above difficulties have led to the development of a number of symbolic manipulation programs to derive the equations of motion by Lagrangian equations [22].

Since the author of this thesis did not have access to any of these programs, a procedure of automatic generation of Lagrangian equations of motion was developed by making use of a powerful commercial software MATHEMATICA [23] available on the Unix System. The final result of eight equations is not printed out because it is quite lengthy. But it is possible and useful to discuss the structure of the eight dynamic motion equations for the upper limb model.

From the above discussion, we know that the upper limb is modeled as a set of three moving rigid bodies connected in a serial chain with one end fixed to the shoulder and the other end free. The bodies are connected together with two three–DOF spherical joints at the shoulder and the wrist, and one two–DOF spherical joint at the elbow. There are three torque actuators (or muscles) acting at each joint with no friction. Generally, the vector equations of motion of such a manipulator can be written in the form

$$H(\mathbf{q})\ddot{\mathbf{q}} + C(\mathbf{q},\dot{\mathbf{q}})\dot{\mathbf{q}} + \mathbf{g}(\mathbf{q}) = \mathbf{Q} \qquad 2.28$$

where $\mathbf{Q}$ is the 8×1 vector of joint torque generated by the muscle, and $\mathbf{q}$ is the 8×1 vector of joint positions (in the form of angular displacement), with $\mathbf{q} = [q_1 \quad q_2 \quad \ldots \quad q_8]^T = [\phi_1 \quad \theta_1 \quad \psi_1 \quad \phi_2 \quad \psi_2 \quad \phi_3 \quad \theta_3 \quad \psi_3]^T$. The matrix, $\mathbf{H(q)}$, is an 8×8 matrix, called manipulator mass or inertia matrix in robotics. The vector $C(\mathbf{q},\dot{\mathbf{q}})\dot{\mathbf{q}}$ represents torques arising from centrifugal and coriolis forces. The vector $\mathbf{g(q)}$ represents torques due to gravity. More properties can be found in [24].

2.6 Anthropometric Joint Model and the Inertial and Segment Parameters

The upper limb is divided into three rigid bodies, which are upper arm, forearm and hand. The anthropometric data for each subject is obtained from the height and weight measurement.

Because of the limitation of the dimensional measurement, the three rigid segments were modeled as three uniform slender rods instead of 3–d geometric shapes as they are in reality. Then the following parameters are derived: mass of each segment, length of each segment, center of mass of each segment, moment of inertia of each segment. All of these parameters were calculated according to [25] where the segment mass is expressed

as a percentage of body weight (W) and the segment length is expressed as a percentage of body height (H). Moments of inertia were calculated from segmental radii of gyration at proximal and distal axes and subsequently translated to the center of mass by the parallel axis theorem [26].

The following formulas were used to calculate the above parameters.

mass of upper arm m_1 =2.8% × W (kg)

mass of forearm m_2 = 1.6% × W (kg)

mass of hand m_3 = 0.6% × W (kg)

length of upper arm l_1 = 17.3% × H (m)

length of forearm l_2 =16% × H (m)

length of hand l_3 = 5.75% × H (m)

center of mass of upper arm c_1 = 43.6% × l_1 (m)

center of mass of forearm c_2 = 43% × l_2 (m)

center of mass of hand c_3 = 50.6% × l_3 (m)

Let I_x , I_y , I_z be moments of inertia with respect to body axis **xyz** with origin at the center of rotation of the shoulder, then

$$I_y = 0$$

$$I_x = I_z = \varrho_o^2.m_1 = (.542l_1)^2.m_1 \qquad (kg.m^2)$$

where ϱ_o is the radius of gyration of the upper arm. Similarly, let I_a , I_b , I_c and I_u , I_v , I_w be the moments of inertia with respect to body axes abc and uvw with origin at the centers of rotation of elbow and wrist, respectively, then

$$I_b = 0$$

$$I_a = I_c = (.526l_2)^2.m_2 \qquad (kgm^2)$$

$$I_v = 0$$

$$I_u = I_w = (.587l_3)^2.m_3 \qquad (kgm^2)$$

Now consider the moments of inertia about the center of mass. The relationship between the above moments of inertia and that about the center of mass is given by the parallel axis theorem:

$$I_o = I - mx^2$$

where I_o = moments of inertia about the center of mass;

x = distance between center of mass and proximal end of the segment;

m = mass of segment

Therefore,

$$I_{oy} = I_{ob} = I_{ov} = 0$$

$$I_{ox} = I_{oz} = (.542l_1)^2m_1 - m_1c_1^2$$

$$I_{oa} = I_{oc} = (.526l_2)^2m_2 - m_2c_2^2$$

$$I_{ou} = I_{ow} = (.587l_3)^2m_3 - m_3c_3^2$$

where I_{ox} I_{oy} I_{oz} , I_{oa} I_{ob} I_{oc} and I_{ou} I_{ov} I_{ow} are the moments of inertia about the centers of mass of upper arm, forearm and hand, respectively.

CHAPTER 3

PROCESSING OF THE RAW MOTION DATA AND ANALYZING THE VELOCITIES AND ACCELERATIONS

3.1 Linear Filtering and Median Filtering

3.1.1 Introduction

Biomechanical studies of movement kinematics and kinetics often involve the measurement of analog quantities through discrete sampling of the signal at regular intervals. The resulting digital data can, in most cases, adequately represent the original signal, providing the sampling frequency is high enough. The ease of computer processing of digital signal data is a distinct advantage over analog data. However, in either case some signal conditioning is usually required before any quantitative analysis is performed because in any case the measurement and data reduction system introduces noise into the signal. Even if the noise is not noticeable in the spatial trajectory or angular plots, the coordinate information may still be too noisy for direct calculation of velocity and acceleration of markers, joint angles, etc.. This is because the amplitude of differentiated noise increases linearly with frequency [1].

Several methods have been described to process noisy biomechanical data to obtain the first (velocity) and second (acceleration) derivatives of the trajectories of body markers. Both time– and frequency–domain approaches have been widely explored. For example, FIR and IIR filters based on frequency–domain techniques were developed by [2] and

[3] and polynomial and spline approximations based on time–domain techniques were developed by [4] and [5]. When the signal is periodic, as it happens in gait analysis, frequency domain techniques are appropriate. For aperiodic signals the use of these techniques requires a forced periodization. In both cases it is necessary to extend the sequence to be filtered.

All approaches based on frequency–domain techniques can be categorized into linear filtering techniques. The theory of linear systems has become well developed in the digital signal processing literature. Its application in biomechanical data processing has been reported by many investigators [6, 7]. The basic concept of a linear filter is the separation of signals based on their nonoverlapping frequency content. For some applications, however, these linear filters are not completely adequate due to the nature of the data being filtered. This inadequateness or failure of the linear filters have been reported in many papers [8, 9] due to the overlapping frequency nature of useful signal with noise. The linear filters tend to smear out the sharp changes in the data and blur the edges in image application.

To overcome this disadvantage of linear filtering, nonlinear filtering techniques have been developed and have become a new direction in the theory and practice of signal processing during the last ten years since J.W. Tukey published his first work [10] on this topic. The basic concept of nonlinear filter is to consider separating signals based on whether they can be considered smooth or rough (noise–like) [9]. In many signal processing applications a nonlinear filtering method called 'median filtering' has achieved some very interesting results.One useful characteristic of median filtering is its ability to preserve signal edges while filtering out impulses. Applications of median filtering can be often found in image processing and speech processing. Its application in biomechanical data

processing has not been reported. The following are reasons why the median filter was applied in this study:

(1) The simplicity of implementation of a median filter which requires a very simple digital nonlinear operation.

(2) Its ability to preserve the occasional signal edge while smoothing out the noise.

(3) The guaranteed convergence of the smoothing as long as the input sequence is limited.

(4) A hope that nonlinear smoothing will take a deserving place in the conditioning of biomechanical signals as well as other physiological signals.

Beside the pioneer work of J.W. Tukey on this topic, one can refer to the publications of several other researchers, such as Arce and Gallagher [11, 12], where it is possible to find references to almost all the main body of research.

3.1.2 Implementation of the Median Filter, Notes on Delay and Convergence and How to Handle the Endpoints of the Data

Unlike linear filters which involve multiplication and summation computation, the median filter computation requires the sorting of a list of numbers. To begin, we take a sampled signal of length L; across this signal we slide a window that spans 2N+1 points. The filter will only affect the center sample of the window. The filter output is set equal to the median value of these 2N+1 signal samples, and is associated with the time sample at the center of the window. For convenience, a symbol, Median[x(n)], will be used to represent the filtered output data obtained after the original data x(n) goes through the median filter. A median filter has no design parameters other than window size 2N+1, so long as we append N values to each end as will be discussed.

By convergence for median filters, we ask if the original signal can be turned into a signal that is invariant to the filter, i.e., the root signal. It has been studied and shown that if the signals are restricted to have a finite length, convergence of the signals to a root signal is guaranteed [11, 13]. If the condition of finite length is removed, oscillations can occur regardless of the number of filter passes.

In order to implement a median filter, one must take care of the initial and ending points, i.e., the delay introduced by it. The delay of the filters is associated with the window size of the median filter; if the window size is 2n+1, the delay is N points. The attempt to compensate the delay leads to the strategies for handling the endpoints data. Several techniques for generating the set of additional initial and final values (i.e., those outside the interval in which the data are defined) have been reported, including constant, linear and quadratic extrapolation. For the applications in this study, constant extrapolation from the initial or final data point proves to be entirely adequate. Constant extrapolation is explained in Figure 3.1.

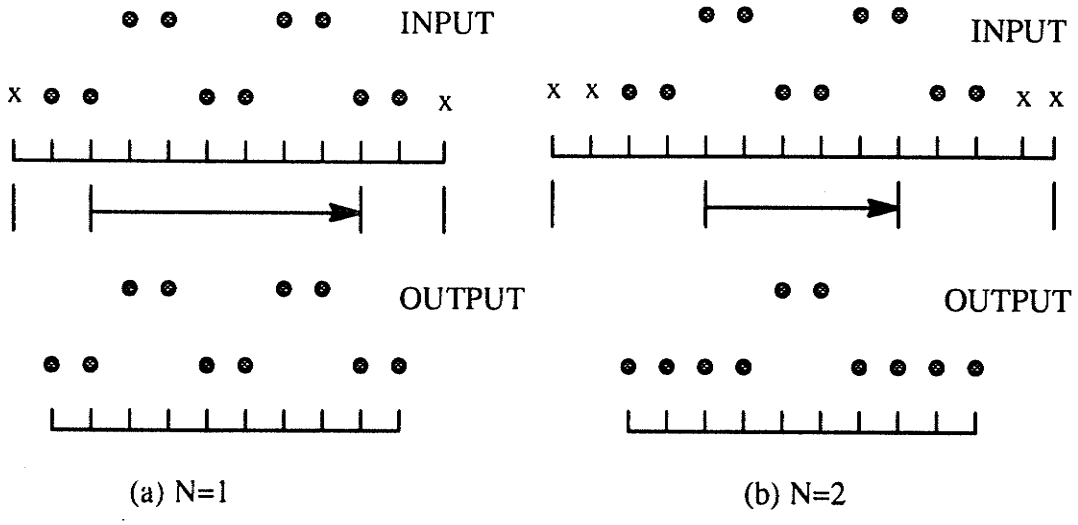

Fig. 3.1 Constant extrapolation when N=1, 2 and 3 (continued)

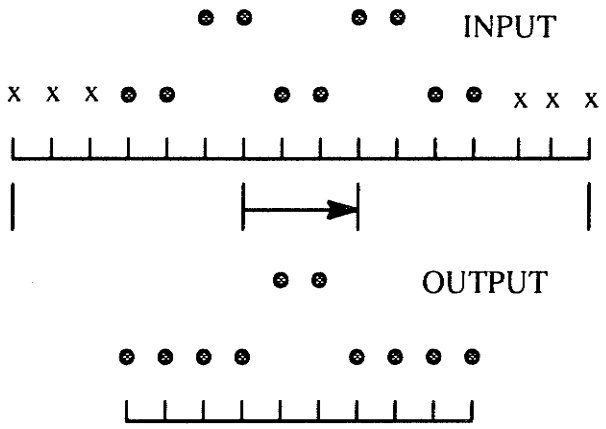

(c) N=3

Fig. 3.1 Constant extrapolation when N=1, 2 and 3

To account for start up and end effects at the two endpoints of the L length signal, N samples each are appended to the beginning and end of the sequence. The value of the appended samples at the beginning is equal to the value of the first sample; similarly, the value of the appended samples at the end of the signal equals the value of the last sample of the signal. Figure 3.1 (a) shows a binary signal of length 10 being filtered by a median filter of window size 3 (N=1). The filtered signal is shown below each input signal in Figure 3.1. The appended bits are shown as crosses (x). Figure 3.1 (b) shows similar results with a larger window (N=2); N=3 in Figure 3.1 (c).

3.2 An Algorithm That Combines a Median Filter and a Linear Filter

3.2.1 Development of the Filtering Algorithm

In order to chose a filtering algorithm, a comparison between several alternative filtering algorithms for an arbitrarily chosen set of motion data was made. Three algorithms were compared. They are:

(1) A linear filter, which produced the output y(n) as the following (x(n–2), x(n–1), x(n), x(n+1), and x(n+2) are the input sequence):

$$y(n) = 1/8x(n-2) + 1/8x(n-1) + 1/2x(n) + 1/8x(n+1) + 1/8x(n+2) \qquad 3.1$$

(2) A 5–point median filter;

(3) A combination of median filter (5–point) and linear filter (3–point Hanning window with coefficients 1/4, 1/2, 1/4).

Figure 3.2 (a) shows the input sequence, and Figure 3.2 (b)–(d) show the outputs of the linear filter, a median filter of 5–point, and a combination of a median filter (5–point) and a linear filter (3–point Hanning window with coefficients 1/4, 1/2, 1/4), respectively.

The smearing effects of the linear filter at each input discontinuity are clearly seen in the Figure 3.2 (b). Although the median filter alone preserves most of the input discontinuities it seems inadequate with a 'rough' output. Finally the combination filter is seen to be a good compromise between the linear filter and median filter. As seen in Fig. 3.2 (d), the noise is smoothed out a great deal, and the discontinuities in the input are fairly well preserved.

In summary, a filtering algorithm consisting of a combination of running median filter and linear filter appears to be a reasonable candidate for smoothing noise sequences with discontinuities.

Figure 3.3 shows a block diagram of the simple filtering algorithm.

For convenience, the smooth part of the signal was denoted as 'smooth', and the rough part of the signal was denoted as 'rough'. A more intelligent strategy than the above simple smoothing algorithm, called 'reroughing' by Tukey, was also utilized in this investi-

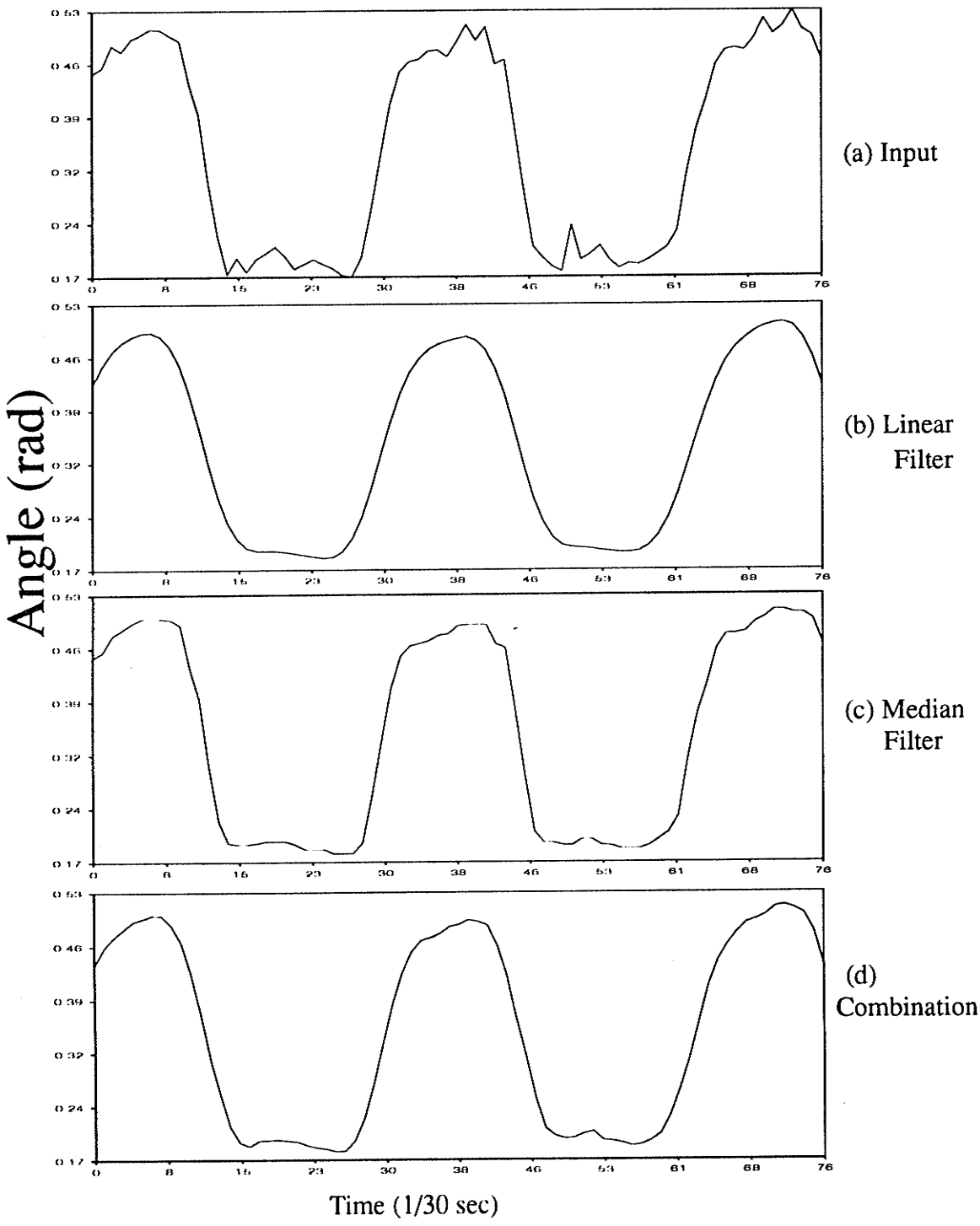

Fig. 3.2 Examples of three smoothed outputs for an arbitrary trajectory data

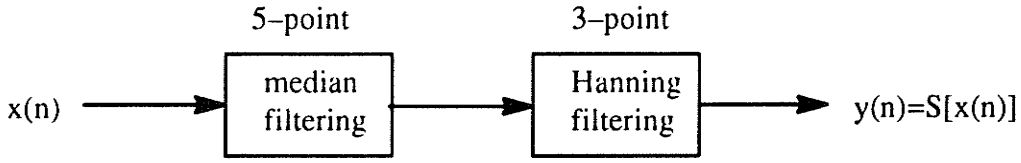

Fig. 3.3 Block diagram of a simple filtering algorithm

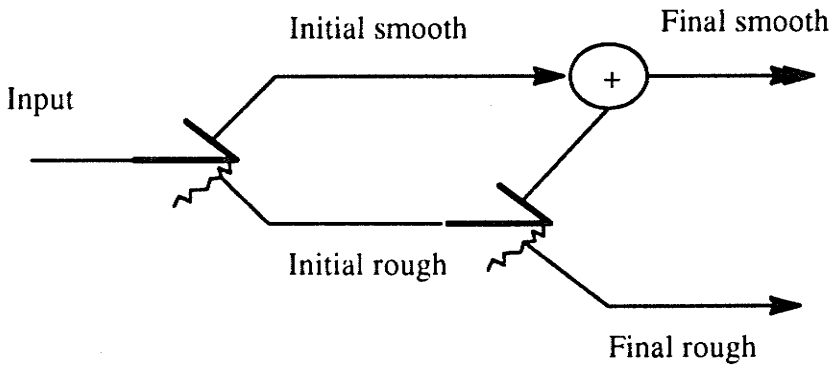

(a) The scheme and algebra of reroughing

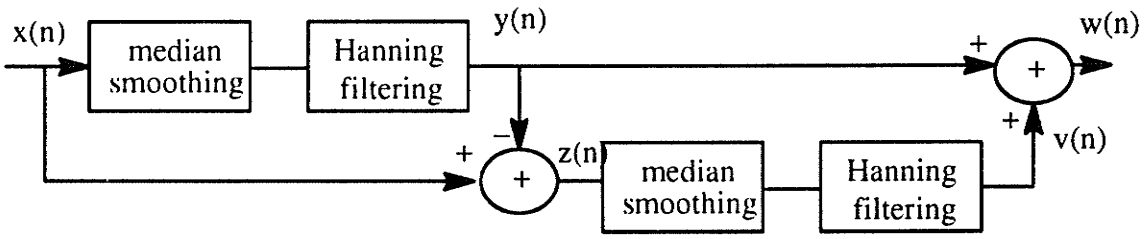

Fig. 3.4 (b) block diagram of 'double–smoothing' algorithm

gation. The basic idea of reroughing is to smooth the rough, and add it back to the smooth we started with. Then we get a final smooth whose rough is precisely the rough of the rough of the original sequence. This process of reroughing extracts the smooth from the

rough of original sequence and leaves the final rough the 'real' rough. The scheme shown in Figure 3.4 (a) is expressed in a verbal algebra first.

Since

$$\text{input} \equiv \text{smooth PLUS rough}, \tag{3.2}$$

and

$$\text{rough} \equiv (\text{smooth of rough}) \text{ PLUS } (\text{rough of rough}), \tag{3.3}$$

we must have, first substituting and then redefining:

$$\text{input} = \text{smooth PLUS} \begin{pmatrix} \textit{smooth} \\ \textit{of rough} \end{pmatrix} \text{ PLUS } \begin{pmatrix} \textit{rough} \\ \textit{of rough} \end{pmatrix}, \tag{3.4}$$

or

$$\text{input} = \text{final smooth PLUS final rough}, \tag{3.5}$$

where

$$\text{final smooth} \equiv \text{smooth PLUS} \begin{pmatrix} \textit{smooth} \\ \textit{of rough} \end{pmatrix} \tag{3.6}$$

and

$$\text{final rough} \equiv \text{rough of rough} \tag{3.7}$$

Now, it is easy to see the following relations in the Figure 3.4 (b).

$$z(n) = \text{initial rough} = x(n) - y(n) \tag{3.8}$$

$$w(n) = \text{final smooth} = \text{smooth PLUS} \begin{pmatrix} \textit{smooth} \\ \textit{of rough} \end{pmatrix}$$

$$= S[x(n)] + S[R[x(n)]] \tag{3.9}$$

The use of this 'double smoothing' or 'reroughing' proved to be very effective.

As we mentioned before, the delays introduced by filtering procedure must be taken care of before the algorithm is implemented. A median filter of 5–point has a delay of 2 samples, and a 3–point Hanning window has a delay of 1 sample. Thus, the total delay of the filtering is 3 samples. The constant extrapolation explained in Section 3.1.2

was applied for both median filter and Hanning window.

3.2.2 Application of the Algorithm to the Upper Limb Motion Data

3.2.2.1 Available Motion Data of Human Upper Limb

The motion data collected by Cooper et al. [14] was used in this study.

Three important activities of daily living were studied in their investigation. These were three feeding tasks: drinking with a cup, eating with a fork and eating with a spoon. A total of 21 human subjects (10 male and 11 female) were used. All were healthy, right–handed and ranging in age from 20–29 years. Total body weight and height were measured as the basis for the calculation of anthropometric parameters.

Twenty–four sets of motion data for 8 female subjects performing the three functional upper limb movements were used in this study

3.2.2.2 Filtered results of the motion data

Although there have been no reports on the application of the combination algorithm of linear and nonlinear filter to the biomechanical motion data, it can be seen that this first attempt has given satisfactory and interesting results. Figure 3.5 shows a set of input signals from Subject 1 when performing the task of drinking with a cup and the resulting outputs from the combinational algorithm.

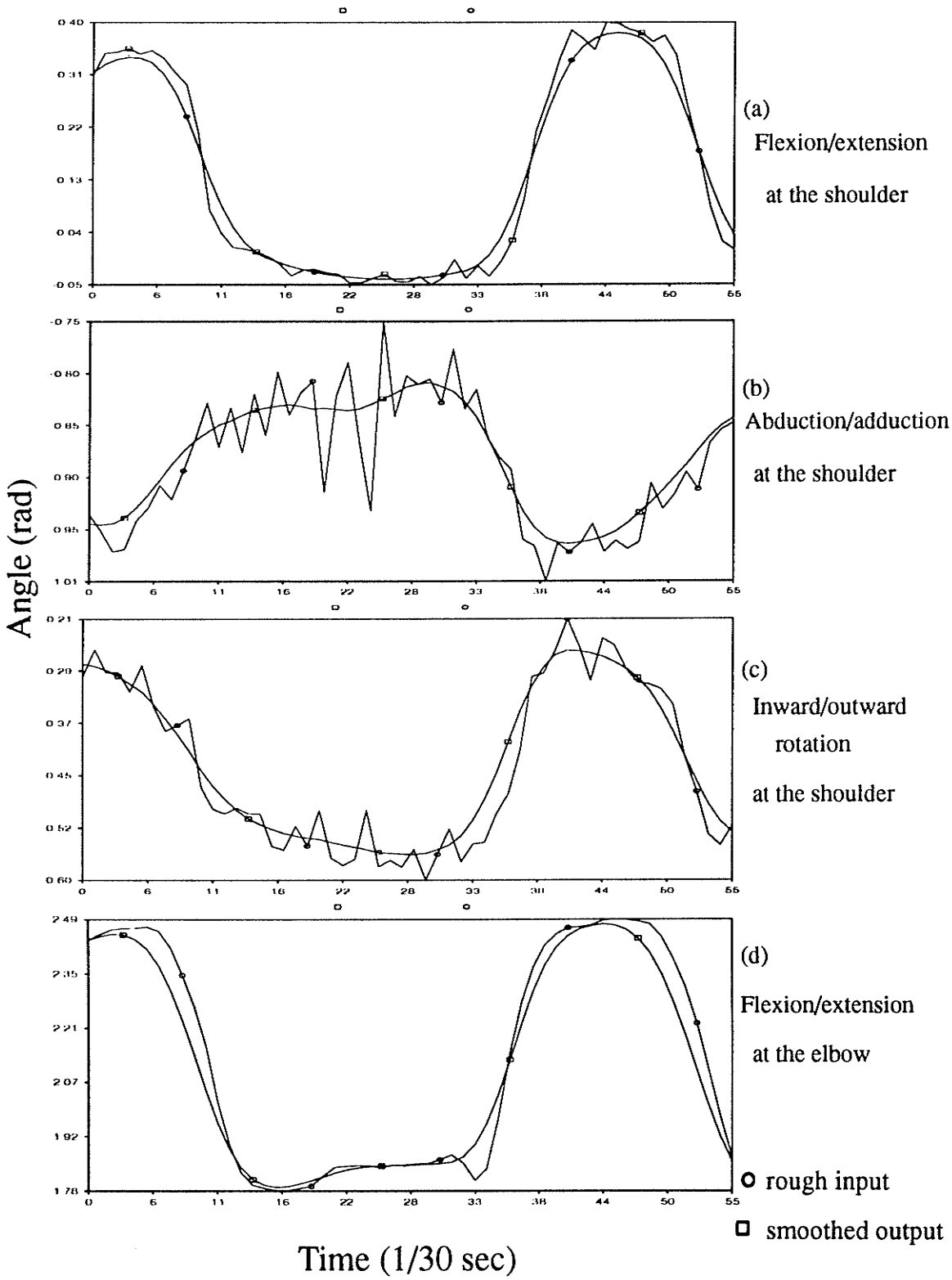

Fig. 3.5 Examples of smoothed trajectory data of the upper limb (Subject 1) (continued)

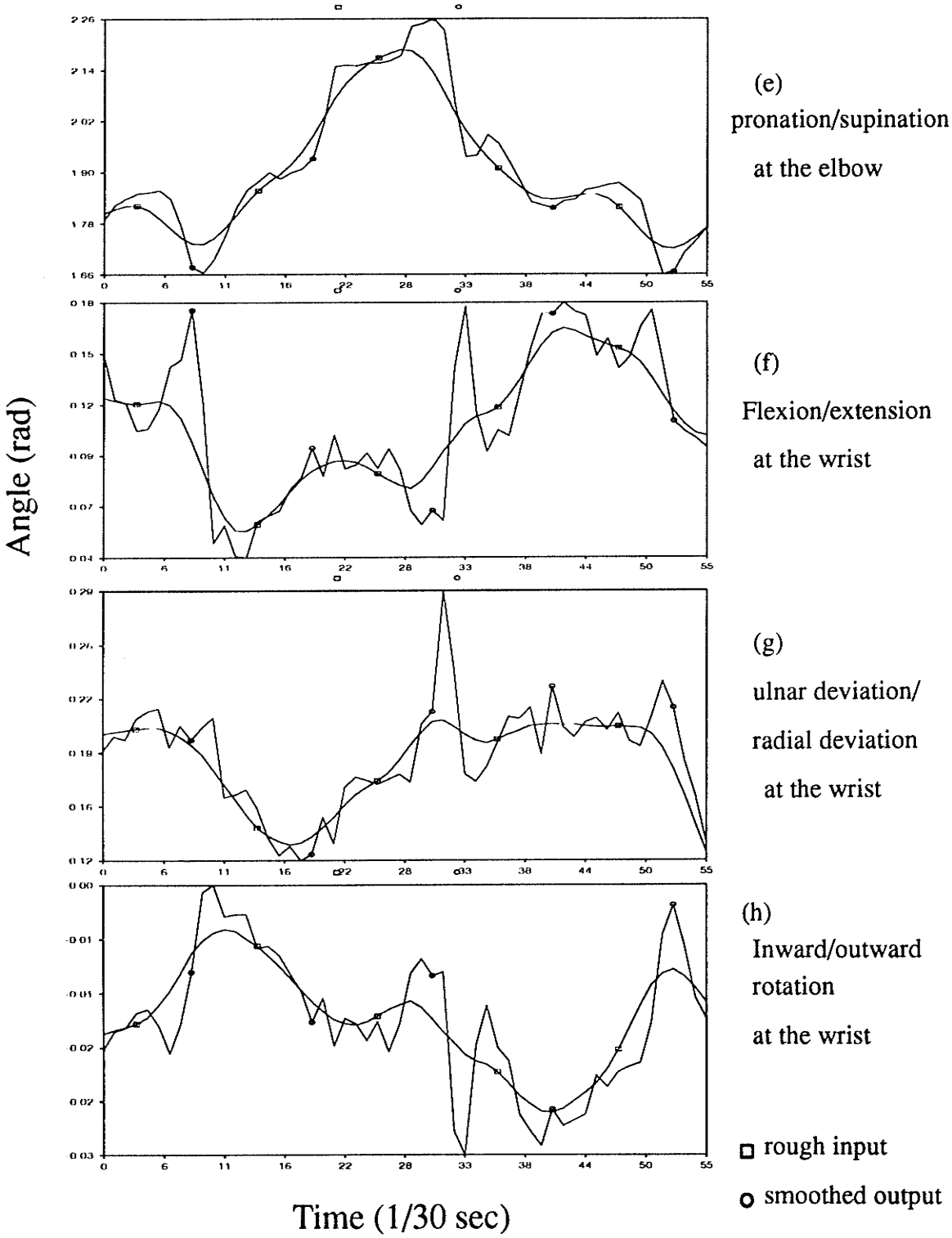

Fig. 3.5 Examples of smoothed trajectory data of the upper limb (Subject 1)

3.3 Calculations of the Velocities and the Accelerations

3.3.1 Methods for Calculating the Velocities and Accelerations

Now all the displacement data of the upper limb have been properly smoothed. To calculate the velocities and accelerations from displacement data, all that is needed is to take the finite differences, i.e., to calculate $\Delta x/\Delta t$.

But the velocity calculated this way does not represent the velocity at either of the sample times. Rather, it represents the velocity of a point in time half way between the samples. This can result in errors later on when we try to relate the velocity–derived information to displacement data, and both results do not occur at the same point in time. A way around this problem is to calculate the velocity and acceleration on the basis of $2\Delta t$ rather than Δt. The the velocity at the ith sample is

$$V_{x_i} = \frac{x_{i+1} - x_{i-1}}{2\Delta t} \qquad 3.10$$

Similarly, the acceleration is

$$A_{x_i} = \frac{V_{x_{i+1}} - V_{x_{i-1}}}{2\Delta t} \qquad 3.11$$

Note the Equation 3.11 requires displacement data from samples i+2 and i–2; thus a total of five successive data points go into the acceleration. An alternative and slightly better calculation of acceleration uses only three successive data points and utilizes calculated velocities halfway between sample times,

$$V_{x_{i+1/2}} = \frac{x_{i+1} - x_i}{\Delta t} \qquad 3.12$$

$$V_{x_{i-1/2}} = \frac{x_i - x_{i-1}}{\Delta t} \qquad 3.13$$

Therefore,

$$A_{x_i} = \frac{x_{i+1} - 2x_i - x_{i-1}}{\Delta t^2} \qquad 3.14$$

3.3.2 Results and Discussions

Figure 3.6 (a)–(h) shows a set of smoothed displacement data from Subject 1 when performing the task of drinking with a cup and their first and second derivatives. Since no studies have been reported on the research, references and comparison are not available. It should be realized that angular velocities instead of the derivatives of the Euler angles are needed in Lagrangian equations and therefore are the most significant variables. Analysis of angular velocities can be found in Chapter 4.

From Figure 3.6, it is seen that both the first and second derivatives are very small. The first derivative, i.e. the speed of the arm, needs some explanation. To understand and analyze the speeds of the arm for the drinking and eating tasks, the mean speeds are tabulated in Table 3.1. In Table 3.1 (a), eight first derivatives of the eight Euler angles of each segment and their mean values for the drinking task are given. It is interesting to see that forearm flexion/extension is the fastest motion for the drinking task, followed by upper arm flexion/extension and forearm pronation/supination. The movements of inward/outward rotation at the shoulder and the wrist are so slow that they can be neglected. This conclusion is also valid for the two eating tasks. But it is important to notice that the motion of pronation/supination , not the flexion/extension, of the forearm is the fastest for the two eating tasks.

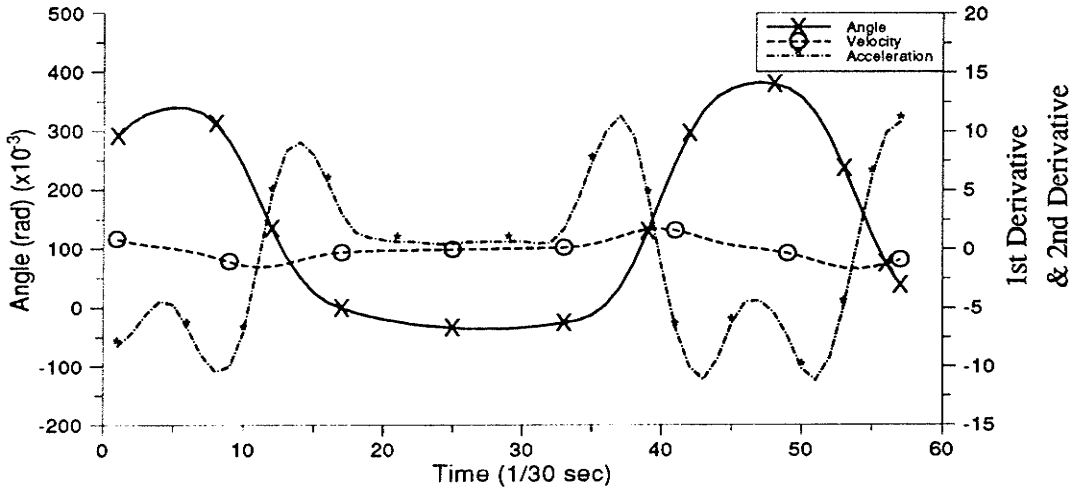

(a) Flexion/extension at the shoulder

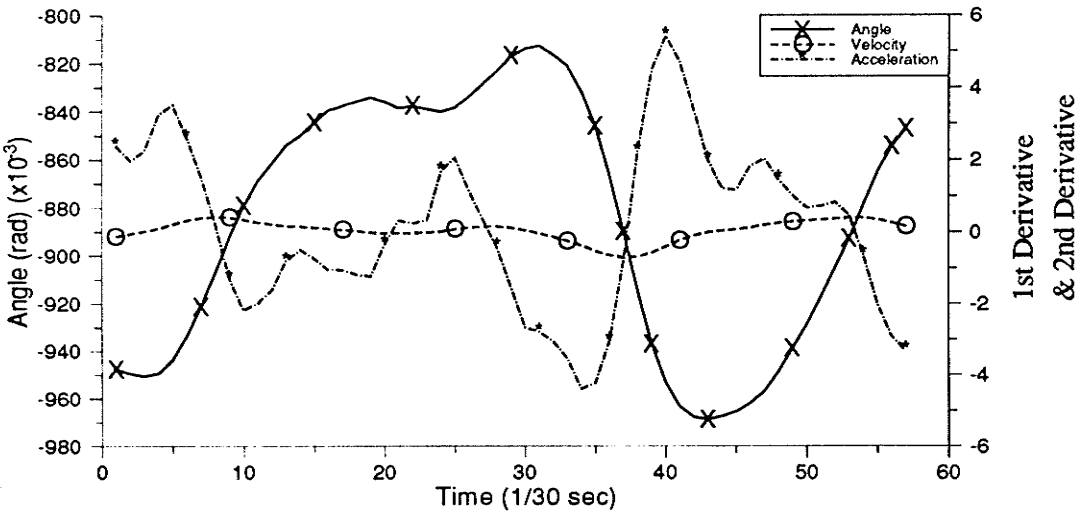

(b) Abduction/adduction at the shoulder

Fig. 3.6 Eight 1st & 2nd derivatives of eight Euler angles form subject 1 when performing the task of drinking with a cup (continued)

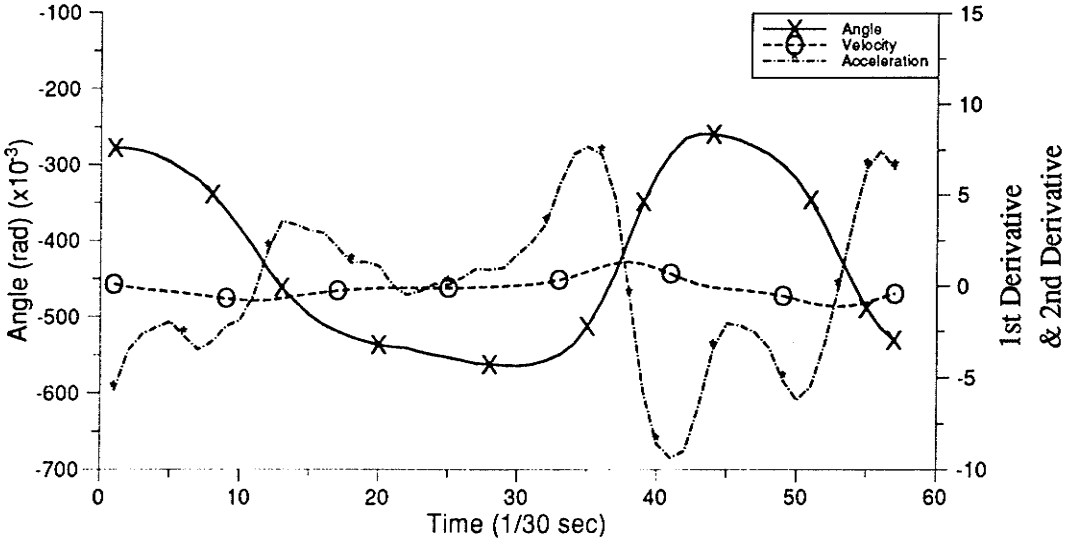

(c) Inward/outward rotation at the shoulder

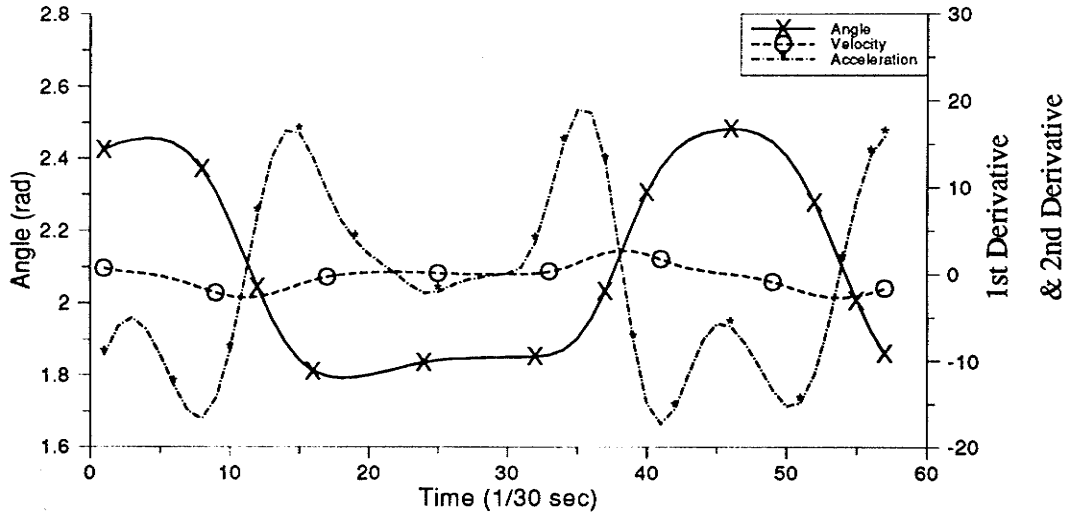

(d) Flexion/extension at the elbow

Fig. 3.6 Eight 1st & 2nd derivatives of eight Euler angles form subject 1 when performing the task of drinking with a cup (continued)

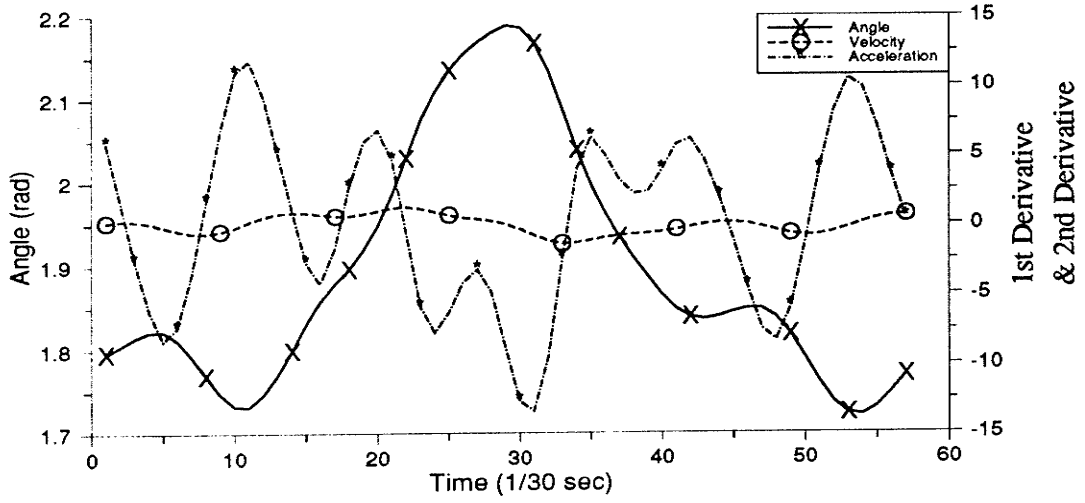

(e) Pronation/supination at the elbow

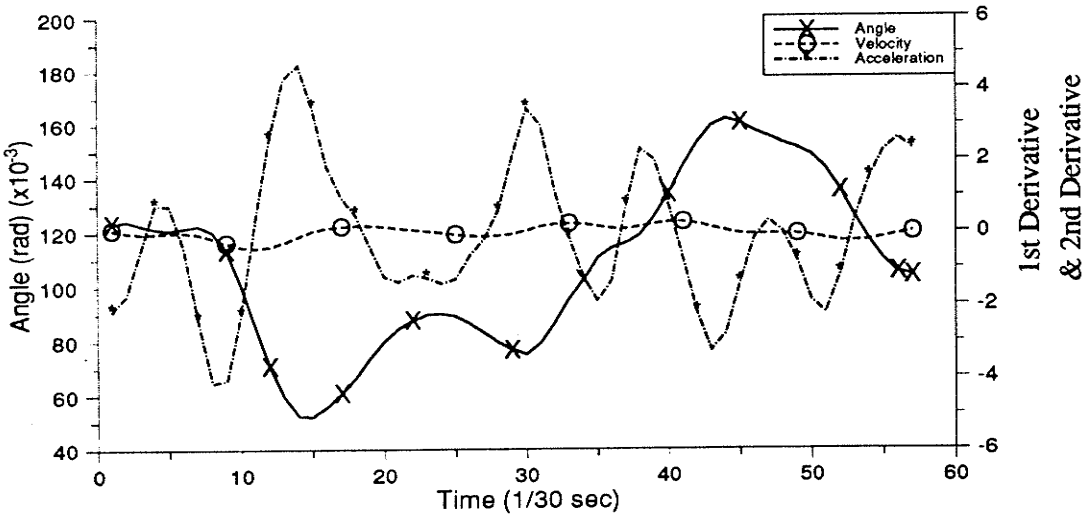

(f) Flexion/extension at the wrist

Fig. 3.6 Eight 1st & 2nd derivatives of eight Euler angles form subject 1 when performing the task of drinking with a cup (continued)

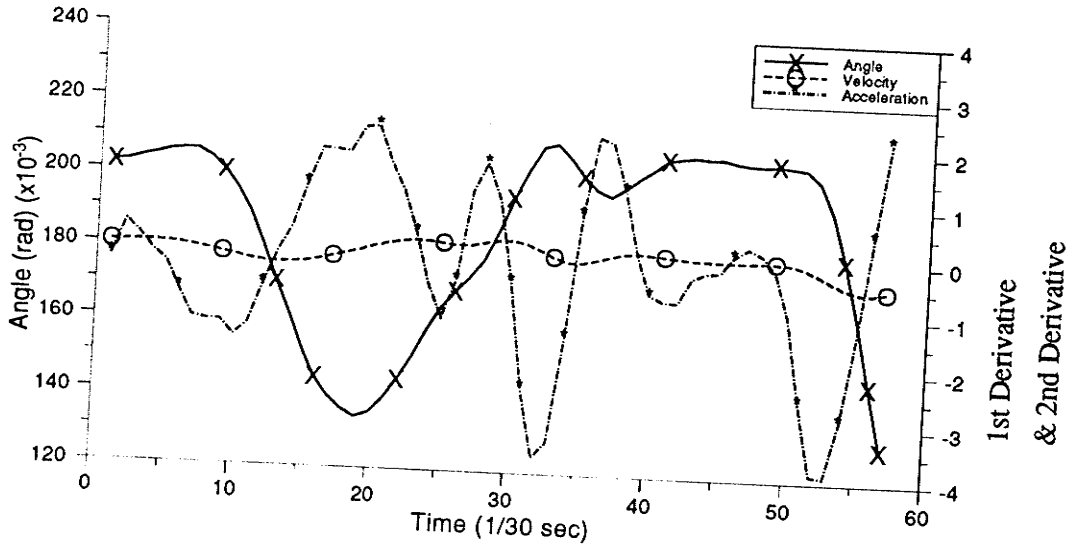

(g) Ulnar deviation/radial deviation at the wrist

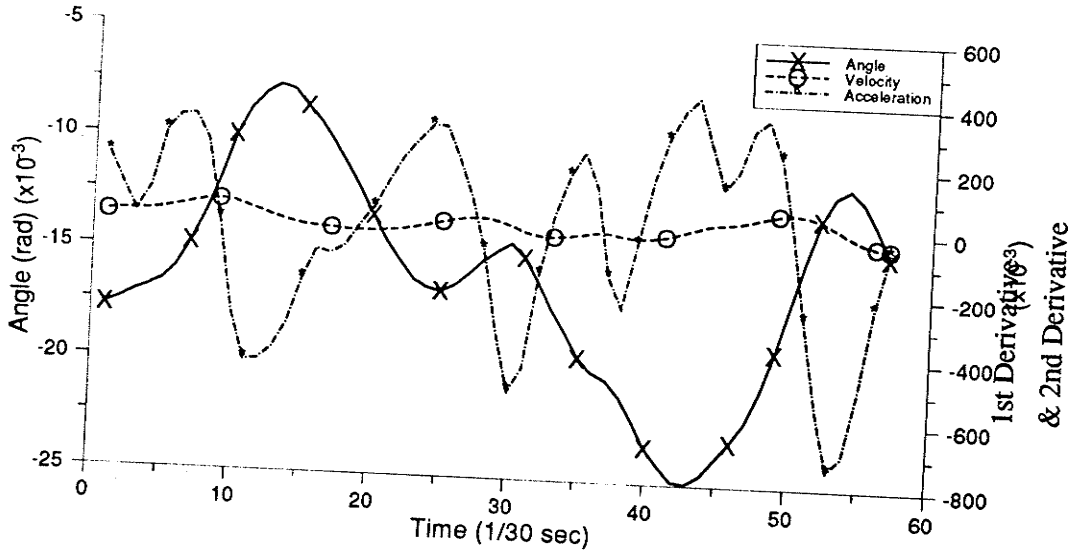

(h) Inward/outward rotation at the wrist

Fig. 3.6 Eight 1st & 2nd derivatives of eight Euler angles form subject I when performing the task of drinking with a cup

TABLE 3.1 MEAN VALUES OF FIRST DERIVATIVES OF THE EIGHT EULER ANGLES FOR THE THREE TASKS

Subject	$\dot{\phi}_1$	$\dot{\theta}_1$	$\dot{\psi}_1$	$\dot{\phi}_2$	$\dot{\psi}_2$	$\dot{\phi}_3$	$\dot{\theta}_3$	$\dot{\psi}_3$
1	0.636	0.224	0.457	1.067	0.567	0.138	0.134	0.025
2	0.538	0.141	0.445	1.869	0.640	0.171	0.409	0.014
3	0.346	0.205	0.442	1.814	0.553	0.301	0.359	0.012
4	0.245	0.146	0.176	1.346	0.414	0.199	0.259	0.044
5	0.353	0.163	0.180	2.224	0.656	1.024	0.580	0.785
6	1.316	0.229	0.711	1.106	0.664	0.348	0.098	0.041
7	0.676	0.245	0.274	1.350	0.383	0.308	0.222	0.007
8	0.884	0.194	0.625	2.110	0.963	0.516	0.421	0.148
Mean	0.624	0.193	0.414	1.611	0.603	0.376	0.310	0.135

(a) Drinking with a cup

TABLE 3.1 MEAN VALUES OF FIRST DERIVATIVES OF THE EIGHT EULER ANGLES FOR THE THREE TASKS

Subject	$\dot{\phi}_1$	$\dot{\theta}_1$	$\dot{\psi}_1$	$\dot{\phi}_2$	$\dot{\psi}_2$	$\dot{\phi}_3$	$\dot{\theta}_3$	$\dot{\psi}_3$
1	0.863	0.186	0.868	0.692	1.689	0.335	0.348	0.043
2	0.527	0.242	0.286	0.401	2.559	0.352	0.459	0.045
3	0.262	0.213	0.214	0.508	2.113	0.464	0.191	0.060
4	0.253	0.148	0.372	0.359	1.375	0.403	0.257	0.032
5	0.403	0.099	0.391	0.415	2.804	0.374	0.413	0.073
6	0.942	0.124	0.495	0.473	2.519	0.814	0.579	0.139
7	0.440	0.333	0.382	0.957	2.975	0.506	0.197	0.095
8	0.538	0.123	0.364	0.946	2.815	0.272	0.293	0.102
Mean	0.529	0.184	0.422	0.594	2.356	0.440	0.342	0.074

(b) Eaing with a fork

TABLE 3.1 MEAN VALUES OF FIRST DERIVATIVES OF THE EIGHT EULER ANGLES FOR THE THREE TASKS

Subject	$\dot{\phi}_1$	$\dot{\theta}_1$	$\dot{\psi}_1$	$\dot{\phi}_2$	$\dot{\psi}_2$	$\dot{\phi}_3$	$\dot{\theta}_3$	$\dot{\psi}_3$
1								
2	1.313	0.546	0.521	0.867	2.382	0.329	0.465	0.022
3	0.521	0.125	0.334	0.950	1.222	0.533	0.630	0.024
4	0.308	0.179	0.316	0.598	0.963	0.147	0.432	0.016
5								
6	1.622	0.135	0.771	0.645	1.436	0.568	0.282	0.063
7								
8	1.372	0.144	0.401	1.029	1.891	0.338	0.515	0.092
Mean	1.027	0.226	0.469	0.818	1.579	0.383	0.465	0.043

Note: the data for subjects 1, 5 and 7 is not available due to missing and corrupted data

(c) Eaing with a spoon

Unit: rad/sec.

$\dot{\phi}_1$: 1st deriv. of the flexion/extension angle at the shoulder

$\dot{\theta}_1$: 1st deriv. of the adduction/abduction angle at the shoulder

$\dot{\psi}_1$: 1st deriv. of the inward/outward rotation angle at the shoulder

$\dot{\phi}_2$: 1st deriv. of the flexion/extension angle at the elbow

$\dot{\psi}_2$: 1st deriv. of the pronation/supination angle at the elbow

$\dot{\phi}_3$: 1st deriv. of the flexion/extension angle at the wrist

$\dot{\theta}_3$: 1st deriv. of the ulnar/radial deviation angle at the wrist

$\dot{\psi}_3$: 1st deriv. of the inward/outward rotation angle at the wrist

CHAPTER 4

MOMENT PATTERNS, ENERGY VARIATION AND WORK/POWER PATTERNS DURING THE FUNCTIONAL MOVEMENT OF THE UPPER LIMB

In Chapter 2 and 3 we have dealt with the upper limb movement itself, without regard to the causes of the movement. In this chapter, analyses of the moments and the resultant energetics, which causes the movement, are presented.

The motion data used in this chapter is the same as described in the Section 3.2.2.1.

4.1 Muscle Moment Patterns Investigation

Knowledge of force patterns (in linear motion) and moment patterns (in angular motion) is necessary for an understanding of any movement.

In Chapter 2 we have illustrated how the moments are related to Lagrangian equations and how they can be solved from the equations. In this section plots of moments versus time are shown and their patterns are investigated.

The moments obtained from the Lagrangian equations of motion are called different names by different researchers. They are named 'generalized muscle moments' in [1] and [2], or 'joint torques' in [3] and [4], or 'moments of force' in [5], [6] and [7], or just 'muscle moments' in [8] and [9]. For convenience the term 'muscle moment' is used

in this study. This term is also consistent with the definition of 'muscle power' (to be discussed in Section 4.3).

Almost all existing investigations on the muscle moment are limited to planar motion because it is assumed that the segment motion is planar. Only a few investigators have reported methods to compute three–dimensional moments [10, 11]. In this study three–dimensional moments at each joint are first solved from the Lagrangian equations of motion and then are analyzed in terms of which group of muscles are active in the particular movement.

It should be noted that the muscle moments are always expressed as components in the direction of the principle axes of the limb segment [6, 11]. Therefore, nine muscle moments (M_x , M_y , M_z at the shoulder, M_a , M_b at the elbow, and M_u , M_v , M_w at the wrist) are obtained from the Lagrangian equations.

To investigate the moment patterns at each joint during the time course of the three movements (drinking with a cup, eating with a fork and a spoon), the moments from each subject were carefully compared. Similar moment patterns among the eight female subjects are found. In this section a detailed analysis of the moment patterns of Subject 5 is presented. The moments of Subject 5 when performing the three tasks of drinking with a cup, eating with a fork and eating with a spoon are plotted vs. time in Figure 4.1, 4.2 and 4.3, respectively. In order to understand and analyze the moments there are two important points that have to be made here:

(1) According to the convention used for interpreting the signs of the moments, the following can be concluded:

<u>At the shoulder</u>

negative ← M_x → positive

extensor moment flexor moment

negative ← M_y → positive

outward rotator moment inward rotator moment

negative ← M_z → positive

abductor moment adductor moment

At the elbow

negative ← M_a → positive

extensor moment flexor moment

negative ← M_b → positive

supinator moment pronator moment

At the wrist

negative ← M_u → positive

extensor moment flexor moment

negative ← M_v → positive

outward rotator moment inward rotator moment

negative ← M_w → positive

ulnar flexor moment radial flexor moment

(2) The time course of each given movement, beginning from the standard position and ending at the standard position was divided into five phases:

(a) *Downward phase* — moving downward from the standard position to where the tool (cup, or fork, or spoon) was.

(c) *Upward phase* — moving upward from where the tool was to the mouth.

(d) *Drinking/Eating phase* — the time course during which the drinking/eating action was finished.

(e) *Reversal phase* — moving downward from the mouth to where the tool was returned.

(f) *Returning phase* — returning to the standard position.

It is most likely that each phase for the different tasks did not happen at the same time. To reduce the 'clutter' in the Figure 4.1 only the five phases for the drinking task are indicated.

First, the moment patterns at the shoulder of Subject 5 are investigated. From Figure 4.1 (a), (b) and (c) it can be concluded:

(1) M_x, the flexion/extension moment at the shoulder, shows one pattern for all three tasks. The extensor generates a moment which acts to control the amount of shoulder extension during the downward phase and extends the upper arm during the upward phase. During the last two phases, the extensor controls the degree of extension at the shoulder in an oscillatory way. The extensor moments for the two eating tasks show very similar trends and less oscillation if compared to the extensor moment for the drinking task.

(2) M_y, the inward/outward rotator moment at the shoulder, shows that for all three tasks and most of the time the inward rotator at the shoulder is an active muscle group. This inward rotator moment shows very similar trend to that of the extensor moment at the shoulder.

(3) M_z, the abductor/adductor moment at the shoulder, shows one pattern for all three tasks. The abductor generates a moment which abducts the upper arm during the downward phase and reduces the degree of the abduction during the upward phase.

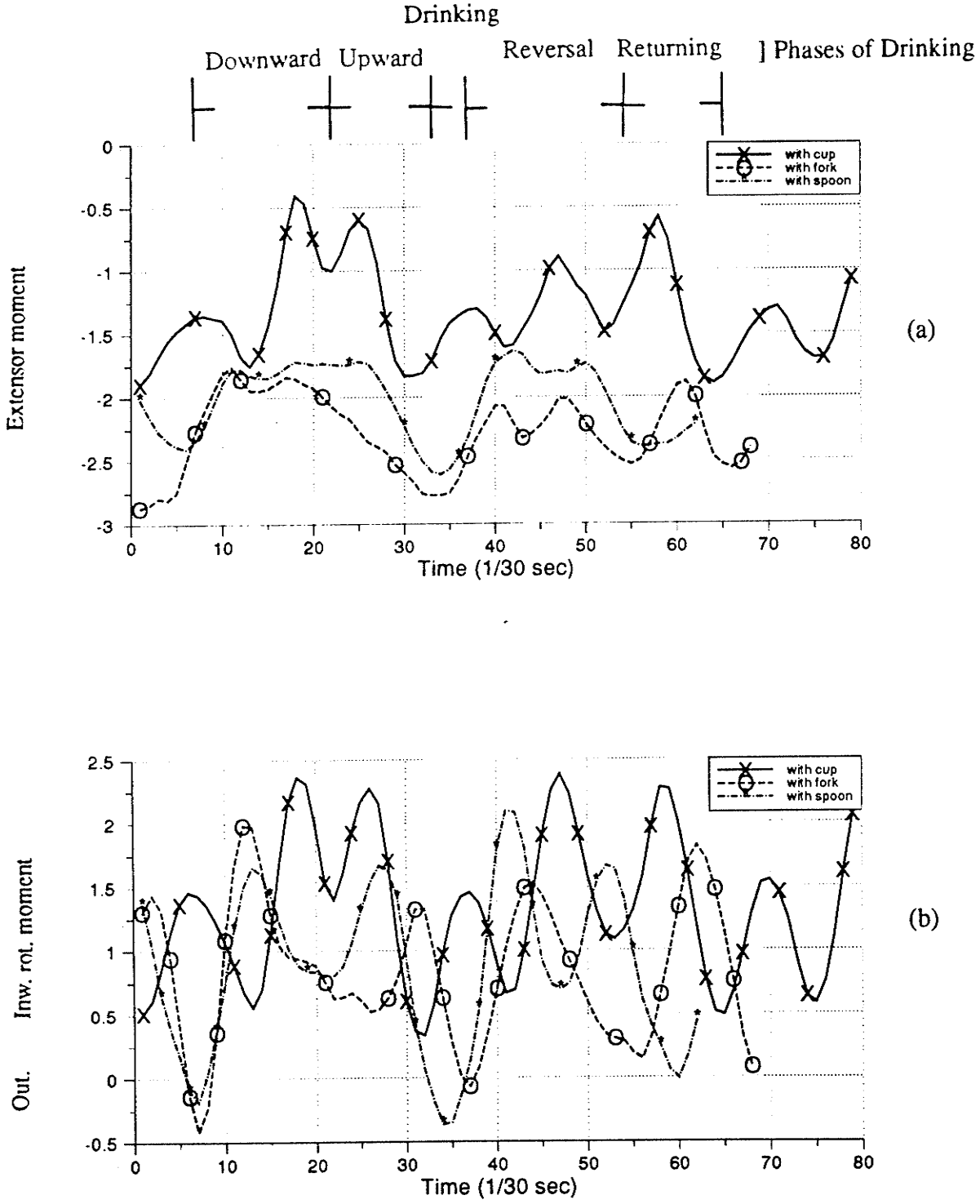

Fig. 4.1 Plots of the moments at the shoulder for the three tasks (continued)

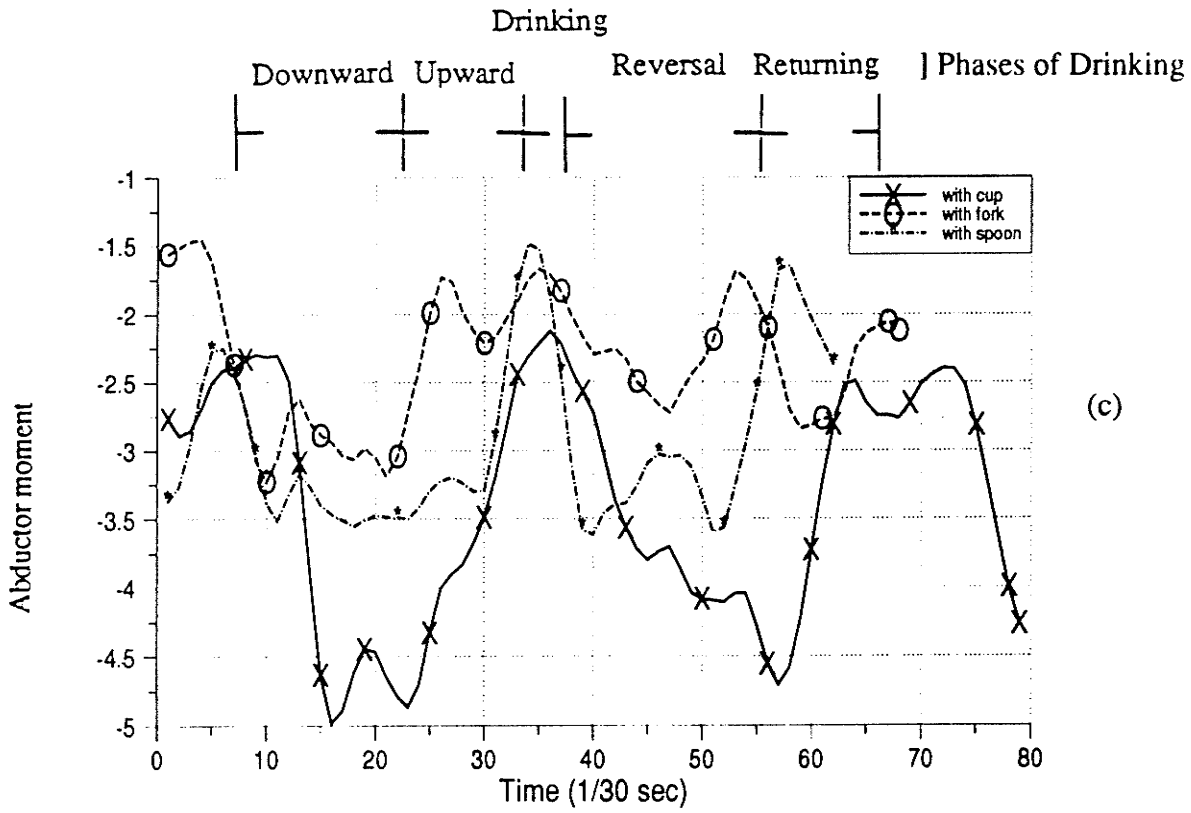

Fig. 4.1 Plots of the moments at the shoulder for the three tasks

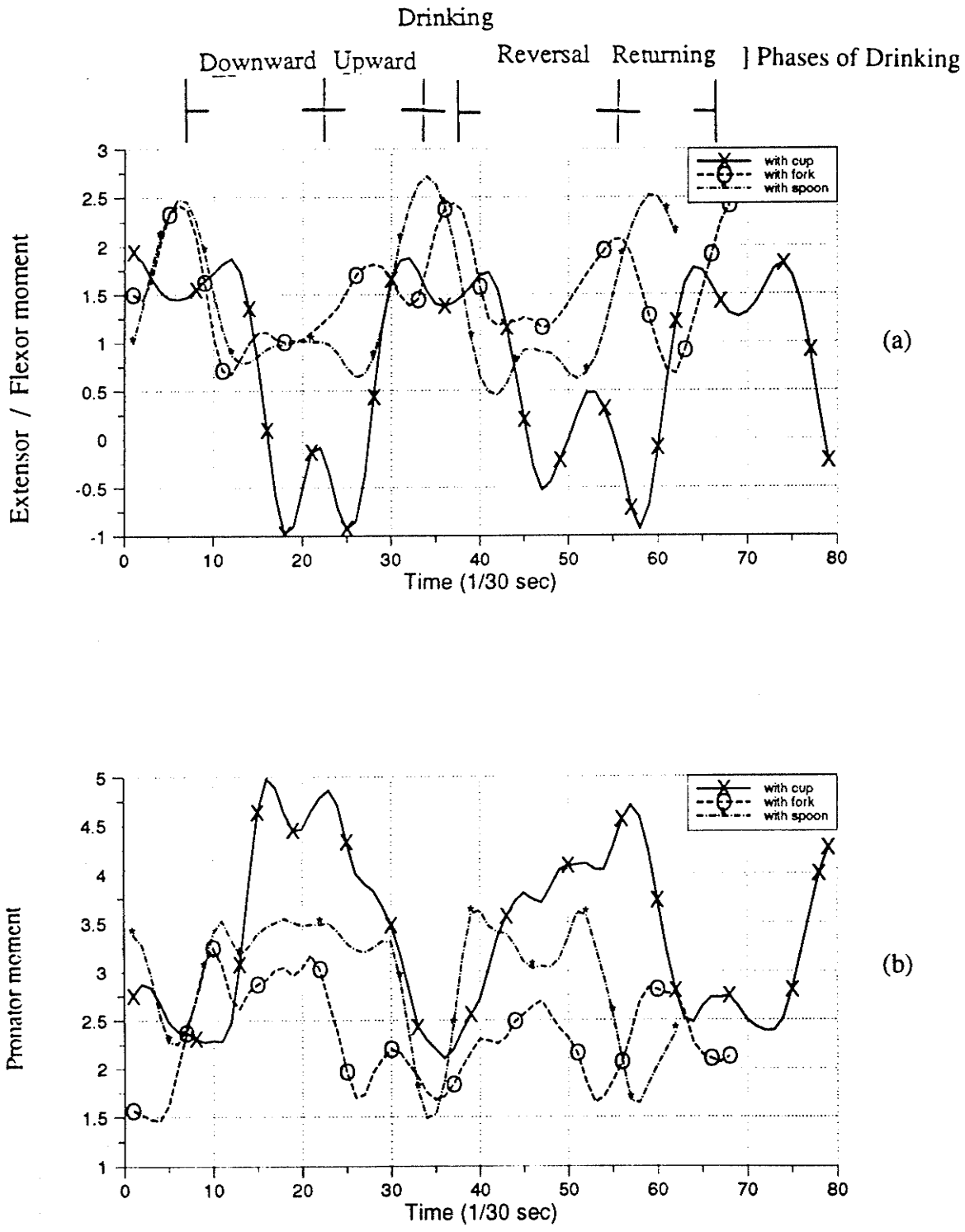

Fig. 4.2 Plots of the moments at the elbow for the three tasks

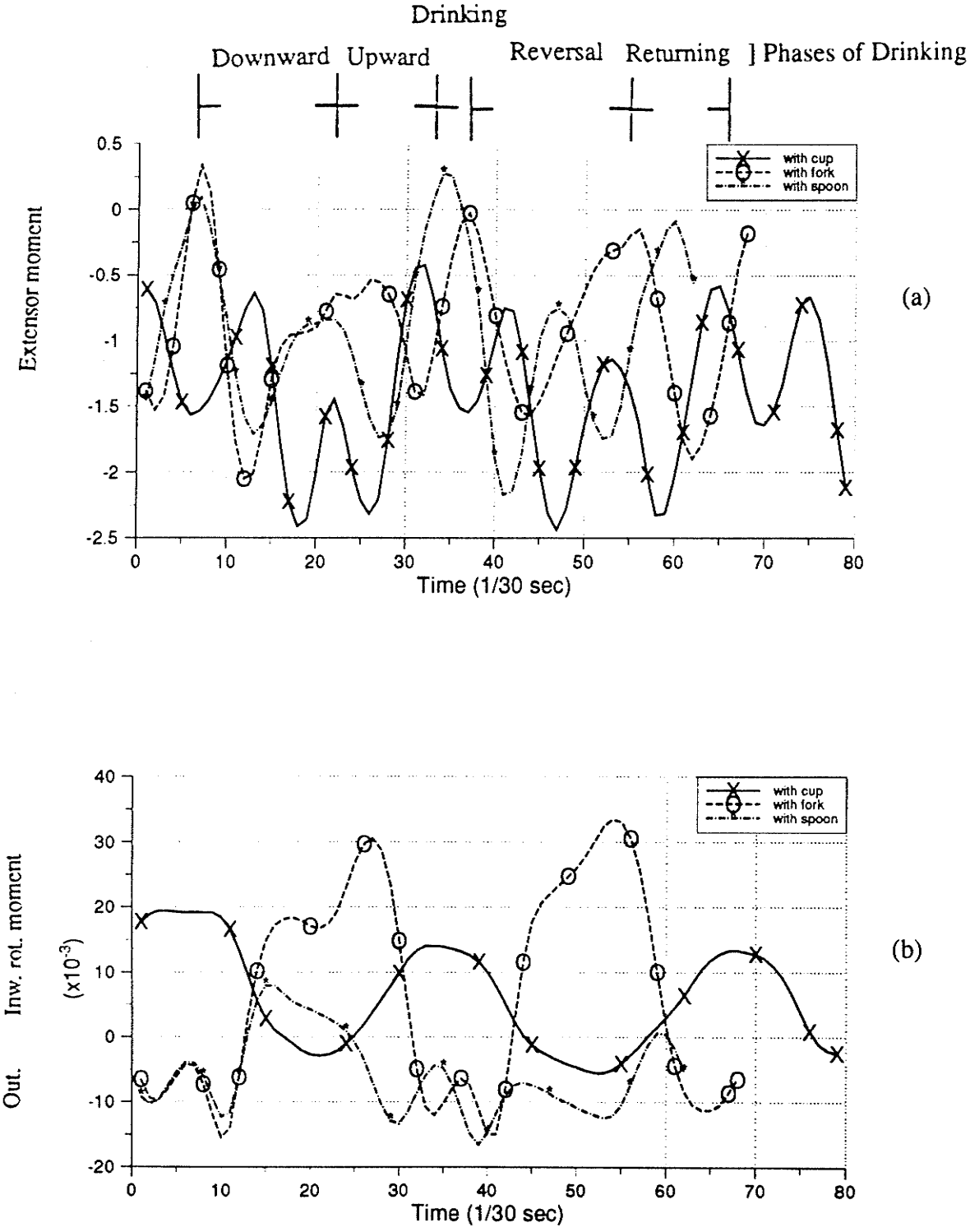

Fig. 4.3 Plots of the moments at the wrist vs. time for the three tasks (continued)

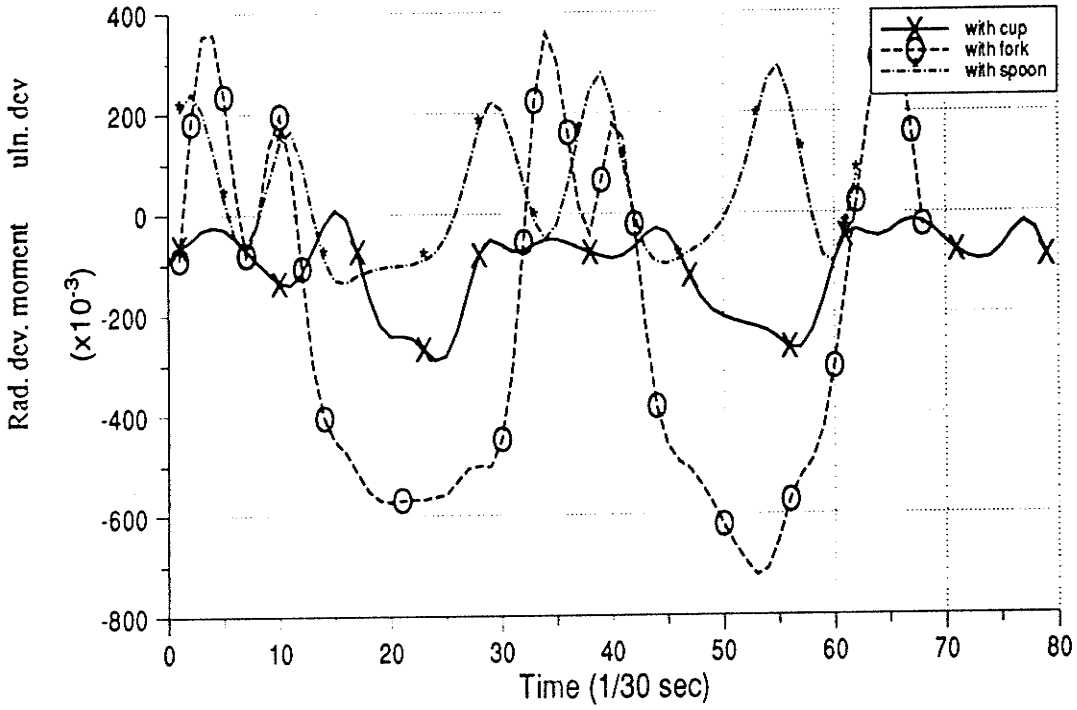

(c)

Fig. 4.3 Plots of the moments at the wrist vs. time for the three tasks

(4) All the three moments show, for each task, very smooth trends during the drinking/eating phase but a very oscillatory trend for the period of fetching and/or returning the tool.

The second important aspect is the differences of the moments for the drinking task as compared to the other two tasks. The magnitude of the flexor moment (M_x) for the drinking task is smaller than the other two flexor moments (Figure 4.1 (a)). An outward rotator moment is not needed for the drinking task, while a small outward rotator moment is present for the other two eating tasks (Figure 4.1 (b)). Finally the magnitude of the abductor moment for the drinking task is larger than for the other two eating tasks.

The difference of the magnitude of the flexor moment between the drinking task and two eating tasks might be explained by the caution the subject took to prevent spilling when drinking. The second difference is due to the different shapes of the tools which require different muscles groups of the upper arm. It is reasonable that a slight outward rotation is needed to send the food into the mouth when one is eating with a fork or spoon. The third difference is due to the fact that the load is heavier when one is drinking with a cup. Therefore the abductor exerts a larger force at the shoulder in comparison with eating with a fork or spoon.

Starting from the flexor/extensor moment in Figure 4.2 (a), it is seen that both the extensor and flexor are active for the drinking task while only the extensor is active for the two eating tasks. Two possible factors cause this difference. First, this subject used a large forward movement of the trunk and head when performing the two eating tasks. This shows an important aspect of arm movement: it is possible to compensate for a large amount of elbow flexion with forward trunk and head movement. This factor was also discussed in [12]. The second factor is the cup position with respect to the subject's body, which requires a larger range of forearm flexion. This factor is consistent with the conclusion that one tends to use her (or his) forearm and/or hand to keep the cup under control rather than her (or his) upperarm. As for the pronator/supinator moment at the elbow, it is seen from the Figure 4.2 (b) that only the forearm pronator is active for all the three tasks with the largest moment magnitude for the drinking task. Overall, the following aspects can be concluded about the elbow joint. First, drinking with a cup requires a larger flexor moment at the elbow joint to compensate for the smaller flexor moment at the shoulder. Second, a large amount of forward trunk and head movement is needed to compensate for the extension of the forearm when performing the two eating tasks.

For the wrist, the first aspect we noticed is that the inward/outward rotator moment as well as the ulnar/radial deviator moment are very small and thus negligible. The second aspect is that no extensor moment is present at the wrist for the drinking task while small extensor moments are needed to fetch the fork and/or spoon for the two eating tasks. This is due to the different shapes of the tools which require different muscle groups at the wrist.

Tables 4.1, 4.2 and 4.3 show the detailed data for the moments of eight female subjects. The mean maximum and minimum moments were calculated. The conclusions from Subject 5 are also valid for the mean values. It is interesting to see that moments of Subject 1 (weight: 65kg, height: 1.55m) are extremely large, especially when she was performing the task of eating with a fork. This might have some relation to the weight/height ratio, which is the largest for this subject. It is possibly true that people with a higher ratio of weight/height have a tendency to use their upper limbs more than moving their trunk or head because of their body configuration.

TABLE 4.1 (a) M_x : extensor moment at the shoulder (continued)

subject	cup		fork		spoon	
	max.	min.	max.	min.	max.	min.
1	0.678	–1.056	6.471	–3.934		
2	–0.702	–2.851	–1.822	–2.790	–1.378	–2.565
3	–1.609	–3.290	–0.899	–2.005	–1.173	–1.988
4	–1.029	–2.171	–0.644	–2.393	–0.816	–2.215
5			–1.264	–2.019		
6	–0.408	–1.901	–1.763	–2.874	–1.633	–2.609
7	–0.915	–2.347	–0.461	–3.324		
8	–0.785	–3.156	–1.622	–2.697	–1.661	–2.633
mean	–0.908	–2.396	–1.211	–2.755	–1.333	–2.402

TABLE 4.1 (b) M_y : inward/outward rotator moment at the shoulder

subject	cup max.	cup min.	fork max.	fork min.	spoon max.	spoon min.
1	2.639	1.217	11.864	0.843		
2	3.998	1.593	3.811	0.137	3.513	0.056
3	1.686	0.611	2.000	–1.236	2.357	–0.173
4	3.218	1.531	3.372	–0.514	3.784	0.697
5			2.567	–0.544		
6	2.382	0.334	1.982	–0.423	2.091	–0.363
7	3.854	0.931	4.272	0.343		
8	3.421	1.337	3.354	1.026	3.446	0.719
mean	3.028	1.079	3.051	–0.046	3.038	0.187

TABLE 4.1 (c) M_z : abductor moment at the shoulder

subject	cup max.	cup min.	fork max.	fork min.	spoon max.	spoon min.
1	–3.133	–5.237	–3.052	–27.106		
2	–1.317	–3.153	–0.393	–2.544	–0.212	–3.892
3	–1.423	–2.357	–0.104	–2.243	–0.890	–2.032
4	–2.705	–4.751	–1.057	–3.569	–0.556	–3.777
5			–1.619	–2.712		
6	–2.296	–4.981	–1.455	–3.229	–1.486	–3.612
7	–3.432	–6.816	–1.236	–7.100		
8	–0.562	–2.223	–0.502	–2.601	–0.574	–2.711
mean	–2.124	–4.217	–0.909	–3.428	–0.744	–3.205

TABLE 4.2 (a) M_a : flexor/extensor moment at the elbow

subject	cup max.	cup min.	fork max.	fork min.	spoon max.	spoon min.
1	1.418	–2.358	4.743	–7.905		
2	1.691	–0.692	2.024	0.011	2.259	–0.331
3	2.058	0.448	0.875	–0.616	0.944	–0.572
4	1.452	–1.338	1.734	–1.903	1.766	–1.522
5			1.350	–0.956		
6	1.939	–0.981	2.443	0.674	2.719	0.455
7	2.281	–2.312	3.100	–1.877		
8	2.635	–0.380	2.984	0.383	2.620	0.680
mean	1.926	–0.979	2.407	–0.612	2.062	–0.258

Table 4.2 (b) M_b : pronator moment at the elbow

subject	cup max.	cup min.	fork max.	fork min.	spoon max.	spoon min.
1	5.184	3.154	27.113	3.028		
2	3.138	1.666	2.563	0.414	3.900	0.240
3	2.346	1.416	2.266	0.130	2.032	0.898
4	4.744	2.451	3.539	1.065	3.777	0.556
5			2.741	1.618		
6	4.981	2.110	3.170	1.464	3.627	1.529
7	6.815	3.451	7.135	1.294		
8	2.221	0.556	2.608	0.523	2.713	0.578
mean	4.204	2.110	3.432	0.930	2.210	0.760

TABLE 4.3 M_u : extensor moment at the wrist

subject	cup		fork		spoon	
	max.	min.	max.	min.	max.	min.
1	–1.239	–2.704	–0.951	–11.962		
2	–1.644	–4.129	–0.271	–3.954	–0.193	–3.613
3	–0.730	–1.809	1.124	–2.331	0.065	–2.494
4	–1.680	–3.363	0.346	–3.836	–0.857	–3.943
5			0.511	–2.676		
6	–0.421	–2.412	0.334	–1.898	0.274	–2.170
7	–1.081	–4.001	–0.524	–4.411		
8	–1.553	–3.477	–1.123	–3.442	–0.672	–3.549
mean	–1.193	–3.128	–0.069	–3.220	–0.277	–3.154

Note: The other two moments at the wrist are small and thus negligible

4.2 Energy Variation Investigation

The analysis of energy variation is a fundamental method to examine the energy exchange within a segment and energy flow between adjacent segments.

The instantaneous energy level of any segment can be defined as the algebraic sum of the potential and kinetic energies, where the kinetic component comprises both translational and rotational components. The potential energy changes are measured from the lowest point the arm took during the given movement. As pointed out in Chapter 1, energy analysis has been criticized for giving erroneous information and that the energy based method and the power/work based method do not lead to the same conclusion. Nevertheless it is possible, by analyzing instantaneous energy levels, to show the energy exchanges within segments, and their individual contributions to the total energy changes during the given movement.

Total energy, potential energy and kinetic energy were analyzed for the five phases of each task on each of eight normal subjects. The pattern of energy changes was very similar for all eight female subjects; the analysis presented here is representative of the group.

Figure 4.4 (a)–(d) present the instantaneous energy of the upperarm, forearm, hand and the whole upper limb of Subject 5, respectively for the drinking task. The kinetic and potential energy components are also plotted. Figure 4.5 (a)–(d) show the instantaneous energy level of each segment of the same subject for the three tasks. Energy changes are emphasized, rather than the absolute energy levels, because an energy change indicates power flow to or from the limb segment in question.

First the energy levels of Subject 5 when performing the drinking task are examined. Two aspects are evident. One is that the energy levels show a similar variation pattern

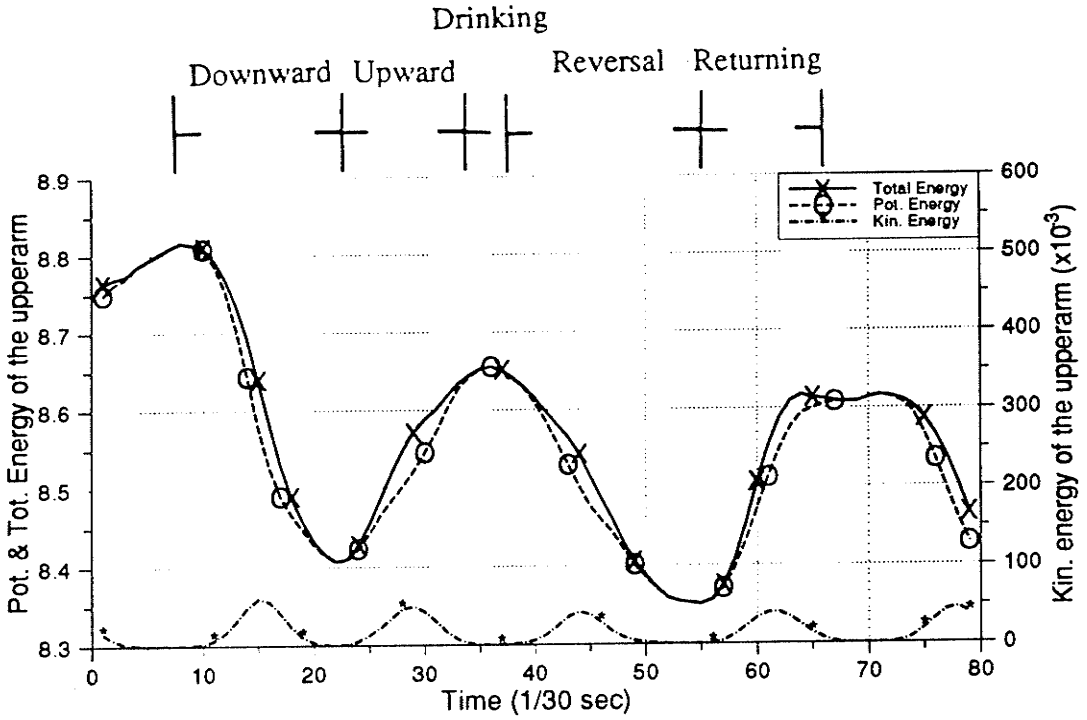

(a)

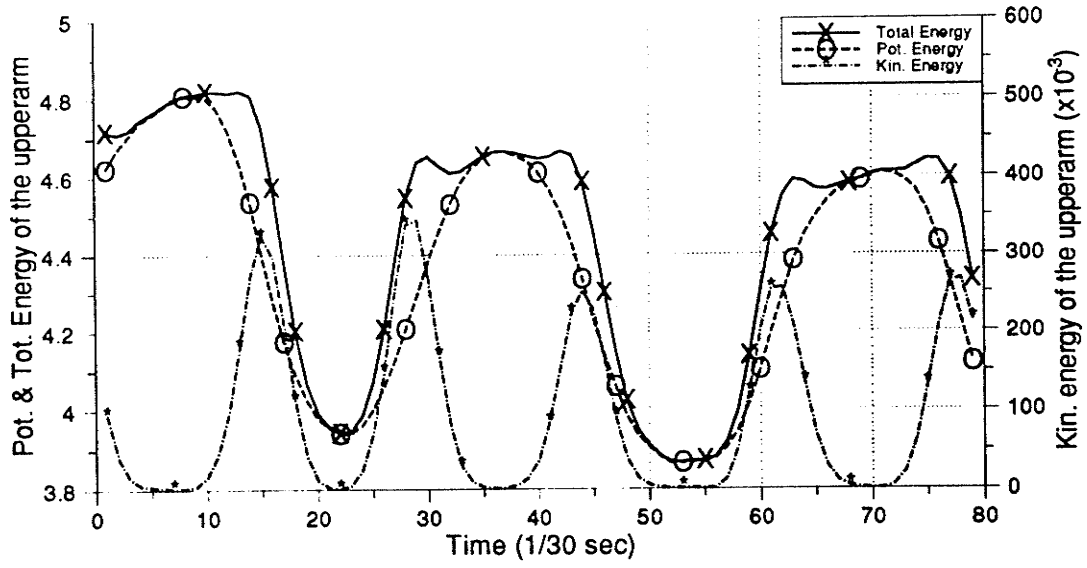

(b)

Fig. 4.4 Energies of Subject 5 when drinking with a cup (continued)

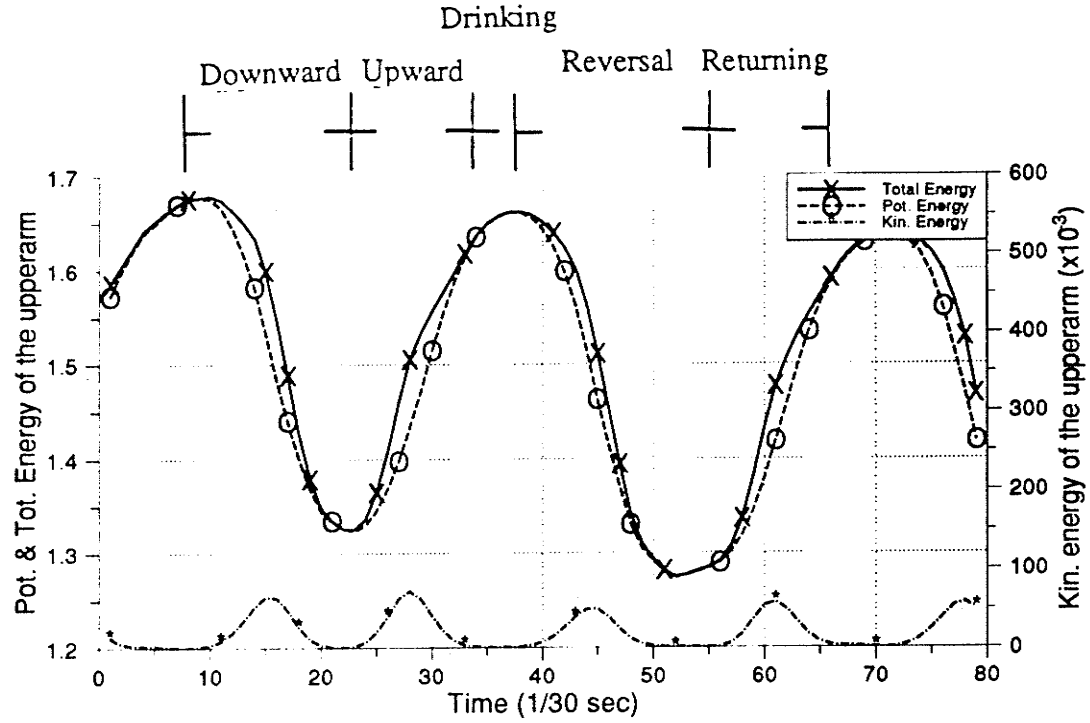

(c)

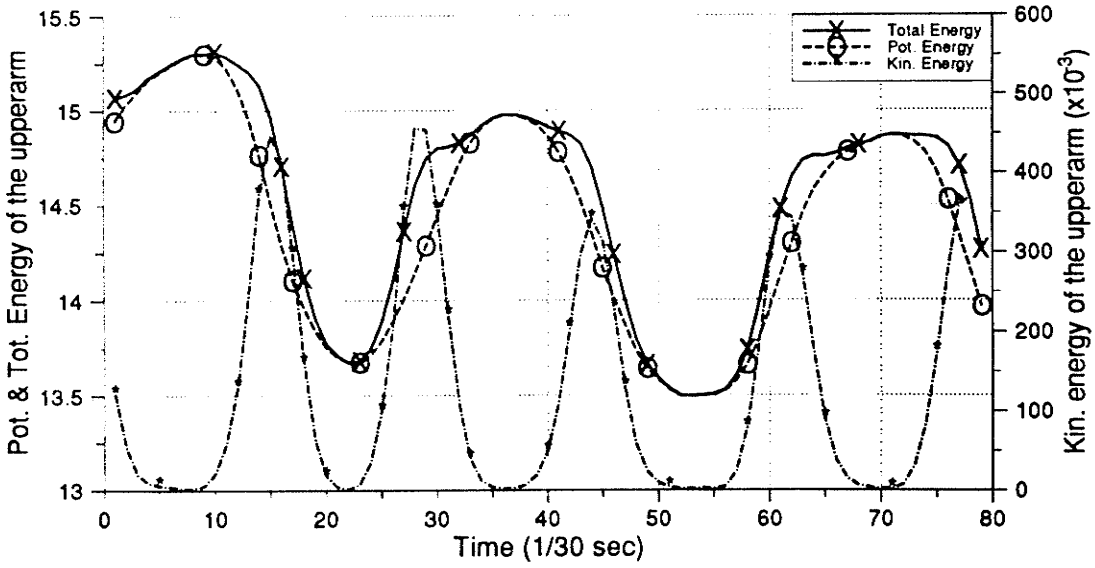

(d)

Fig. 4.4 Energies of the subject 5 when drinking with a cup

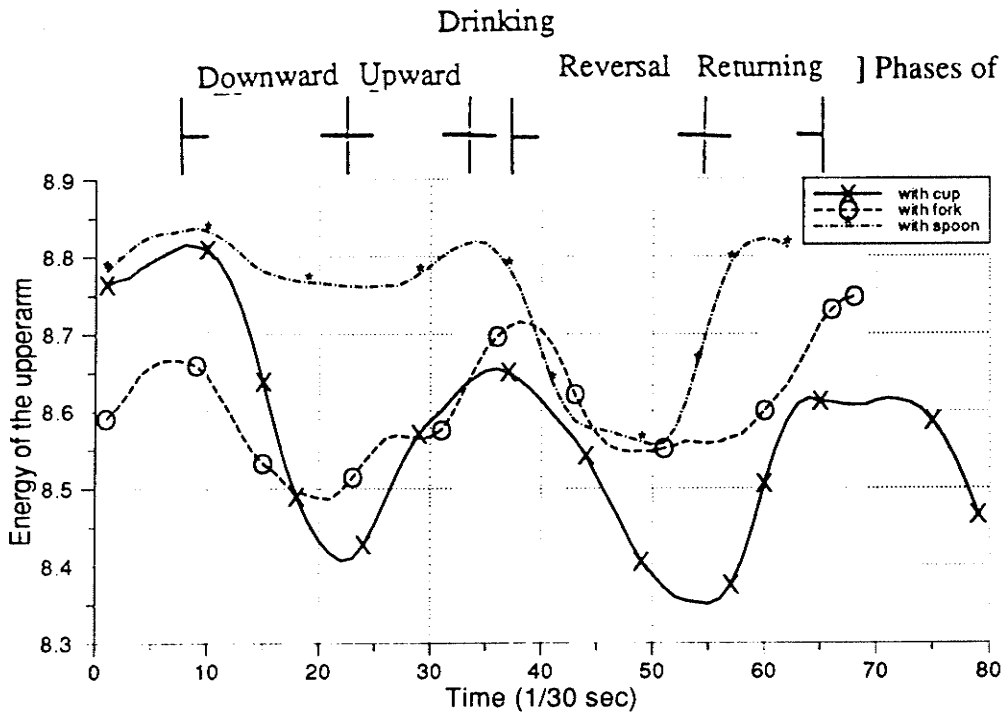

(a)

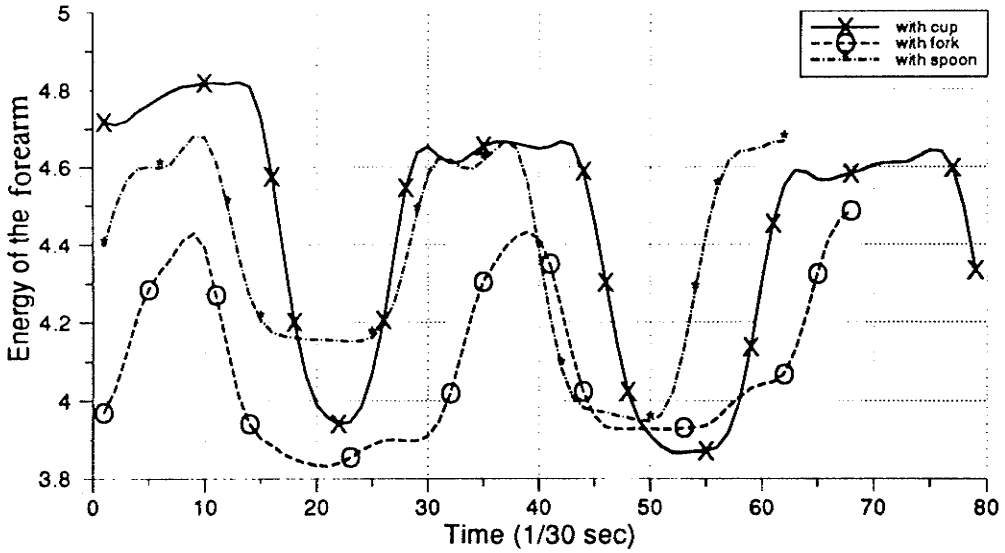

(b)

Fig. 4.5 Energies of the subject 5 for the three tasks (continued)

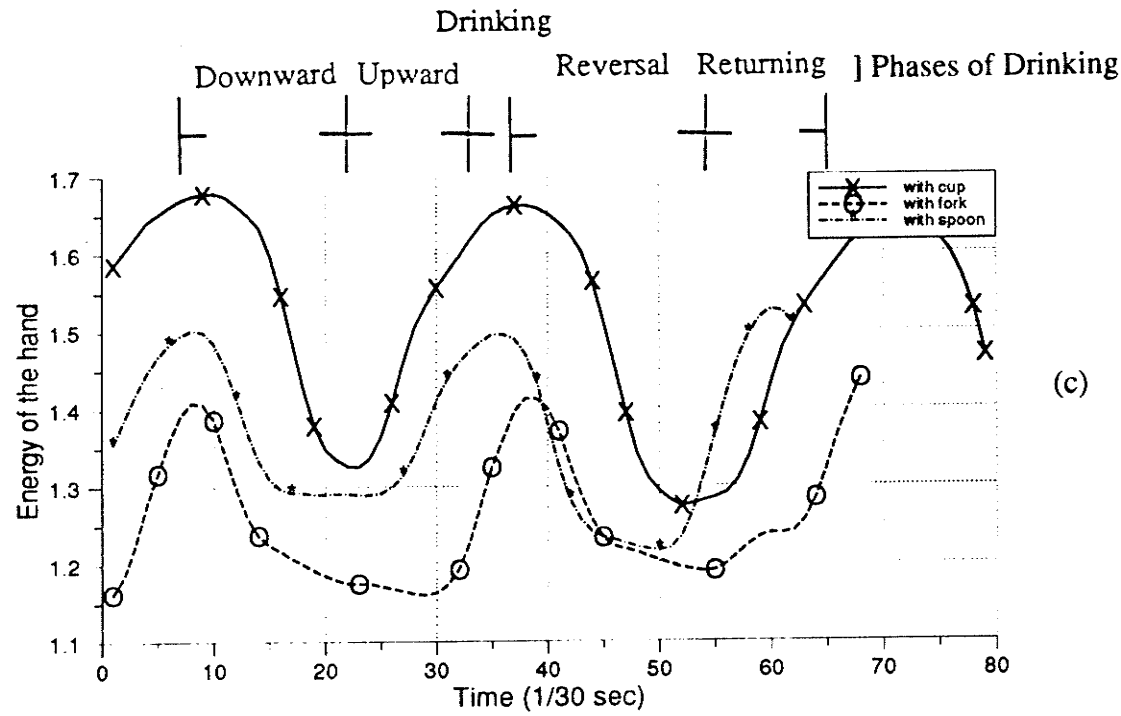

(c)

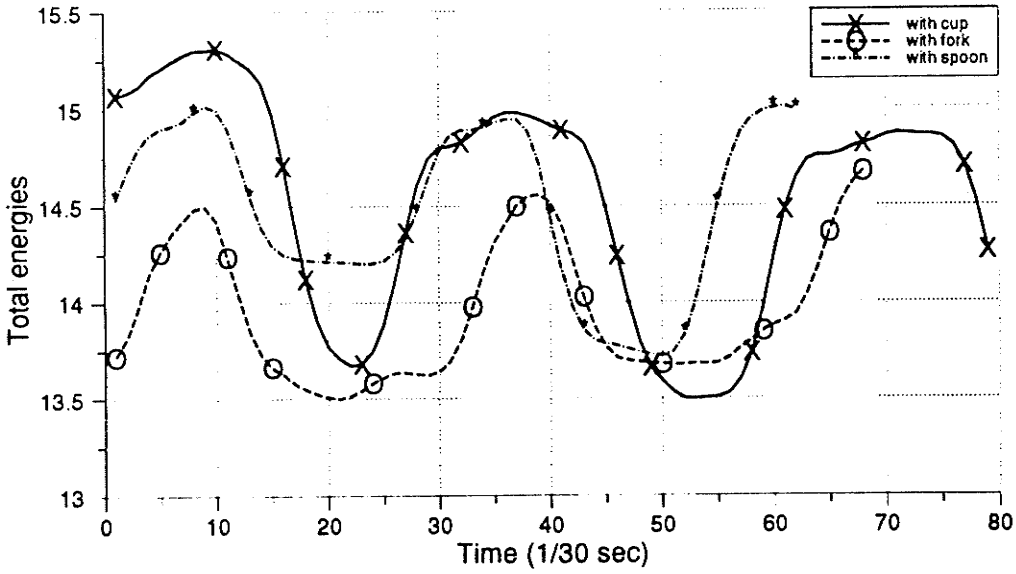

(d)

Fig. 4.5 Energies of the subject 5 for the three tasks

at each joint and for the whole upper limb. Another one is that the kinetic energy levels are small compared to the potential levels. But an energy exchange within each segment is still significant. For the upperarm, ΔKE (Δ = Max. – Min.) is ca. 50mJ while ΔPE is ca. 250mJ which is a small fraction of its mean potential energy (8.56J). For the forearm, ΔKE is 350mJ while ΔPE is 900mJ. For the hand ΔKE is 50mJ and ΔPE is 400mJ. Energy exchanges within each segment are all in phase. The first exchange of energy takes place at the early period of the downward phase. Here the kinetic energy increases while the potential energy decreases as the arm is moved from the standard position to fetch the tool. The second exchange happened at the late part of the upward phase. The kinetic energy is converted into potential energy. During the drinking phase both kinetic and potential energies are kept constant and then during the early part of the reversal phase some of the store potential energy is converted back into kinetic energy.

If we investigate the energy difference of each segment for the three different tasks, the following observations can be obtained from the Figure 4.5.

For the upperarm

the energy variation ΔE = 400mJ for the drinking task

= 200mJ for the task of eating with a fork

= 300mJ for the task of eating with a spoon

For the forearm

the energy variation ΔE = 900mJ for the drinking task

= 600mJ for the task of eating with a fork

= 700mJ for the task of eating with a spoon

For the hand

the energy variation ΔE = 400mJ for the drinking task

= 250mJ for the task of eating with a fork

= 300mJ for the task of eating with a spoon

It is concluded that each segment presents the largest peak energy for the drinking task, and the smallest peak energy for the task of eating with a spoon. When drinking with a cup, the energy of each segment decreases faster during the downward phase and also increases faster during the upward phase as compared with the two eating tasks. The energy, though, keeps constant for a longer duration around the drinking phase.

4.3 Power/Work Pattern Investigation

In the first two sections of this chapter, the mechanical energy aspects and muscle moment patterns of the upper limb motion have been investigated. The mechanical energy is an excellent means of quantifying and describing human movement but, unfortunately, yields no information as to the source of generation and absorption of that energy, or which muscle groups control the movement and how much they contribute to the segments' motion. Similarly, resultant muscle moment information quantifies which muscles are active but does not indicate where the mechanical energy generated by muscles goes, where the energy absorbed by muscles comes from or where energy is transferred between segments.

In this section, an analysis of the patterns of mechanical power generation and absorption at each of the joints is presented, aimed at determining the major function of each muscle group in terms of positive and negative work.

4.3.1 Methodology

From many previous reports, it is known that there are two main methods to compute the mechanical work of human movement: (1) to infer the work performed by examining the energy changes of the body and its constituent segments (energy based approach); (2) to compute the work from the knowledge of the resultant muscle moments at the joint and their angular velocities (joint–work approach) [12]. The energy variation patterns have been investigated in Section 4.2. No attempt was made to infer the work done from energy changes of the segments. In this section, the joint–work approach is developed to get information on generation and absorption of the energy.

The basic idea of the joint–work approach has been reported by a number of investigators. There are two kinds of power [8]. One is called joint power, which is the rate of work done, positively or negatively, by the joint forces. This joint power P_j can be calculated from:

$$P_j\ (j, s) = \vec{F}\ (j, s) \quad \cdot \quad \vec{V}\ (j) \qquad 4.1$$

where P_j (j, s) is the power delivered to or if negative taken from segment s at its joint j due to the work done by the joint reaction forces. $\vec{F}$ (j, s) is the joint reaction force vector acting on segment s at joint j and $\vec{V}$ (j) is the linear velocity vector of that joint. The other power is called muscle power, which is the rate of work done by the muscle moments. The muscle power P_m can be calculated from

$$P_m\ (j, s) = \vec{M}\ (j, s) \quad \cdot \quad \vec{\omega}\ (s) \qquad 4.2$$

where P_m (j, s) is the mechanical power delivered to or taken from segment s at joint j due to the work done by the muscle moments, $\vec{M}$ (j, s) is the muscle moment vector acting on segment s at joint j and $\vec{\omega}$ (s) is the angular velocity vector of segment s. A positive rate again indicates the rate of mechanical work done by the muscle on segment s, while a negative rate shows the rate of mechanical work done by segment s on the muscle. Contrary to the situation for the joint power, the two segments connected at joint

j do not necessarily have the same angular velocity, consequently, there can be more than simply a transfer of energy from segment to segment through the muscles. The muscles can also generate mechanical energy or absorb mechanical energy by concentrically or eccentrically contracting, respectively [6, 8].

Before proceeding, three points need to be clarified:

(1) Joint reaction forces are not available from Lagrangian formulation; rather only muscle moments. Therefore, only the muscle powers can be calculated.

(2) Because relative joint angular velocities were used instead of the absolute angular velocities of each segment, information concerning energy transfers between adjacent segments is not available.

(3) When the total power of each segment, which is the sum of the joint and muscle powers of each segment, is positive it signifies that the segment is gaining mechanical energy implying a net increase in potential and/or kinetic energies. Conversely, a negative power indicates the rate of loss in the segment's total mechanical energies. Since only the muscle power of each segment is available, there is no way to relate the sign of the muscle power to the energy pattern of each segment. But the sign of the muscle power is an indication of where the energy flows. A positive power indicates rate of energy inflow from the particular source plotted; negative powers show the rates of the energy outflow. When the energy flows into the particular segment, the segment is said to absorb the energy and is called a 'sink'. When the energy flows out of the particular segment, the segment is said to generate the energy and is called a 'source'.

From Equation 4.2, three muscle powers can be calculated at the shoulder and the wrist joint. Two muscle powers can be calculated at the elbow joint.

where ω_x, ω_y, ω_z, ω_a, ω_b, ω_c, and ω_u, ω_v, ω_w are the respective angular velocity components in the direction of the principle axes **xyz**, **abc** and **uvw**.

At the shoulder $P_{s,x} = M_x\omega_x$, $P_{s,y} = M_y\omega_y$, $P_{s,z} = M_z\omega_z$

At the elbow $P_{e,a} = M_a\omega_a$, $P_{e,b} = M_b\omega_b$

At the wrist $P_{w,u} = M_u\omega_u$, $P_{w,v} = M_v\omega_v$, $P_{w,w} = M_w\omega_w$

M_x , M_y , M_z , M_a , M_b , M_c , and M_u , M_v , M_w are the respective muscle moment components in the direction of the principle axes **xyz**, **abc** and **uvw**, $P_{s,x}$, $P_{s,y}$ $P_{s,z}$ are the powers at the shoulder, $P_{e,a}$, $P_{e,b}$ are the powers at the elbow, and $P_{w,u}$, $P_{w,v}$, $P_{w,w}$ are the powers at the wrist joint.

4.3.2 Results and Discussions

The purpose of the section is to analyze the patterns of mechanical power generation and absorption at each joint, aimed at determining the major function of each muscle group in terms of positive and negative power.

For the purposes of documentation the detailed curves for each subject will not be presented; rather an example calculation of power and work for Subject 5 is presented. Figure 4.6, 4.7 and 4.8 show the power and work of each segment for the drinking task. To investigate the function of each major muscle group, the three powers of the three moment components in the direction of the three orthognal axes at each joint are shown. The area under each phase of the power curve is the work done at each joint by the particular muscle group and is expressed in Joules. The major phases of power generation and absorption are labelled. The power bursts at the wrist for the drinking task (Figure 4.8) were either large nor consistent in their patterns, thus no label was given.

It is seen in Figure 4.6 (a) that the shoulder is flexed at the downward phase. During this time the extensor moment is reduced and as the major extensor muscles shortened

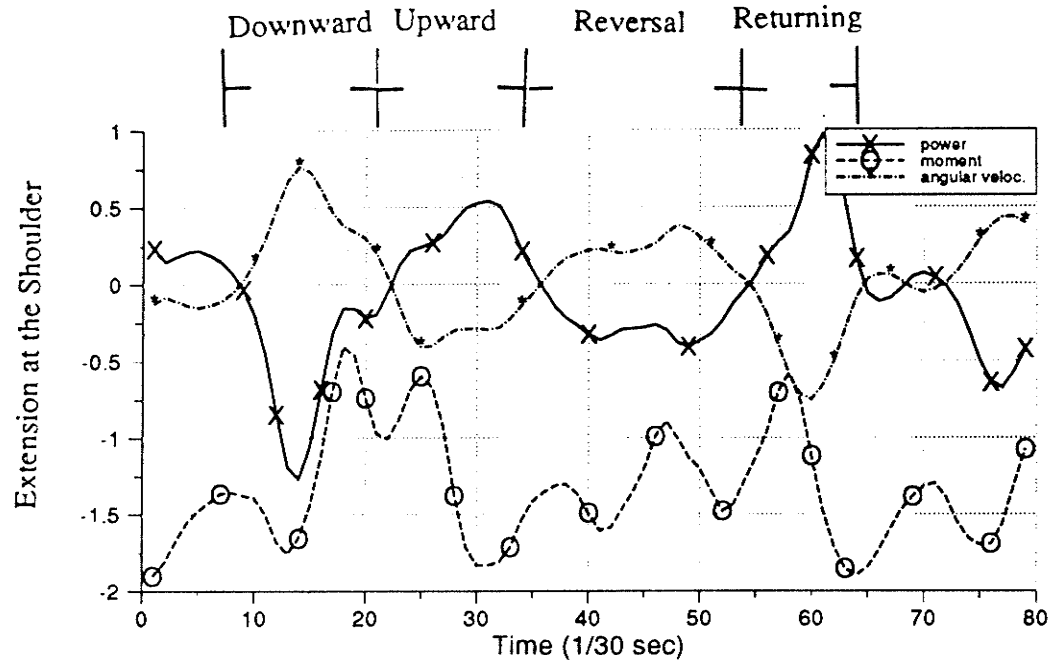

(a)

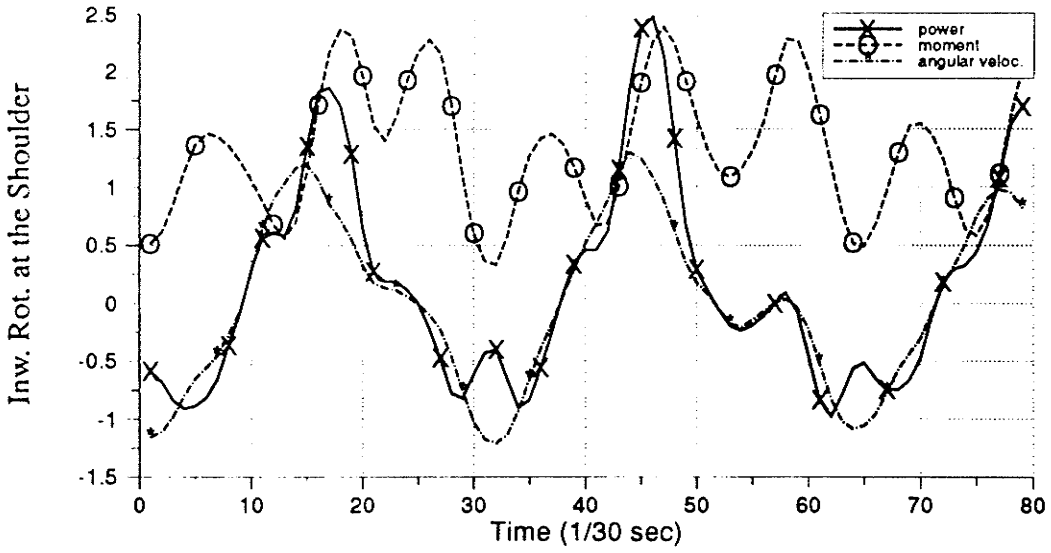

(b)

power: W; moment: N.M; angular velocity: rad/s.

Fig. 4.6 Work/Power at the shoulder joint of subject 5 for the drinking task (continued)

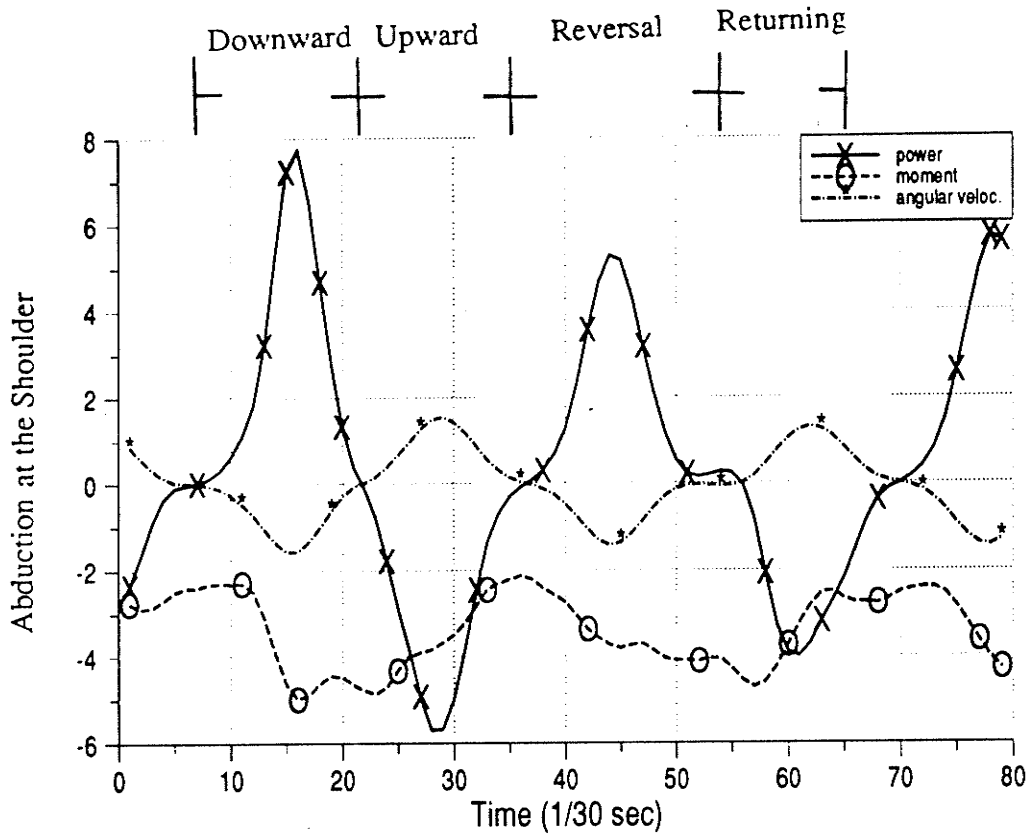

(c)

power: W; moment: N.M; angular velocity: rad/s.

Fig. 4.6 Work/Power at the shoulder joint of subject 5 for the drinking task

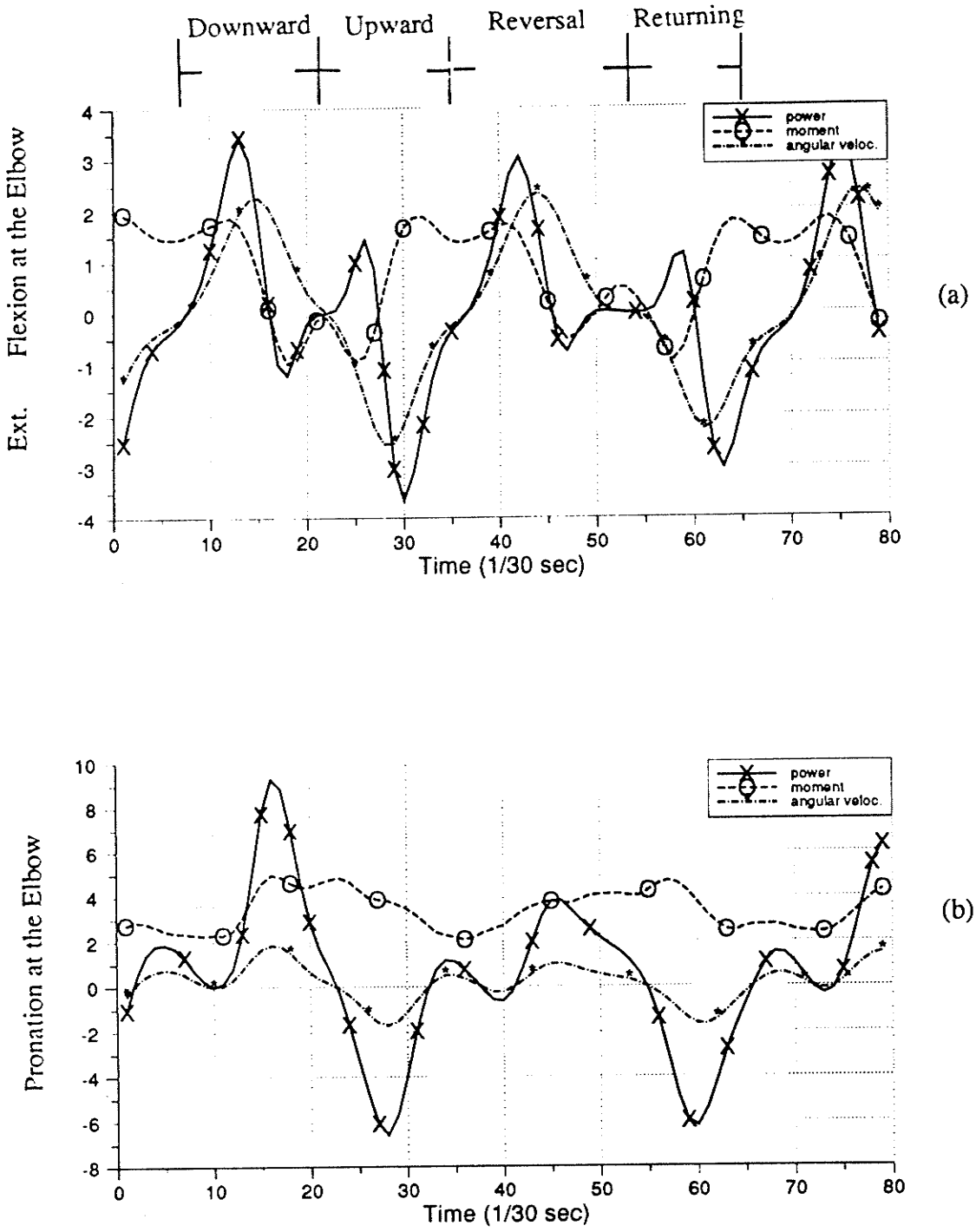

Power: W; Moment: N.M; Angular velocity: Rad/s.

Fig. 4.7 Power/Work at the elbow of subject 5 for the drinking task

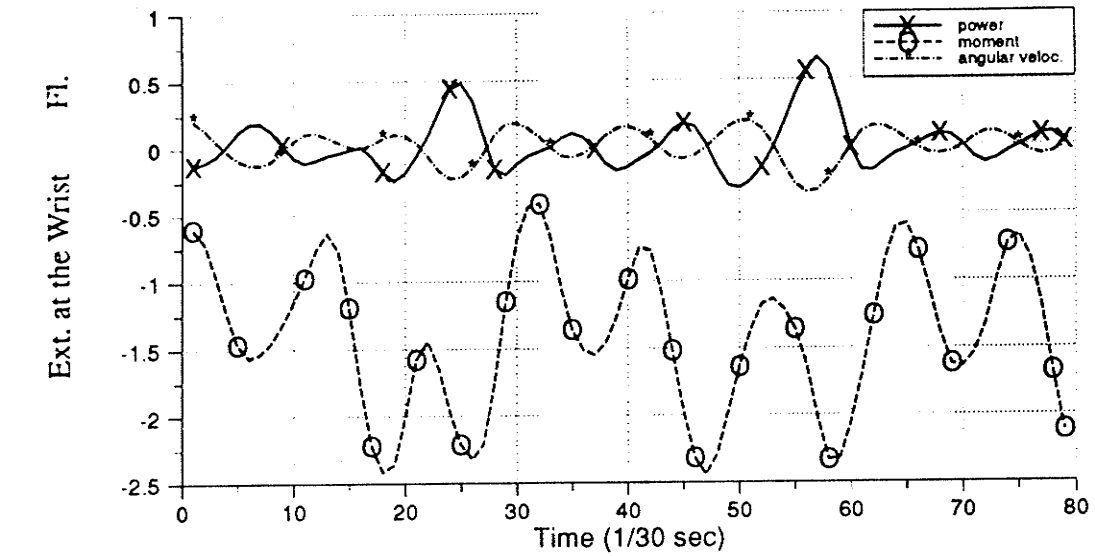

(a)

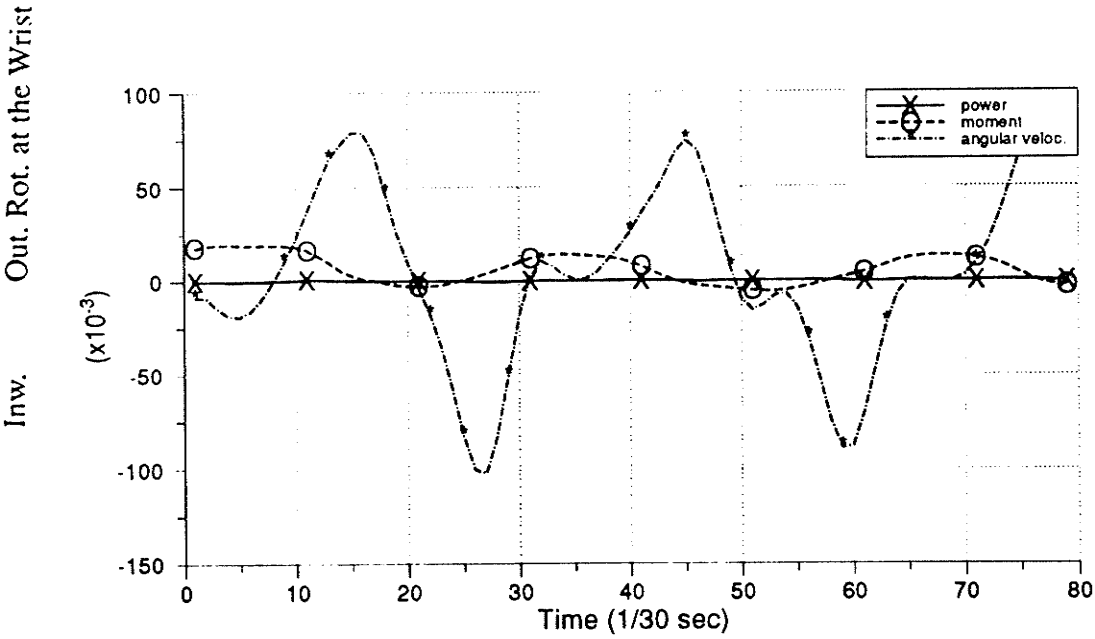

(b)

Power: W; Moment: N.M; Angular velocity: Rad/s.

Fig. 4.8 Power/Work at the wrist of subject 5 for the drinking task (continued)

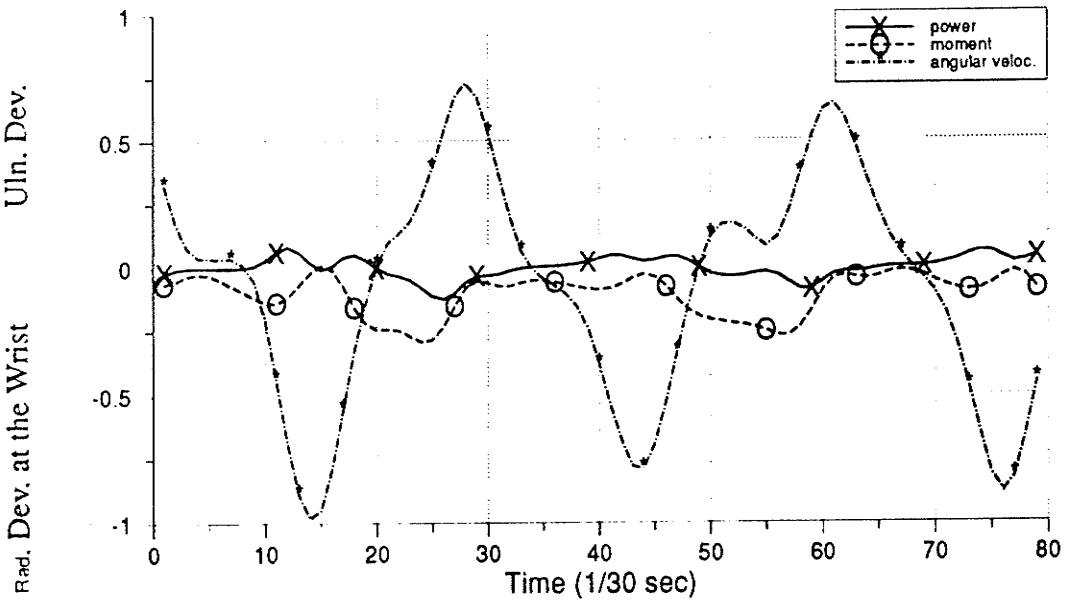

(c)

Power: W; Moment: N.M; Angular velocity: Rad/s.

Fig. 4.8 Power/Work at the wrist of subject 5 for the drinking task

under tension, they absorbed 226mJ (A_1) of mechanical energy. The power peak during this phase was 1.75W. During the upward phase the shoulder started to extend and as these extensor muscles lengthened energy was generated. The positive work done was 142mJ (A_2). During the reversal phase, this moment is highly unstable but it is seen that the extensor muscles absorbed 164mJ (A_3) work during the reversal phase. The shoulder extended again during the returning phase and 154mJ (A_4) work was generated by the extensor muscles. By comparing $A_1 + A_3$ and $A_2 + A_4$ it can be said that the extensor muscles at the shoulder mainly absorb energy ($A_1 + A_3 > A_2 + A_4$).

Figure 4.6 (b) is a plot showing the power associated with the inward rotator moment at the shoulder. Four power phases are seen in all the subjects; here they are labelled B_1, B_2, B_3 and B_4. An inward rotator moment developed during the downward phase and this group of inward rotator muscles resulted in a peak positive power of 1.8W with a corresponding energy generation of 408mJ (B_1). From the end of the downward phase until late upward phase the shoulder rotates outward and during this lengthening of the inward rotator muscles 227mJ work was absorbed. Then the power repeats the same pattern with a higher positive peak power 2.5W during the reversal phase than during the downward phase.

It is evident in Figure 4.6 (c) that as compared with the extensors and the inward rotators at the shoulder the abductors at the shoulder generated and absorbed the largest mechanical energy. The pattern of this power is similar to that in Figure 4.6 (b). The difference is that the abductors generated larger mechanical energy during the downward phase while the inward rotators generated a larger mechanical energy during the reversal phase.Unlike the extensors at the shoulder which mainly absorb energy, both the inward rotators and the adductors at the shoulder mainly generate energy.

Figure 4.7 shows three similar plots for the elbow joint. Figure 4.7 (a) shows the power due to the flexor/extensor moment at the elbow. Figure 4.7 (b) shows the power associated with the pronator moment at the elbow. There are eight evident power phases in Figure 4.7 (a). There are two interesting aspects about this power. First, it is interesting to notice two pairs of smaller work bursts corresponding to the times when the cup is picked up and when the cup was returned to the original place. At these two times the extensors switch from absorption of energy to generation of energy. Second, the amount of energy generated by the flexors is almost equal to the amount of energy absorbed by themselves. These two observations hold for all the subjects. Figure 4.7 (b) shows that a large mechanical energy generated and absorbed by the pronators at the elbow. Seven power phases can be seen for all the subjects. If the power phase E_1 is compared with the power phase E_5 we find that the mechanical energy generated by the pronators during the reversal phase is much smaller than that generated during the downward phase. It is logical to assume that this smaller energy generated by the pronators at the elbow is compensated by a larger energy generated by the inward rotators at the shoulder. By comparing the energy generated and absorbed by the pronators at the elbow it is clear that the pronators are an energy generator.

Figure 4.8 shows the power/work curves at the wrist. The wrist had relatively low power levels, and when different trials are compared no consistent patterns are seen. The major conclusion that results is that this lack of pattern appears to be due to the complicated role of the wrist flexors during the drinking task. They are obviously involved with the upper limb in supporting the cup and initiating and controlling the feeding action. However, these muscles are also responsible for maintaining a stable cup and a stable upper limb, and it is probably fine adjustments of the balance between the cup and the upper limb that increased the variability that marked major patterns.

4.4 Conclusions

The muscle moments at each joint, which are solved from the Lagrangian equations of motion, are analyzed. The conclusions are:

(1) The active groups of muscles for the three functional upper limb movements at the shoulder are the extensors, inward rotators and abductors.

(2) At the elbow the extensors are active for the two eating tasks while a small flexor moment of the forearm is needed for the drinking task, and pronators are active for all the three tasks with the largest magnitude of the moment for the drinking task.

(3) At the wrist the inward/outward rotator moment as well as the ulnar/radial deviator moment are very small and thus negligible; only a flexor moment is present for the drinking task while small extensor moments are needed to fetch the fork and/or the spoon for the two eating tasks.

From the analysis of each segment's energy levels it is concluded that:

(1) Energy levels show similar variation patterns for all the human subjects.

(2) Kinetic energy levels are small compared to the potential energy levels.

(3) Three energy exchanges are noticeable and all in phase.

(4) Each segment presents the largest peak energy level for the drinking task, and the smallest for the task of eating with a spoon.

The power/work patterns for the drinking task have been also analyzed. The conclusions are:

(1) All the power curves for the drinking task show similar patterns among all the subjects except that the power bursts at the wrist are neither large nor consistent in their patterns.

(2) The extensor muscles at the shoulder mainly absorb energy and the inward rotators and abductors at the shoulder mainly generate energy.

(3) The amount of energy generated by the flexors at the elbow is almost equal to the amount of energy absorbed by themselves; the group of pronators at the elbow is an energy generator.

(4) The lack of well–defined patterns at the wrist are explained by the complicated roles of the flexors at the wrist.

CHAPTER 5

SUMMARY, CONCLUSIONS AND RECOMMENDATIONS

An approach to analyze the muscle moments and the resultant energetics of three functional human upper limb movements, which are drinking with a cup, eating with a fork and eating with a spoon, was developed. A 3–D kinematic model of human upper limb was developed. This 3–D model of the upper limb has 8–DOF (degrees of freedom) with 3–DOF at the shoulder, 2 DOF at the elbow and 3 DOF at the wrist. To establish the equations of motion for the upper limb, a Lagrangian formulation was utilized. Muscle moments at each joint were then solved from the Lagrangian equations of motion.

The motion data of the three functional human upper limb movements was collected by Cooper et al. [1]. The motion data was conditioned before used in the Lagrangian equations because of the noise introduced by the measurement system and/or the data quantization. A simple but effective filtering algorithm, which is a combination of a median smoother and a Hanning filter, was developed to filter out the noises without smearing out sharp discontinuities in the motion data. Then the first and second derivatives of the motion data were obtained by taking the finite differences. It is concluded from analyzing the first derivatives that the motion of flexion/extension of the forearm is the fastest for the drinking task, followed by the motion of flexion/extension of the upperarm and the motion of pronation/supination of the forearm. The movement of inward/outward rotation at the shoulder and the wrist is so slow that it can be neglected. For the two eating tasks the motion of pronation/supination of the forearm, not the motion of flexion/extension of the forearm, is the fastest.

To gain an understanding of the causes of the functional movement of the upper limb, muscle moments at each joint, energy variation of each segment and the power/work patterns were analyzed. The analysis of energy variation is a fundamental method to examine the energy exchange within a segment and energy flow between adjacent segments. It is concluded that energy levels show similar variation patterns at each joint; kinetic energy levels are small compared to the potential energy levels; three energy exchanges are noticeable and all are in phase. Each segment has the largest peak energy for the drinking task, and the smallest for the task of eating with a spoon.

Unfortunately, this energy method can not answer either of the following two basic questions: (1) which group of muscles contribute to the particular motion; (2) where the energy comes and where it goes.

The first question can be answered by examining the muscle moment pattern at each joint. The active groups of muscles for the three functional upper limb motion at the shoulder are the extensors, inward rotators and the abductors. At the elbow only extensors are active for the two eating tasks while a small flexor moment of the forearm is needed for the drinking task. This shows an important aspect of the arm movement: it is possible to compensate for a large amount of elbow flexion with trunk and/or head forward movement. At the wrist it is concluded that the inward/outward rotator moment as well as the ulnar/radial deviator moment are very small and thus negligible; only the flexor moment is present for the drinking task while small extensor moments are needed to fetch the fork and/or spoon for the two eating tasks.

The power/work approach focuses on the human muslces themselves as generators and absorbers of energy; thus this method can answer the question of where the energy was generated and where it was absorbed. It is concluded that all the power curves for the drinking task show certain similar patterns among all the subjects except that the power

bursts at the wrist were neither large nor consistent in their patterns. Mechanical energies generated and/or absorbed by the particular group of muscles were then calculated. It is concluded that the extensor muscles at the shoulder mainly absorb energy and that the inward rotators and the abductors at the shoulder mainly generate energy. The amount of energy generated by the flexors at the elbow is almost equal to the amount of energy absorbed by themselves. The pronator group at the elbow is an energy generator. The lack of well defined patterns at the wrist was explained by the complicated role of the flexors at the wrist. They are involved with the upper limb in supporting the cup, initiating and controlling the feeding action, and are also responsible for maintaining a stable cup and a stable upper limb. It is the fine adjustments of the balance between the cup and the upper limb that causes the uncertain and inconsistent patterns at the wrist.

Overall, the following conclusions can be made;

(1) An approach to analyze the muscle moments and the resultant energetics of functional human upper limb motion was formulated.

(2) The fundamental bases for this approach were developed, i.e.,

(a) a 3–D kinematical model of human upper limb with 3–DOF at the shoulder, 2–DOF at the elbow and 3–DOF at the wrist.

(b) the equations of motion of the upper limb, which was derived by using the Lagrangian dynamic formulation.

(c) the muscle moments at each joint which were solved from the equations of motion.

(3) A simple but effective smoothing algorithm was developed to smooth out the noises in the raw human motion data while preserving the useful sharp edges in the data.

(4) Three important aspects of human upper limb motion are analyzed.

(a) muscle moments at each joint;

(b) energy levels of each segment;

(c) power/work patterns of each segment;

(5) All the above three analyses are valid and provide correct information on the causes of human upper limb motion.

(6) From all the analyses, the 3–D kinematic model of human upper limb appears to be reasonable. All the analyses give the author confidence in the model even though no direct comparisons to the work of this thesis is available.

At last, problems that should be solved in order to improve the kinematical model of human upper limb and those aspects that should be studied in the future to provide more thorough and detailed information for analyzing the energetics of functional human arm motion are suggested here:

(1) The accuracy and reliability of the kinematic model of the upper limb should be tested. This can be done by the simulation of the upper limb movement through the model. By viewing the muscle moments at each joint as the inputs of Lagrangian equations of motion, the output motion should be a specific motion corresponding to the moments. It is obvious that the closer this simulated motion is to the real motion, the better the model is.

(2) To improve the kinematic model of the upper limb, each rigid body of the upper limb can be modeled as a 3–D solid, which is more realistic than a uniform slender rod.

(3) To gain knowledge of male subject upper limb motion, study of the moments and the resultant energetics for the male subjects (the motion data is available in the Laboratory) is necessary.

(4) In addition to the two main energy forms, which are kinetic and potential energy, other forms, such as the energy stored in springs due to the elastic deformation and the dissipation energy due to friction of the system, and their contributions to the total body energy are worth studying.

(5) Energy transfer between adjacent joints should be studied. To do so the absolute angular velocity of each segment needs to be known.

(6) Even with the detailed analysis described in the section 4.3, the work done by cocontracting muscles is underestimated. Muscle power, as calculated, is the product of the muscle moment M and the angular velocity ω . M is the net muscle moment resulting from all agonist and antagonist activity and therefore can not account for simultaneous generation by one muscle group and absorption by the antagonist group, or vice versa. Unfortunately, to date there has been very limited progress to calculate the power and work associated with each muscle's action. The major problem is to partition the contribution of each muscle to the net moment. Solving this problem will provide significant insight into the function of each muscle.

REFERENCES

CHAPTER 1

[1] Kromodihardjo, s. and Mital, A., "Biomechanical Analysis of Manual Lifting Tasks," Transactions of the ASME, Vol. 109, pp. 132–138, May 1987.

[2] Frievalds, A., Chaffin, D. B., Garg, A. and Lee, K. S., "A Dynamic Biomechanical Evaluation of Lifting Maxium Acceptable Loads," J. Biomechanics, Vol. 17, pp. 251–262, 1984.

[3] Lucas, W. T., "Measuring Hand Forces and Wrist Motions For Preventing Injures In The Workplace," Bioengineering, Proceedings of the Northeast Conf., pp. 143–144, 1990.

[4] Safaee–Rad, R., Shwedyk, E., Quanbury, A.O. and Cooper, J.E., "Normal Functional Range of Motion of Upper Limb Joints During Performance of Three Feeding Sctivities," Arch. Phys. Med. Rehabil., Vol. 71, pp. 505–509, June 1990.

[5] Sperling, L. and Jacobsen–Sollerman, C., "The Grip Pattern of the Health Hand During Eating," Scand. J. Rehab. Ded., 9: 115–121, 1977.

[6] Brumfeild, R.H. and Champoux, J.A., "A Biomechnical Study of Normal Functional Wrist Motion," Clin. Ortho. Rel. Res., 187: 23–25, 1984.

[7] Cooper, J.E., Shwedyk, E. and Quanbury, A.O., "The Effect of ElbowJoint Restriction on Functional Upper Limb Motion During Performance of Three Eating Activities," CMBEC–16–CCGB, pp. 161–162, Winnipeg, 1990.

[8] George, V.K., "Computation of Functional Capacity: Stradege and Example for Should," IEEE Ninth Conf. of the Engg. In Med. and Biolog. Society, pp. 477–478, 1987.

[9] Wood, J.E., Meek, S.G. and Jacobson, S.C., "Quantitation of Human Shoulder Anatomy for Prosthetic Arm Control–I. Surface Moddling," J. Biomechanics, Vol. 22, No. 3, pp. 273–292, 1989.

[10] Lara–Feria, A. and Verdeguer–Codina, J., "Simulation of movements for a Prosthesis Finger and Hand by Quanternions," IEEE Engg. in Med. and Biology Society 10th Annual Int. Conf., pp. 1513–1514, 1988.

[11] Baer, P.C. and Seliktar, R., "Arm Prosthesis for Above Elbow Amputees Based on Extended Physioloigcal Proprioception," IEEE Ninth Annual Conf. of the Engg. in Med. and Biology Society, pp. 1066–1067, 1987.

[12] Harris, G.F., Acharya, K.R., Benson, L.J., Light, T.R. and Matesi, D.V., "Biomechanical Assessment of Active and Passive Unit Joint Control in Children with Cerebral Palsy," IEEE Engg. in Med. and Biology Soceity 11th Annual Int. Conf., pp. 820–821, 1989.

[13] Fukamachi, H., Handa, Y., Naito, A., Ichie, M., Yajima, M., Ushikoshi, K., Tuchya, M., Matsushita, N. and Hoshimiya, N., "Improvement of Finger Movement by Intrinsic Muscles Stimulation of the Hand," IEEE Ninth Annual Conf. of the Engg. in Med. and Biology Society, pp. 361–362, 1987.

[14] Della Santina, C.C., DeAngelis, G.L. and Lehman, S., "Exploring Neuromotor Control of the Forearm Reaction to Perturbation," IEEE Engg. in Med. and Biology Society 11th Annual Int. Conf., pp. 951–952, 1989.

[15] Flash, T. and Cohen, M., "Learning and Control of Arm Impedance," IEEE Engg. in Med. and Biology Sciety 11th Annual Int. Conf., pp. 900–901, 1989.

[16] Asada, H. and Goldfine, N., "Optimal Compliance Design for Grinding Robot Tool Holders," Proc. 1985 IEEE Int. Conf. on Robotics and Automation, pp. 316–322, 1985.

[17] Mussa–Ivaldi, F. A., Hogan, N., and Bizzi, E., " Neural, Mechanical and Geometric Factors Subserving Arm Posture in Humans," J. Neurosci., Vol. 5, pp.2732–2743, 1985.

[18] Safaee–Rad, R., Shwedyk, E., Quanbury, A. O., " Functional Human moyion Study with a New 3–D Measurement System," IEEE/Ninth Annual Conference of the Engineering in Medicine and Biology Society, pp.54–55, 1987.

[19] Langrana, N. A., " Spatial Kinetic Analysis of the Upper Extremity Using a Biplanar Videotaping Method," J. Biomechanical Engineering, Vol. 103, Feb. 1981, pp.11–17.

[20] Hart, R. L., Peckham, P. H., and Crago, P. E., " Evaluation of a Three–Dimensional Tracking System to Monitor Hand Kinematics," IEEE/Ninth Annual Conference of the Engineering in Medicine and Biology Society, pp.353–354, 1987.

[21] Suntay, W. J., Grood, E. S., Hefry, M. S., Butler, D. L., and Noyes, K. R., " Error Analysis of a System for Measuring Three–Dimensional Joint Motion," J. Biomechanics Engineering, Vol. 1, No. 5, pp.127–135, May 1983.

[22] Yeadon, M. R., and Morlock, M., " The appropriate Use of Regression Equations for the Estimation of Segment Inertia Parameters," J. Biomechanics, Vol. 22, No. 6/7, pp.683–689, 1989.

[23] Yeadon, M. R., " The Simulation of Aerial Movement, Part II: a Mathematical Inertia Model of the Human Body," J. Biomechanics, Vol. 23, N0. 1, pp.67–74, 1990.

[24] Jensen, R. K., " Body Segment Mass, Radius and Radius of Gyration Proportions of Children," J. Biomechancis, Vol. 19, pp.359–368, 1986.

[25] Forwood, M. R., Neal, R. J., and Wilson, B. D., " Scaling Segmental Moments of Inertia for Individual Subjects," J. Biomechanics 18, pp.755–761, 1985.

[26] King, A. I., " A Review of Biomechanicsl Models," J. Biomechanical Engineering, Vol. 106, May 1984, pp.97–104.

[27] Kinzel, G. L., and Gutkowski, L. J., " Joint Models, Deree of Freedom, and Anatomical Motion Measurement," J. Biomechanical Engineering, Vol. 105, Feb. 1983, pp.55–62.

[28] Jackson, K. M., Joseph, J., and Wyard, S. J., " A Mathematical Model of Arm Swing During Human Locomotion," J. Biomechanics, Vol. 11, pp.277–289, 1978.

[29] Engin, A. E., and TÜmer, S. T., " Three–Dimensinal Kinematic Modelling of the Human Shoulder Complex—Part I: Physical Model and Determination of Joint Sinus Cones," J. Biomechanical Engineering, Vol. 111, May 1989, pp.107–112.

[30] Audu, M. L., and Dory, D. T., " The Influence of Muscle Model Complexity in Musculoskeletal Motion Modelling," J. Biomechanical Engineering, Vol.107, May 1985, pp.147–.

[31] Andrews, J. G., " A General Model for Detecting the Functional Role of a Muscle," Transactiona of ASME, Vol. 107, Nov. 1985, pp348–.

[32] Winters, J. M., and Stark, L., " Estimated Mechanical Properties of Synergestic Muscles Involked in Movements of a Variety of Human Joints," J. Biomechanics, Vol. 21, No. 12, pp.1027–1041, 1988.

[33] Van Zuylen, E. J., Van Velzen, A., and Van Der Gon, J. J. D., " A Biomechanical Model for Flexion Torques of Human Arm Muscles As a Function of Elbow Angle," J. Biomechanics, Vol.21, No. 3, pp.183–190, 1988.

[34] An, K. N., Kwak, B. M., Chao, E. Y., and Morrey, B. F., " Determination of Muscle and Joint Forces: a New Technique to Solve the Indeterminate Problem," J. Biomech. Engng. 106, pp.364–367, 1984.

[35] An, K. N., Kanfman, K. R., and Chao, E. Y. S., " Physiological Considerations of Muscle Force Through the Elbow Joint," J. Biomechanics, Vol. 22, No. 11/12, pp.1249–1256, 1989.

[36] Bassett, R. W., Browne, A. O., Morrey, B. F., and An K. N., " Glenohumeral Muscle Force and Moment Mechanics in a Position of Shoulder Instability," J. Biomechanics, Vol. 23, No. 5, pp.405–415, 1990.

[37] Schneider, K., Zernicke, R. F., Schmidt, R. A., and Hart, T. J., " Changes in Limb Dynamics During the Practice of Rapid Arm Movement," J. Biomechanics, Vol. 22, No. 8/9, pp.805–817, 1989.

[38] Gagnon, M., and Smyth, G., " Muscular Mechanical Energy Expenditure as a Process for Detecting Potential Risks in Manual Materials Handing," J. Biomechanics, Vol. 24, No. 3/4, pp.191–203, 1991.

[39] JÖris, H. J. J., Van Muyen, A. J. E., Van Ingen Schnau, G. J., and Kemper, H. L. G., " Force, Velocity and Energy Flow During the Overarm Throw in Female Handball Players," J. Biomechanics, Vol. 18, No. 6, pp.409–414, 1985.

[40] Naito, A. et al., " EMG Analysis of Elbow Movements and its Application to FNS," IEEE/Ninth Annual Conference of the Enginerring in Medicine and Biology Society," pp.46–47, 1987.

[41] An, K. E., and chao, E. Y., " Kinematic Analysis of Human Movement," Annals of Biomedical Engineering, Vol. 12, pp.585–597, 1984.

[42] Goldstein, H., *Classical Mechanics*, Addison–Wesley, New York, 1960, pp.107–109.

[43] Beggs, J. S., *Advanced Mechanics*, The Macmillan Co., New York, 1966.

[44] Panjabi, M., and White, A. A., " A Mathematical Approach for Three–Dimensinal Analysis of the Mechanics of the Spine," J. Biomechanics, Vol. 4, pp.203–211, 1977.

[45] Brown, R. H., Burstain, A. H., Nash, C. L., and Schock, C. C., " Spinal Analysis using a Three–Dimensinal Radiographic Technique," J. Biomechanics, Vol. 9, pp.355–366, 1976.

[46] Youm, Y., amd Yoon, Y. S., " Analytical Development in Investigation of Wrist Kinematics," J. Biomechanics, Vol. 12, pp.613–621, 1979.

[47] Blacharski, D. A., and Somerset, J. H., " A Three Dimensinal Study of the Kinematics of the Human Knee," J. Biomechanics, Vol. 8, pp.375–384, 1975.

[48] Kinzel, G. L., " On the Design of Instrumented Linkage for the Measurement of Relative Motion Between Two Rigid Bodies," Ph. D. thesis, Purdue University, 1973.

[49] Grood, E. S., and Suntay, W. J., " A Joint Coordinate System for the Clinical Description of Three–Dimensional Motions: Application to the Knee," Transactions of the ASME, Vol. 105, May 1983, pp.136–144.

[50] Sommer, J. J., and Miller, N. R., " A Technique for the Estimation of the Kinematic Parameters of a Spatial Anatomical Joint Model," Biomechanics Symposium, pp.291–222, 1979.

[51] Murray, M. P., Sepic, S. B., and Barnard, E. J., " Patterns of Sagittal Rotation of the Upper Limbs in Walking," Physical Therapy, Vol. 47, pp.272–282, 1967.

[52] Ringer, L. B., and Adrian, M. J., " An Electrogoniometric Study of the Wrist and Elbow in the Crawl Arm Stroke," The Research Qarterly, Vol. 40, pp.353–363, 1969.

[53] Freedman, L., and Munro, R. H., " Abduction of the Arm in the Scapular Plane: Scapular and Glenohumeral Movement," The J. of Bone and Joint Surgery, Vol. 48–A, pp.1503–1510, 1966.

[54] Feldman, M. C., " Mini–Goniometer for Finger Range of Motion," Physical Therapy, Vol. 50, p.1348, 1970.

[55] Shoup, J. E., " Optical Measurement of the Center of Rotation for Human Joints," J. Biomechanics, Vol. 9, pp.241–242, 1976.

[56] Dempster, S. T., " The Anthropometry of Body Motion," Annals New York Academy of Sciences, Vol. 63, pp.559–585, 1955.

[57] Dimnet, J., et al., " A Technique for Joint Analysis Using a Stored Program Calculator," J. Biomechanics, Vol. 9, pp.771–778, 1976.

[58] Soudan, K., Van Andekercke, R., and Martens, M., " Methods, Difficulties and Inaccuracies in the Study of Human Joint Kinematics and Pathokinematics by the Instant Axis Concept," J. Biomechanics, Vol. 12, pp.27–33, 1979.

[59] Chao, E. Y., " Experimental Methods for Biomechanical Measurements of Joint Kinematics," CRC Handbook of Engineering in Medicine and Biology, 1978, pp.385–411.

[60] Suntay, W. J., et al., " A Coordinate System for Descibing Joint Position," Advanced in Bioengineering, ASME, pp.59–62, 1978.

[61] Shames, I. H., *Engineering Mechanics*, 2nd Edition, Prentice Hall, Englewood cliff, N. J., p.653.

[62] Chao, E. Y., " Justification of Triaxial Goniometer for the Measurement of Joint Rotation," J. Biomechanics 13, pp.989–1006, 1980.

[63] Anonymous, Joint Motion, Method of Measuring and Recording, American Academy of Orthopaedic Surgeon, 1965.

[64] Engen, T. J., and Spencer, W. A., " Method of Kinematic Study of Normal Upper Extremity Movement," Archives of Physical Medicine and Rehabilitation, Vol. 49, pp.9–12, 1968.

[65] Kinzel, G. L. et al., " Preliminary Study of the in Vivo Motion in the Canine Shoulder," American J. of Veterinary Research, Vol. 37, No. 12, pp.1505–1510, 1976.

[66] Brady, M. et al., *Robot Motion: Planning and Control*, The MIT Press, 1982.

[67] Chao, E. Y., and Rim, K., " Application of Optimization Principles in Determining the Applied Moments in Human Leg Joints During Gait," J. Biomechanics, Vol. 6, pp.497–510, 1973.

[68] Hemami, H., Jaswa, V. C., and Mcghee, R. B., " Some Alternative Formulations of Manipulator Dynamics for Computer Simulation Studies," Proceedings of 13th Allerton Conference On Circuit and System Theory, pp.1–17, 1975.

[69] Asada, H., and Slotine, J. J. E., Robot Analysis and Control, Wiley–Interscience, 1986.

[70] Winter, D. A., Biomechanics and Motor Control of Human Movement, 2nd Edition, Wiley Interscience, 1990.

[72] Komi, P. V., " Relevance of In Vivo Force Measurements to Human Biomechanics, J. Biomechanics, Vol. 23, Suppl. 1, pp.23–34, 1990.

[73] Bean, J. C., Chaffin, D. B., and Schultz, A. B., " Biomechanical Model Calculation of Muscle Contraction Forces: A Double Linear Programming Method," J. Biomechanics, Vol. 21, No. 1, pp.59–66, 1988.

[74] Pedersen, D. R., Brand, R. A., Cheng, C., and Aroro, U. S., " Direct Comparison of Muscle Force Prediction Using Linear and Nonlinear Programming," Transactions of the ASME, Vol. 109, August 1987, pp.192–.

[75] An, K. N., Kwak, B. M., Chao, E. Y., and Morrey, B. F., " Dtermination of Muscle and Joint Forces: A New Technique to Solve the Indeterminate Problem," ZTransactions of the ASME, Vol. 106, Nov. 1984, pp.364–367.

[75] TÜmer, S. T., and Engin, A. E., " Three–Dimensinal Kinematic Modelling of the Human Shoulder Complex—Part II: Mathematical Modelling and Solution Via Optimization," J. Biomechanical Engineering, Vol. 111, May 1989, pp.113–121.

[76] Herzog, W., " Individual Muscle Force Estimations Using a Nonlinear Optimal Design," J. Neurosci. Meth. 21, pp.167–179, 1987.

[77] Crowninshield, R. D., and Bran, R. A., " A Physiologically Based Criterion of Muscle Force Prediction in Locomotion," J. Biomechanics, 14, pp.793–802, 1981

[78] Verstraete, M. C., " A Method for Computing the Three–Dimensional Forces and Moments at the Knee During Gait," International Society of Biomechanics XI Congress, 1988, p.875.

[79] Bahamonde, R E., " Kinematic Analysis of the Serving Arm During the Performance of the Tennis Serve," International Society of Biomechanics XII, 1989, p.983.

[80] Hoy, M. G., and Zernicke, R. F., " The Role of Intersegmental Dynamics During Rapid Limb Oscillations," J. Biomechanics 19, pp.867–877, 1986.

[81] Smith, J. L., and Zernicke, R. F., " Prediction for Neural Control Based on Limb Dynamics," Trends Neurosci. 10, pp.123–128, 1987.

[82] Atkeson, C. G., and Hollerback, J. M., " Kinematic Features of Unrestrained Vertical Arm Movements," J. Neurosci. 5, pp.2318–2330, 1985.

[83] Robertson, D. G. E., and Winter, D. A., " Mechanical Energy Generation, Absorption and Transfer amongst Segments during Walking," J. Biomechanics 13, pp.845–854, 1980.

[84] Winter, D. A., " Moments of Force and Mechanical Power in Jogging," J. Biomechanics, Vol.10, No. 1, pp.91–97, 1983.

[85] Jensen, R. K., and Bellow, D. G., " Upper Extremity Contraction Moments and Their Relationship to Swimming Training," J. Biomechanics, vol.9, pp.219–225, 1976.

[86] Anderson, G. B. J., and Schultz, A. B., " Transmission of Moments across the Elbow Joint and the Lumber Spine," J. Biomechanics, Vol. 12, pp.747–755, 1979.

[87] Wells, R. P., " Mechanical Energy Costs of Human Movement: An Approach to Evaluating the Transfer Possibilities of Two–Joint Muscles," J. Biomechanics, Vol. 21, No. 11, pp.955–964, 1988.

[88] Fenn, W. O., " Frictional and Kinetic Factors in the Work of Spring Running," Am. J. Physiol. 92, pp.583–611, 1929.

[89] Ralston, H. J., and Lukin, L., " Energy Level of Human Body Segments During Level Walking," Ergonomics, Vol. 12, No. 1, pp.39–46, 1969.

[90] Winter, D. A., Quanbury, A. O., and Reimer, G. D., " Analysis of Instantaneous Energy of Normal Gait," J. Biomechanics, Vl. 9, pp.253–257, 1976.

[91] Wells, R. P., " The Kinematics and Energy Variations of Swing Through Crutch Gait," J. Biomechanics, Vol. 12, pp.579–585, 1979.

[92] Winter, D. A., " A New Definition of Mechanical Work Done in Human Movement," J. Appl. Physiol. Resp. Env. Exercise Physiol. 46, pp.79–83, 1979.

[93] Williams, K., and Cavanagh, P., " A Model for the Calculation of Mechanical Work During Distance Running," J. Biomechanics 66, pp.115–128, 1983.

[94] Zatsiorski, V., Mikhailov, N. G., and Yakunin, N. A., " Mechanical Work Done During Walking and Running: Comparison of Six Different Ways of Calculations," II Conference of the European Society of Biomechanics, Nijmegen, Netherlands, 1982.

[95] Hubley, C. L., and Wells, R., " A Work–Energy Approach to Determine Individual Joint Contributions to Vertical Jump Performance," Eur. J. Appl. Physiol. 50, pp.247–254, 1983.

[96] Winter, D. A., and Robertson, G. E., " Joint Torque and Energy Patterns in Normal Gait," Biol. Cybernetics 29, pp.137–142, 1978.

[97] Bresler, B., and Frankel, J. P., " The Forces and Moments in the Leg during Leval Walking," Transactions of the ASME 72, pp.27–36, 1950.

CHAPTER 2

[1]. Onyshko, S. and Winter, D.A., " A Mathematical Model for the Dynamics of Human Locomotion," J. Biomechanics, Vol.13, pp.361–368, 1980.

[2]. Hatze, H., " A Complete Set of Control Equations for the Human Musculo–skeletal Systems," J. Biomechanics, Vol. 10, pp.799–805, 1977.

[3]. Kilmister, C.W., *Lagrangian Dynamics*: An Introduction for Students, 1967.

[4] Engin, A.E., " On the Biomechanics of the Shoulder Complex," J. Biomechanics, Vol. 13, No. 7, pp.575–590, 1980.

[5]. Steiner, A., *Kinesiology of the Human Body*, Charlse C. Thomas, Springfield, III, 1955.

[6]. Engin, A. E., and TÜmer, S. T., " Three–Dimensinal Kinematic Modelling of the Human Shoulder Complex—Part I: Physical Model and Determination of Joint Sinus Cones," J. Biomechanical Engineering, Vol. 111, May 1989, pp.107–112.

[7]. Engin, A.E., Peindl, R.D., Berme, N. and Kaleps, I., " Kinematic and Force Data Collection in Biomechanics by means of Sonic Emitters— II: Force Data Collection and Application to the Human Shoulder Complex," transactions of the ASME, Vol. 106, August 1984, pp.212–219.

[8]. Engin, A.E. and Chen, S.–M., " Statistical Data Base for the Biomechanical Properties of the Human Shoulder Complex— I: Kinematics of the Shoulder Complex," J. Biomechanical Engineering, Vol. 108, August 1986, pp.215–221.

[9]. TÜmer, S. T., and Engin, A. E., " Three–Dimensinal Kinematic Modelling of the Human Shoulder Complex—Part II: Mathematical Modelling and Solution Via Optimization," J. Biomechanical Engineering, Vol. 111, May 1989, pp.113–121.

[10]. Youm, Y., dryer, R.F., Thambyrajah, K. and Flatt, A.E., " Biomechanical Analyses of Forearm Pronation–Supination and Elbow Flexion–Extension," J. Biomechanics, Vol. 12, pp.245–255, 1979.

[11]. Menli, H.C., " Arthroplastry of the Wrist," Clinical Orthopaedics and Related Research, Vol. 149, p.118, 1980.

[12]. Hamas, R.S., " A Quqntitative Approach to tatol Wrist Arthroplastry: Development of a 'Precentered' total Wrist Prosthesis," Orthopaedics, Vol. 2, No. 2, p.245, 1979.

[13]. Brumbaugh, R.B., Crowninshield, R.D., Blair, W.F. and Andrews, J.G., " An In–Vivo Study of Normal Wrist Kinematics," Transactions of the ASME, Vol. 104, August 1982, pp.176–181.

[14]. Langrana, N. A., " Spatial Kinetic Analysis of the Upper Extremity Using a Biplanar Videotaping Method," J. Biomechanical Engineering, Vol. 103, Feb. 1981, pp.11–17.

[15]. Jackson, K. M., Joseph, J., and Wyard, S. J., " A Mathematical Model of Arm Swing During Human Locomotion," J. Biomechanics, Vol. 11, pp.277–289, 1978.

[16]. Luttgens &Wells, *Kinesiology, Scientific Basis of Human Motion*, 1982.

[17]. J.E. Cooper, E. Shwedyk, A. Quanbery and J. Miller, " 3–D Kinematic Analysis of the Effect of Elbow Joint Restriction on Upper Limb Motion during Performance of the Feeding

Activities," Conference on 3–D Kinematic Analysis of Human Motion, July 28–31, 1991, Montreal.

[18]. Greenwood, D.T., *Principles of Dynamics*, Prentice–Hall Inc., 1965.

[19]. Winter, D. A., Biomechanics and Motor Control of Human Movement, 2nd Edition, Wiley Interscience, 1990.

[20]. Niku, S. and Henderson, J.M., " Viscocity of the Flexor Muscles of the Elbow Joint under Contraction Condition," J. Biomechanics, Vol. 22, No. 6/7, pp.523–527, 1989.

[21]. Niku, S. and Henderson, J.M., " Determination of the Parameters for an Athetotic Arm Model," J. Biomechanics, Vol. 18, No. 3, pp.209–215, 1985.

[22]. Singhal, K. and Kesavan, H.K., " Dynamic Analysis of Mechacnism via Vector Network Model," J. Mechacnisms Mach. Theory 18, pp.175–180, 1983.

[23]. Wolfram, S., *Mathematica: A System for Doing Mathematics by Computer*, Addison–Wesley Pub. Comp., 1988.

[24]. Spong, M.W. and Vidyasagar, M., *Robot Dynamics and Control*, John Wiley and Sons, 1989.

[25]. Plagenhoef, S., Erans, F.G. and Abdelnour, T., " Anatomical Data for Analyzing Human Motion," Res. Q. Exerc. Sport 54, p.169, 1983.

[26]. Mclean and Nelson, Engineering Mechanics, 2/ed., Mcgraw–Hill Book Comp., 1962.

CHAPTER 3

[1] Winter, D.A., Sidwall, H.G. and Hobson, D.A., " Measurement and Reduction of Noise in Kinematics of Locomotion," J. Biomechanics, Vol. 7, pp.157–159, 1974.

[2] Lesh, M.D., Mansour, J.M. and Simon, S.R., " A Gait Analysis Subsystem for Smoothing and Differentiation of Human Motion Data," J. Biomechanics, Vol. 101, pp.205–212, 1979.

[3] Pezzack, J.C., Norman, R.W. and Winter, D.A., " An Assessment of Derivative Dtermining Techniques Used for Motion Analysis," J. Biomechanics, Vol. 10, pp.377–382, 1977.

[4] Plagenhoef, S.C., " Computer Program for Obtaining Kinetic Data on Human Movement," J. Biomechanics, Vol. 1, pp.221–234, 1968.

[5] Wood, G. and Jennings, L., " On the Use of Spline Functions for Data Smoothing," J. Biomechanics, Vol. 12, pp.477–479, 1979.

[6] Busby, H.R. and Trujillo, D.M., " Numerical Experiments with a New Differentiation Filter," J. of Biomechanical Engineering, Vol. 107, pp.293–299, 1985.

[7] Verstraete, M.C. and Soutas–Little, R.W., " A Method for Computing the Three–Dimensional Angular Velocity and Acceleration of a Body Segment from Three–Dimensional Position Data," Transactions of the ASME, Vol. 112, pp.114–118, 1990.

[8] Marble, A.E. and Zayezdny, A.M., " Adaptive Numerical Smoothing: An Effecient Method of Conditioning Physiological Signals," Med. & Biolo. Eng. & Comput., pp.171–180, 1989.

[9] Rabiner, L.R., Sambur, M.R. and Schmidt, C.E., " Applications of a Nonlinear Smoothing Algorithm to Speech Processing," IEEE Trans., ASSP–23, pp.552–557, Dec. 1975.

[10] Tukey, J.W., *Exploratory Data Analysis*, Addison–Wesley, 1977.

[11] Arce, G.R. and Gallagher, N.C., " State Description of the Root Signal Set of Median Filters," IEEE Trans., ASSP–30, pp.894–902, 1982.

[12] Kasparis, T. and Eichmann, G., " Vector Median Filters," Sig. Proc., Vol. 13, pp.287–299, 1987.

[13] Gallagher, N.C. and Wise, G.L., " A Theoretical Analysis of the Properties of Median Filters," IEEE Trans., ASSP–29, pp.1136–1141, Dec. 1981.

[14]. J.E. Cooper, E. Shwedyk, A. Quanbery and J. Miller, " 3–D Kinematic Analysis of the Effect of Elbow Joint Restriction on Upper Limb Motion during Performance of the Feeding Activities," Conference on 3–D Kinematic Analysis of Human Motion, July 28–31, 1991, Montreal.

CHAPTER 4

[1] Schneider, K., Zernicke, R. F., Schmidt, R. A., and Hart, T. J., " Changes in Limb Dynamics During the Practice of Rapid Arm Movement," J. Biomechanics, Vol. 22, No. 8/9, pp.805–817, 1989.

[2] Hoy, M.G. and Zernicke, R.F., " Modulation of Limb Dynamics in the Swing Phase of Locomotion," J. Biomechanics, Vol. 18, No. 1, pp.49–60, 1985.

[3] Atkeson, C. G., and Hollerback, J. M., " Kinematic Features of Unrestrained Vertical Arm Movements," J. Neurosci. 5, pp.2318–2330, 1985.

[4] Hamilton, N. and Myers, A., " A Preliminary Study of Joint Torques in the Lower Extremity in a Plyometric Jump," International Society of Biomechanics XI Congress, 1988.

[5] Jensen, R. K., and Bellow, D. G., " Upper Extremity Contraction Moments and Their Relationship to Swimming Training," J. Biomechanics, vol.9, pp.219–225, 1976.

[6] Winter, D. A., Biomechanics and Motor Control of Human Movement, 2nd Edition, Wiley Interscience, 1990.

[7] Winter, D. A., " Moments of Force and Mechanical Power in Jogging," J. Biomechanics, Vol.10, No. 1, pp.91–97, 1983.

[8] Robertson, D. G. E., and Winter, D. A., " Mechanical Energy Generation, Absorption and Transfer amongst Segments during Walking," J. Biomechanics 13, pp.845–854, 1980.

[9] Chapman, A.E. and Caldwell, G.E., " Factors Determing Changes in Lower Limb Energy during Swing in Treadmill Running," J. Bimechanics, Vol. 16, No. 1, pp.69–77, 1983.

[10] Bahamonde, R E., " Kinematic Analysis of the Serving Arm During the Performance of the Tennis Serve," International Society of Biomechanics XII, 1989, p.983.

[11] Verstraete, M. C., " A Method for Computing the Three–Dimensional Forces and Moments at the Knee During Gait," International Society of Biomechanics XI Congress, 1988, p.875.

[12] Safaee–Rad, R., Functional Human Arm Motion Study with a New 3–D Measurement System, M. Sc. Thesis, University of manitoba, 1987.

[13] Winter, D. A., Quanbury, A. O., and Reimer, G. D., " Analysis of Instantaneous Energy of Normal Gait," J. Biomechanics, Vl. 9, pp.253–257, 1976.

[14] Wells, R. P., " The Kinematics and Energy Variations of Swing Through Crutch Gait," J. Biomechanics, Vol. 12, pp.579–585, 1979.

[15] Wells, R. P., " Mechanical Energy Costs of Human Movement: An Approach to Evaluating the Transfer Possibilities of Two–Joint Muscles," J. Biomechanics, Vol. 21, No. 11, pp.955–964, 1988.

CHAPTER 5

[1]. J.E. Cooper, E. Shwedyk, A. Quanbery and J. Miller, " 3–D Kinematic Analysis of the Effect of Elbow Joint Restriction on Upper Limb Motion during Performance of the Feeding Activities," Conference on 3–D Kinematic Analysis of Human Motion, July 28–31, 1991, Montreal.